

# Recent measurement of isolated $\gamma$ with

ALICE 

- Cross section in pp and Pb-Pb collisions at  $\sqrt{s_{\text{NN}}} = 5.02$  TeV
  - Also pp and p-Pb at different energies
- Isolated  $\gamma$ -hadron correlation in Pb-Pb at  $\sqrt{s_{\text{NN}}} = 5.02$  TeV
- Run 2 measurements at mid-rapidity  $|\eta| < 0.67$

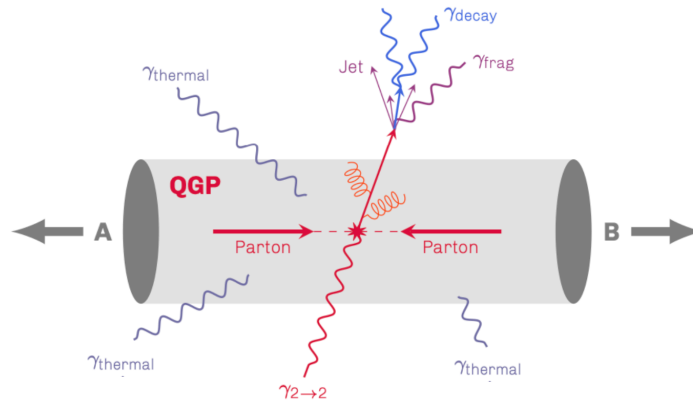
Preliminary results shown at HEP-EPS 23 (G. Conesa),  
QM 23 and GDR-QCD (C. Arata)

# Motivation

- $\gamma$  are **color neutral**: **not affected** by “*quark-gluon plasma*” (QGP) presence in *heavy-ion collisions* unlike **partons** that **lose energy**
- Direct  $\gamma$ , *not originated by hadronic decays*

Nuclear modification factor:  
 $p_T$  yield modification from AA to pp coll. due to QGP and other effects

$$R_{AA} = \frac{1}{N_{\text{coll}}} \frac{d^2\sigma_{AA} / (dp_T d\eta)}{d^2\sigma_{pp} / (dp_T d\eta)}$$

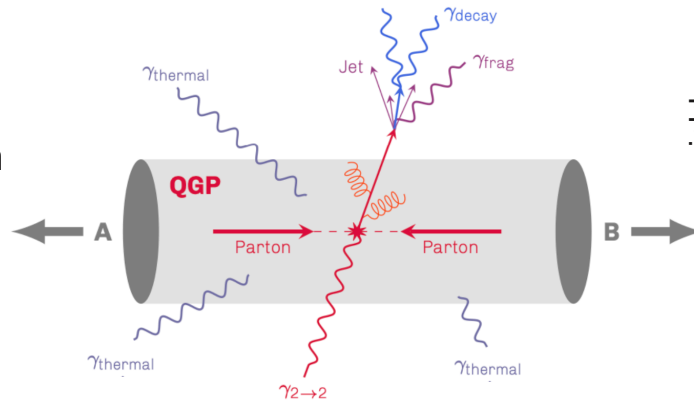


# Motivation

- $\gamma$  are **color neutral**: not affected by “quark-gluon plasma” (QGP) presence in heavy-ion collisions unlike **partons** that **lose energy**
- Direct  $\gamma$ , not originated by hadronic decays

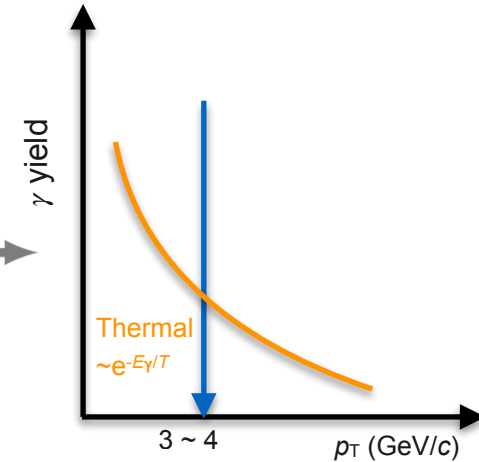
➔ **Direct thermal  $\gamma$ :  $R_{AA} \gg 1$**

- QGP thermal radiation
- Measure  **$T$  & time/size evolution**



Nuclear modification factor:  
 $p_T$  yield modification from AA to pp coll. due to QGP and other effects

$$R_{AA} = \frac{1}{N_{\text{coll}}} \frac{d^2\sigma_{AA} / (dp_T d\eta)}{d^2\sigma_{pp} / (dp_T d\eta)}$$



# Motivation

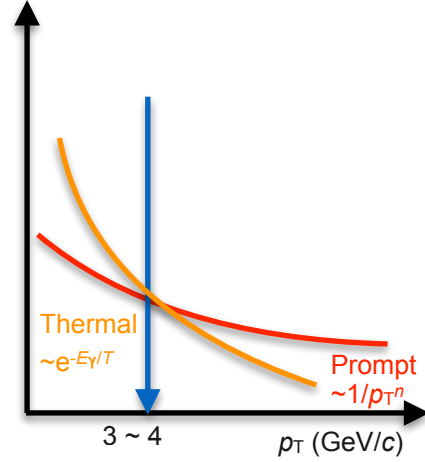
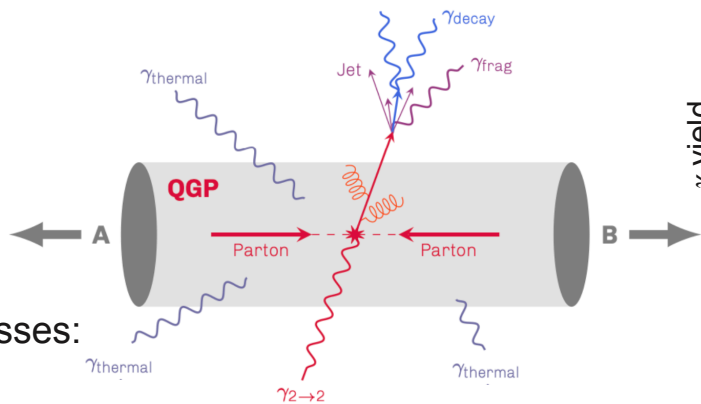
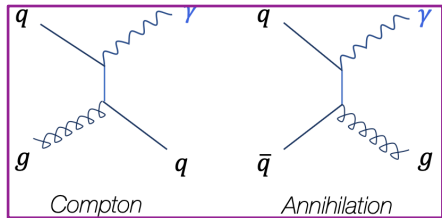
- $\gamma$  are **color neutral**: not affected by “quark-gluon plasma” (QGP) presence in heavy-ion collisions unlike **partons** that lose energy
- Direct  $\gamma$ , not originated by hadronic decays

Nuclear modification factor:  
 $p_T$  yield modification from AA to pp coll. due to QGP and other effects

$$R_{AA} = \frac{1}{N_{\text{coll}}} \frac{d^2\sigma_{AA} / (dp_T d\eta)}{d^2\sigma_{pp} / (dp_T d\eta)}$$

- ➔ **Direct thermal  $\gamma$ :  $R_{AA} \gg 1$** 
  - QGP thermal radiation
  - Measure  $T$  & time/size evolution

- ➔ **Direct prompt  $\gamma$ :  $R_{AA} \approx 1$** 
  - Initial hard scattering,  $2 \rightarrow 2$  processes:



$$d\sigma_{AB \rightarrow h}^{\text{hard}} = f_{a/A}(x_1, Q^2) \otimes f_{b/B}(x_2, Q^2) \otimes d\sigma_{ab \rightarrow c}^{\text{hard}}(x_1, x_2, Q^2) \otimes D_{c \rightarrow h}(z, Q^2)$$

PDFs      Hard scattering (pQCD)      Fragmentation function

- Test pQCD predictions, **constrain (n)PDFs & FF**
- $p_T^\gamma \simeq p_T^{\text{parton}}$ , before parton loses  $\Delta E$  in QGP
- Measure **FF modifications**, where is the  $\Delta E$  radiated?

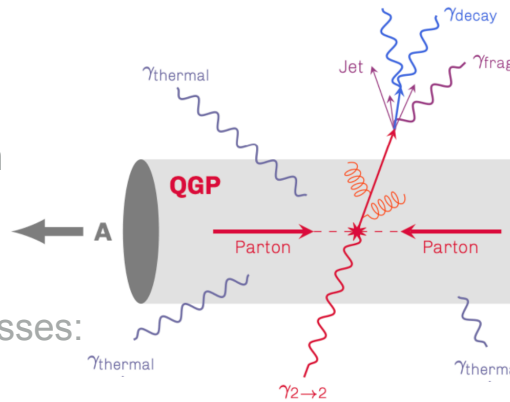
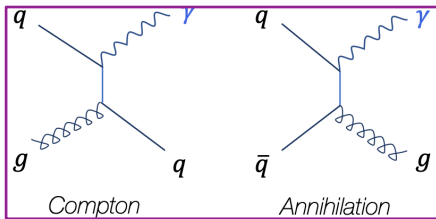


# Motivation

- $\gamma$  are **color neutral**: not affected by “*quark-gluon plasma*” (QGP) presence in *heavy-ion collisions* unlike **partons** that lose energy
- Direct  $\gamma$ , not originated by hadronic decays

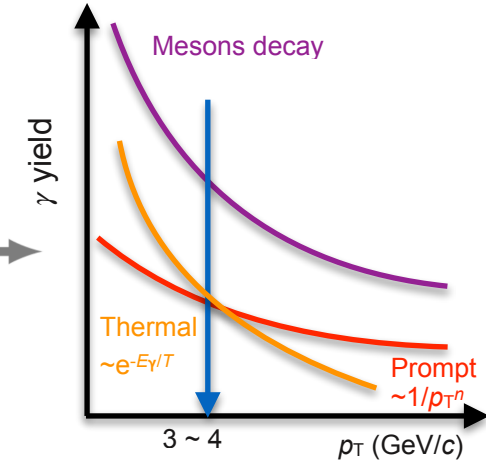
- ➔ **Direct thermal  $\gamma$** :  $R_{AA} \gg 1$ 
  - QGP thermal radiation
  - Measure  $T$  & time/size evolution

- ➔ **Direct prompt  $\gamma$** :  $R_{AA} \approx 1$ 
  - Initial hard scattering,  $2 \rightarrow 2$  processes:



Nuclear modification factor:  
 $p_T$  yield modification from AA to pp coll. due to QGP and other effects

$$R_{AA} = \frac{1}{N_{\text{coll}}} \frac{d^2\sigma_{AA} / (dp_T d\eta)}{d^2\sigma_{pp} / (dp_T d\eta)}$$



$$d\sigma_{AB \rightarrow h}^{\text{hard}} = f_{a/A}(x_1, Q^2) \otimes f_{b/B}(x_2, Q^2) \otimes d\sigma_{ab \rightarrow c}^{\text{hard}}(x_1, x_2, Q^2) \otimes D_{c \rightarrow h}(z, Q^2)$$

PDFs                                      Hard scattering (pQCD)                                      Fragmentation function

- Test pQCD predictions, constrain (n)PDFs & FF
- $p_T^\gamma \simeq p_T^{\text{parton}}$ , before parton loses  $\Delta E$  in QGP
- Measure FF modifications, where is the  $\Delta E$  radiated?

- **Decay  $\gamma$  ( $\pi^0$  &  $\eta$ )**:  $R_{AA} \ll 1$ 
  - Main background for direct  $\gamma$  measurements

# Motivation

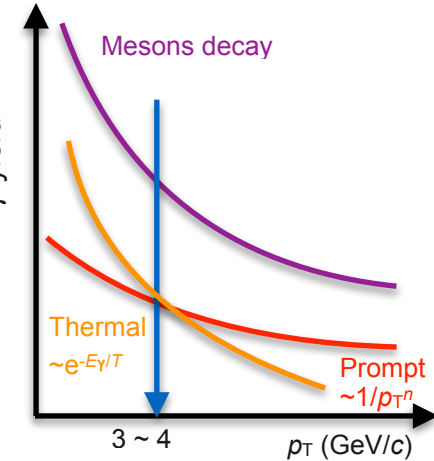
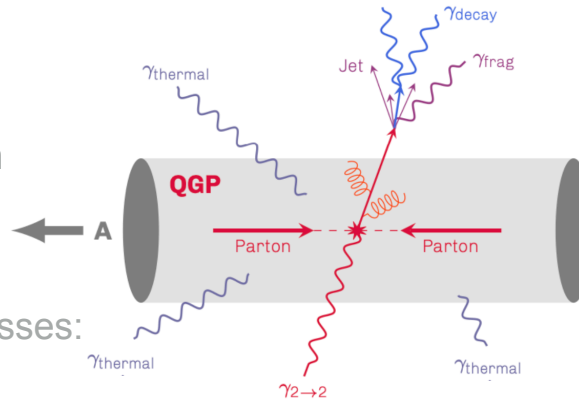
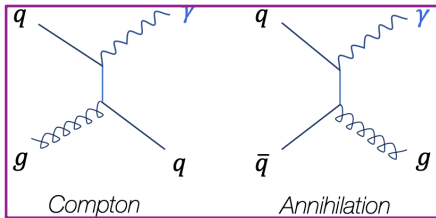
- $\gamma$  are **color neutral**: **not affected** by “*quark-gluon plasma*” (QGP) presence in heavy-ion collisions unlike **partons** that **lose energy**
- Direct  $\gamma$ , not originated by hadronic decays

Nuclear modification factor:  
 $p_T$  yield modification from AA to pp coll. due to QGP and other effects

$$R_{AA} = \frac{1}{N_{\text{coll}}} \frac{d^2\sigma_{AA} / (dp_T d\eta)}{d^2\sigma_{pp} / (dp_T d\eta)}$$

- ➔ **Direct thermal  $\gamma$ :  $R_{AA} \gg 1$** 
  - QGP thermal radiation
  - Measure  $T$  & time/size evolution

- ➔ **Direct prompt  $\gamma$ :  $R_{AA} \approx 1$** 
  - Initial hard scattering,  $2 \rightarrow 2$  processes:



$$d\sigma_{AB \rightarrow h}^{\text{hard}} = \underbrace{f_{a/A}(x_1, Q^2)}_{\text{PDFs}} \otimes \underbrace{f_{b/B}(x_2, Q^2)}_{\text{PDFs}} \otimes \underbrace{d\sigma_{ab \rightarrow c}^{\text{hard}}(x_1, x_2, Q^2)}_{\text{Hard scattering (pQCD)}} \otimes \underbrace{D_{c \rightarrow h}(z, Q^2)}_{\text{Fragmentation function}}$$

- Test pQCD predictions, **constrain (n)PDFs & FF**
- $p_T^\gamma \simeq p_T^{\text{parton}}$ , before parton loses  $\Delta E$  in QGP
- Measure **FF modifications**, where is the  $\Delta E$  radiated?
- **Decay  $\gamma$  ( $\pi^0$  &  $\eta$ ):  $R_{AA} \ll 1$** 
  - Main background for direct  $\gamma$  measurements

- **Other  $\gamma$  sources:**
  - Fragmentation  $\gamma$ :  $R_{AA} < 1$   
**comparable yield to direct prompt  $\gamma$**
  - QGP pre-equilibrium  $\gamma$ ?  $R_{AA} \gg 1$  (glasma phase)
  - Jet-QGP interaction  $\gamma$ ?  $R_{AA} \gg 1$  (hard partons scattering)

# Prompt $\gamma$ identification in ALICE: EM shower spread shape & isolation with tracks

$$R = \sqrt{(\eta_{\text{track}} - \eta_{\gamma})^2 + (\varphi_{\text{track}} - \varphi_{\gamma})^2} < 0.2 \text{ or } 0.4$$

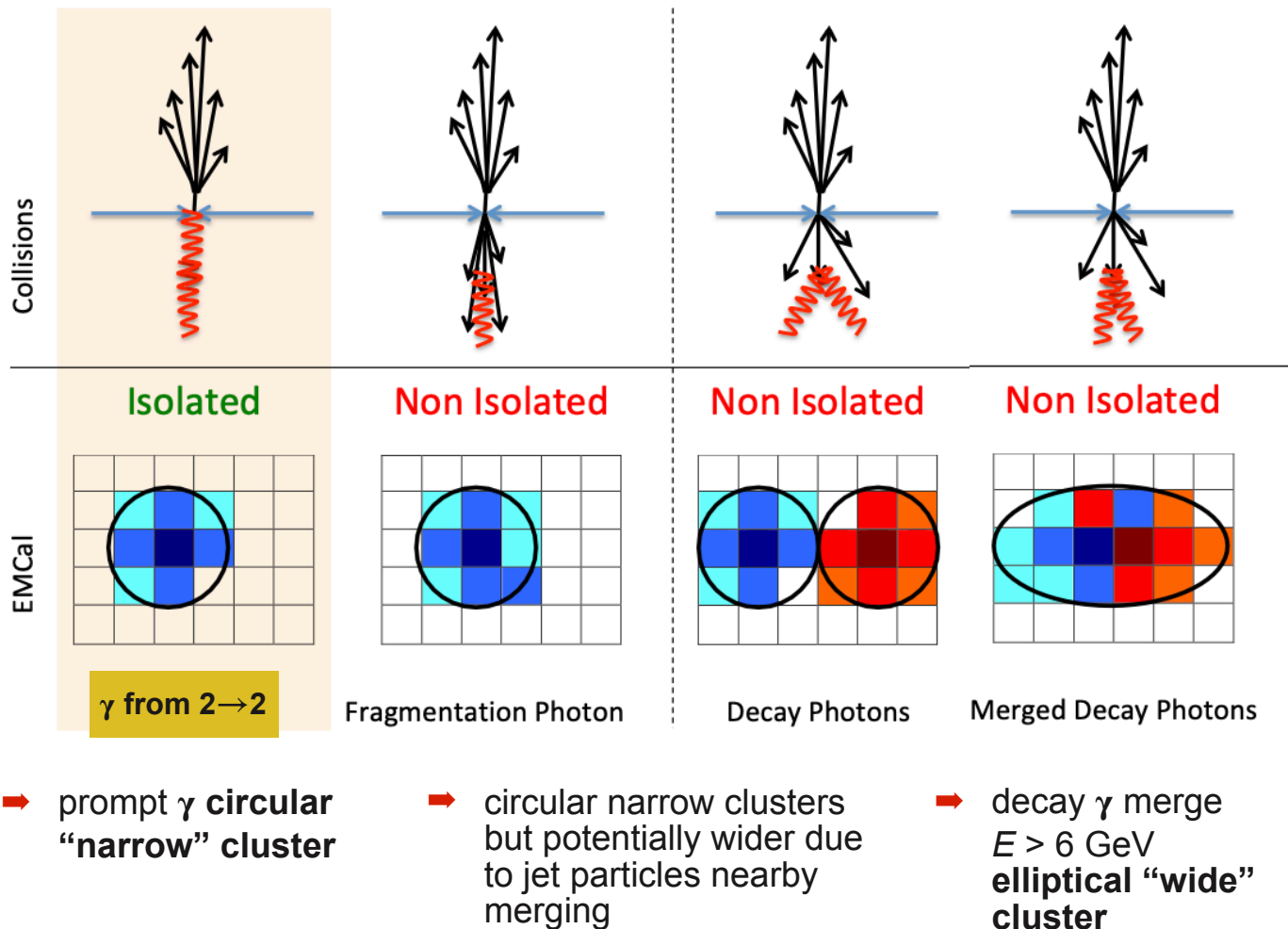
$$p_{\text{T}}^{\text{iso, ch}} = \sum p_{\text{T}}^{\text{tracks in cone}} - \rho_{\text{UE}} \cdot \pi \cdot R^2 < 1.5 \text{ GeV}/c$$

## $\gamma$ from 2 $\rightarrow$ 2: isolated

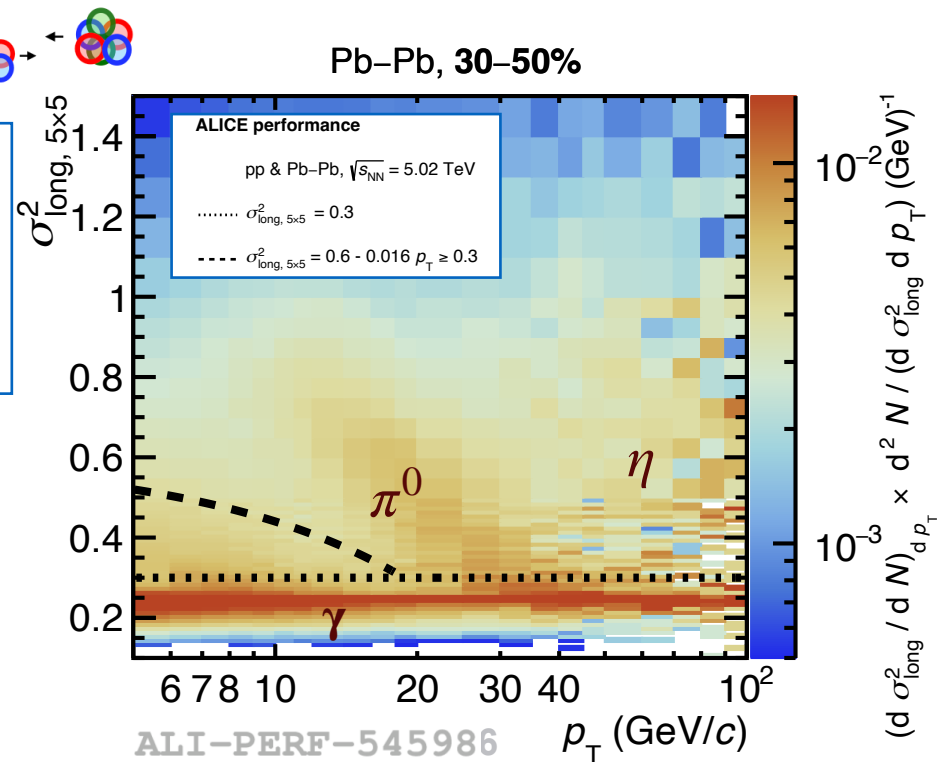
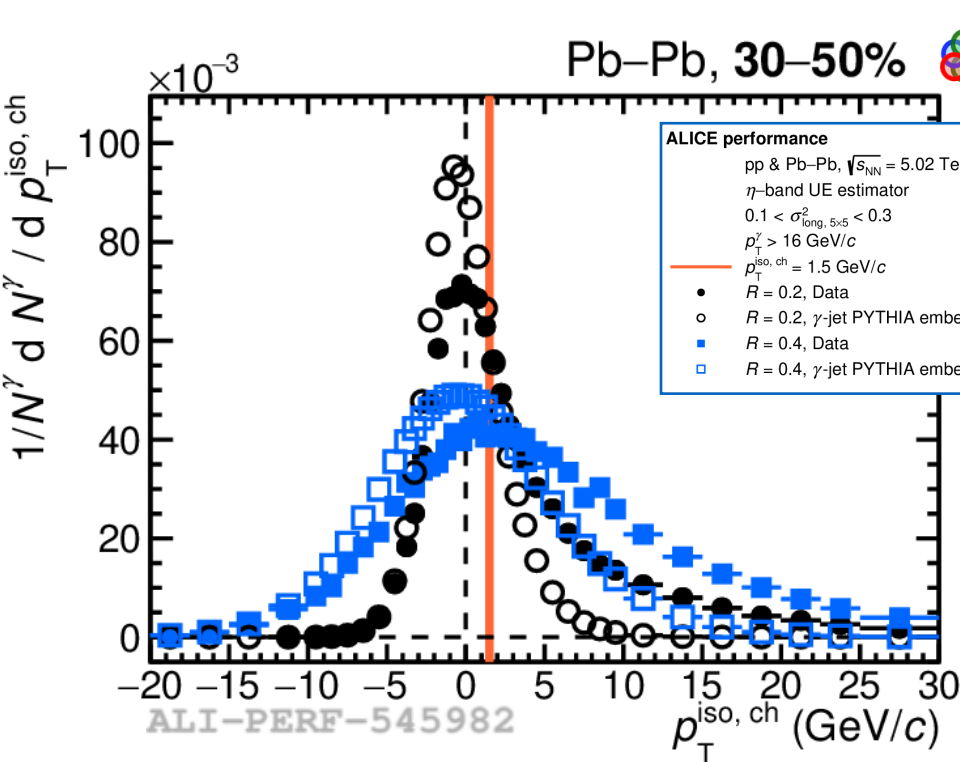
- ➔ TPC+ITS charged tracks
- ➔ Select  $\gamma$  with low hadronic activity in  $R$ , small  $p_{\text{T}}^{\text{iso, ch}}$
- ◆ Underlying event (UE) subtracted event-by-event,  $\rho_{\text{UE}}$  density estimated in  $\eta$ -band

## EM shower discrimination

- ➔ EMCal
- ➔ lateral dispersion  $\sigma_{\text{long}, 5 \times 5}^2$  calculated in  $5 \times 5$  cells around the highest energy cell



# Prompt $\gamma$ identification in ALICE: EM shape & isolation



- Embedded pp PYTHIA simulation into MB data, symmetric distribution
- In data, more asymmetric distribution due to jet contribution
- Significantly wider distributions for  $R = 0.4$
- Isolated if  $p_T^{\text{iso, ch}} < 1.5$  GeV/c (orange line)

- Bands for  $\gamma$  (narrow clusters) &  $\pi^0$  (wide clusters) visible from pp to Pb-Pb
- Select as  $\gamma$  clusters with
  - $0.1 < \sigma_{\text{long}, 5 \times 5}^2 < 0.6 - 0.016 \cdot p_T$  for Pb-Pb  $p_T < 18$  GeV/c
  - $0.1 < \sigma_{\text{long}, 5 \times 5}^2 < 0.3$  for pp & Pb-Pb,  $p_T > 18$  GeV/c

# Purity, $R = 0.2$ & $0.4$

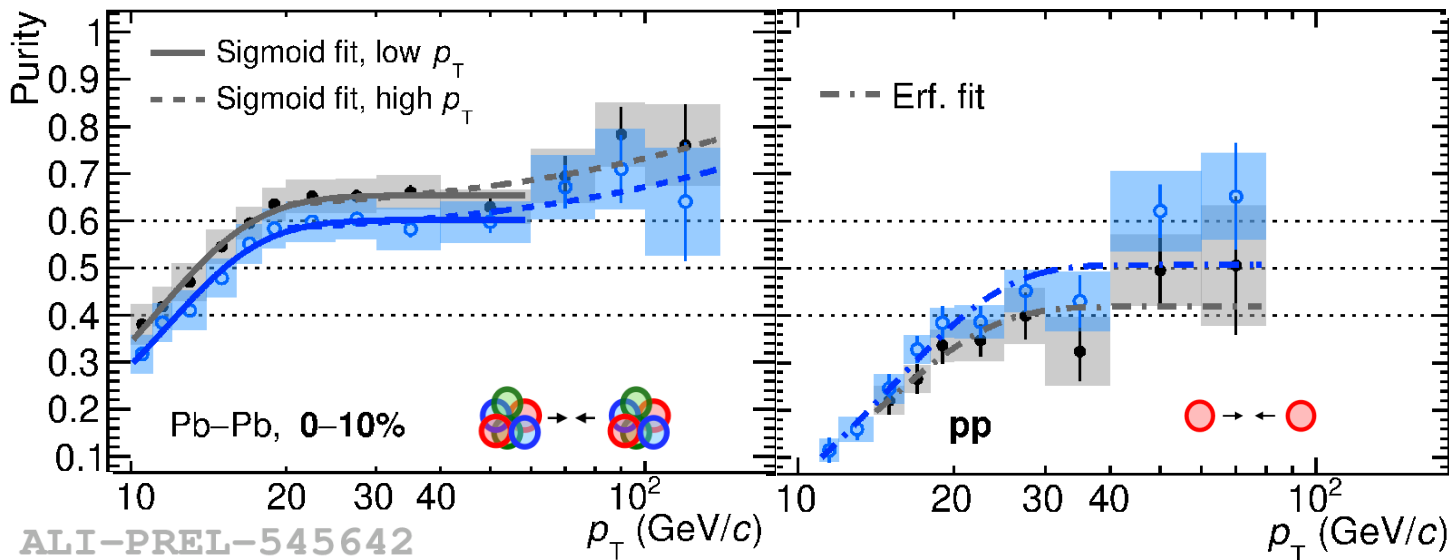
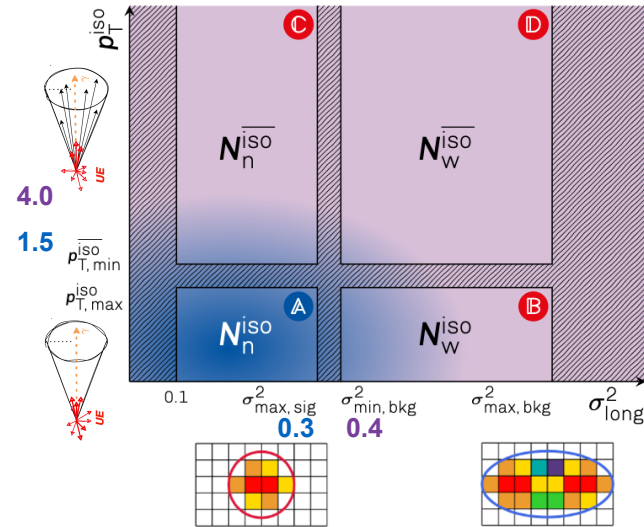
- Phase space of calorimeter clusters divided in 4 regions:
  - A, signal dominated & B-C-D, background dominated

$$P = 1 - \left( \frac{N_n^{\text{iso}} / N_n^{\text{iso}}}{N_w^{\text{iso}} / N_w^{\text{iso}}} \right)_{\text{data}} \times \left( \frac{B_n^{\text{iso}} / N_n^{\text{iso}}}{N_w^{\text{iso}} / N_w^{\text{iso}}} \right)_{\text{MC}}$$

data-driven      PYTHIA

$N_{n,w}^{\text{iso,iso}} = \text{jet-jet } (B_{n,w}^{\text{iso,iso}}) + \gamma\text{-jet } (S_{n,w}^{\text{iso,iso}})$

- Semi data-driven approach, simulation used to correct correlations between  $p_T^{\text{iso, ch}}$  and  $\sigma_{\text{long}}^2$ ,  $5 \times 5$

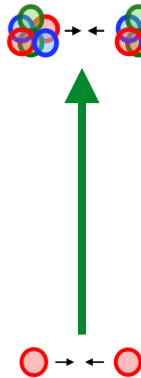
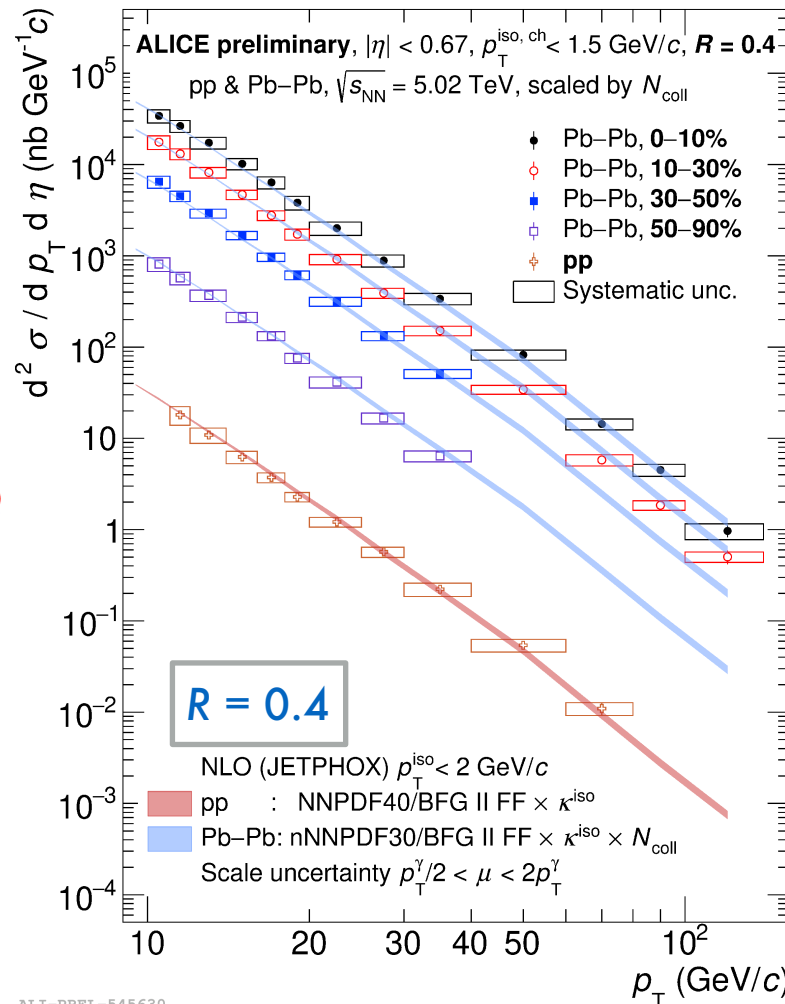
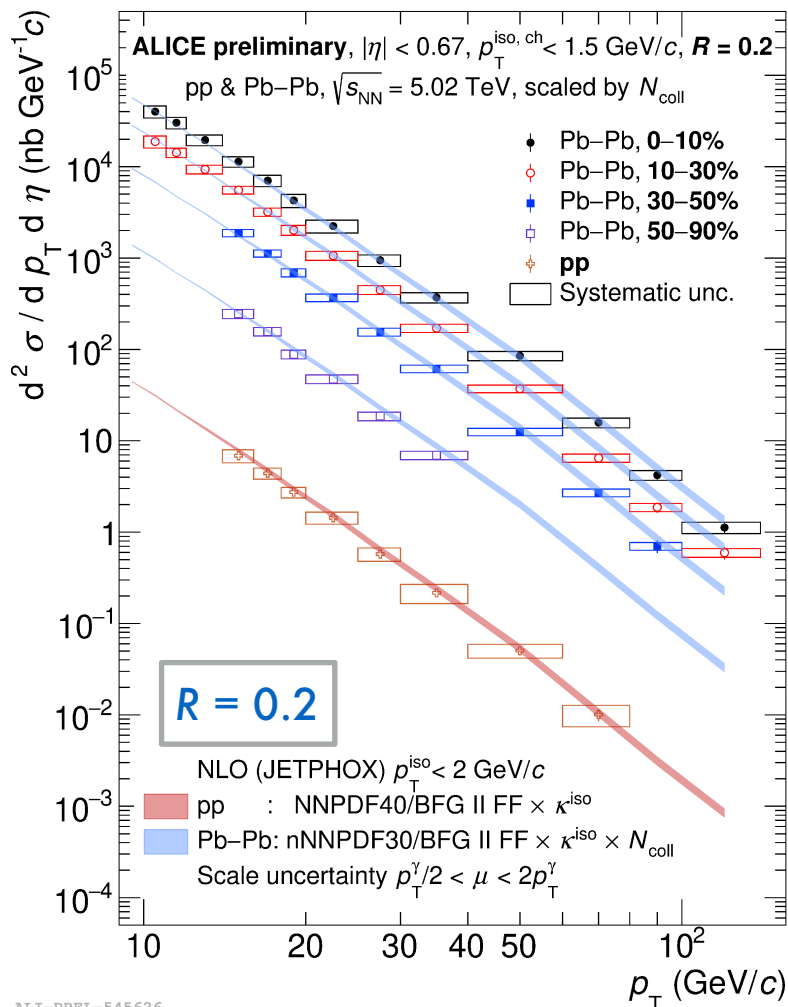


- Reduce influence of statistical fluctuations with Sigmoid or Erf functions fits  
→ used in spectra

- $P(R = 0.4) > P(R = 0.2)$  in pp coll., more jet particles in cone, but  $P(R = 0.2) > P(R = 0.4)$  in 0-10% Pb-Pb coll., due to UE fluctuations, but not significantly different
- $P(\text{Pb-Pb}) > P(\text{pp})$ , better tracking & higher  $N(\gamma) / N(\pi^0)$  ratio

# Cross section, $R = 0.2$ & $0.4$

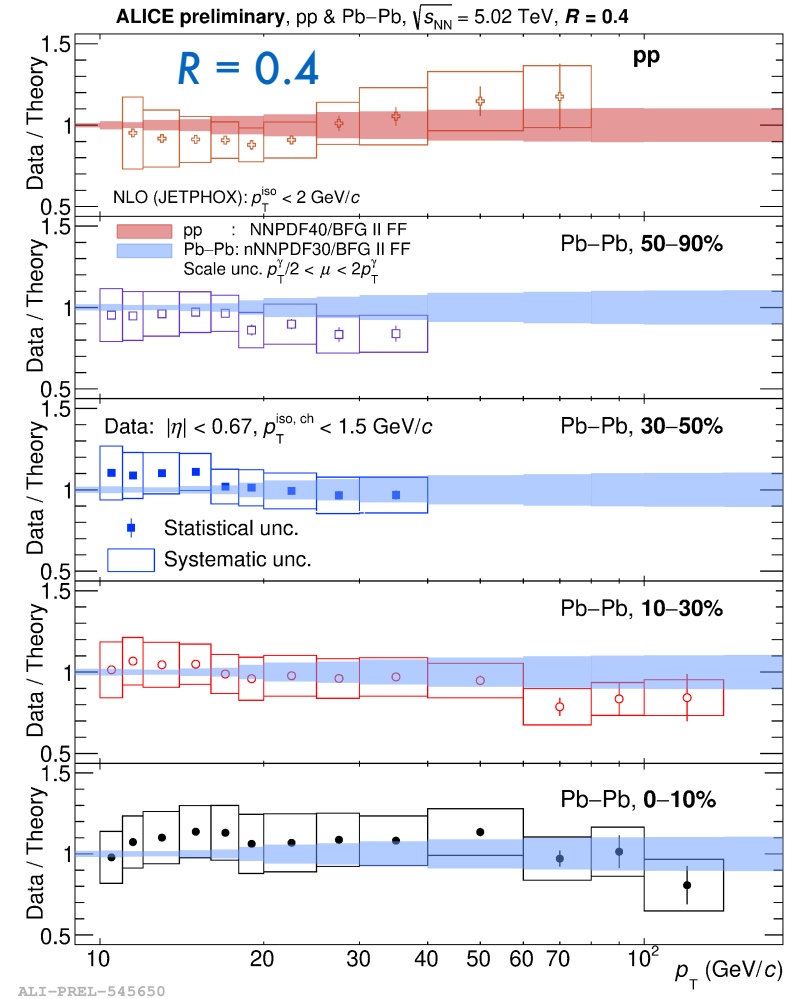
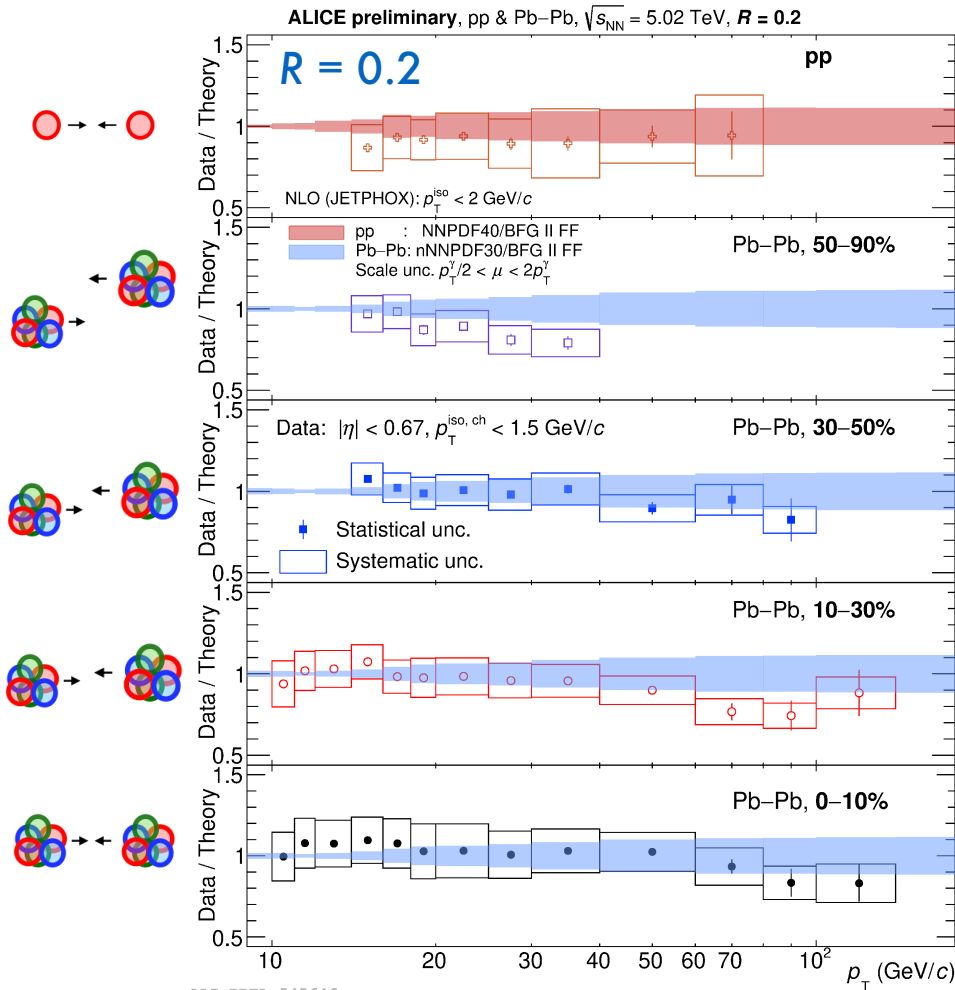
$$\frac{d^2 \sigma}{d p_T d \eta} = \frac{\sigma_{\text{MB}}}{N_{\text{events}} \times R F_{\epsilon_{\text{trig}}}} \times \frac{d^2 N}{d p_T d \eta} \times \frac{P}{\text{Acc} \times \epsilon_{\gamma}^{\text{iso}} \times \epsilon_{\text{trig}}}$$



- Wide range:  $10 < p_T < 140$  GeV/c in Pb-Pb 0-30% coll. &  $11-14 < p_T < 60$  GeV/c in pp coll.
- NLO pQCD predictions (JETPHOX)

➔ Note: **Theory is centrality independent!** only difference is PDF (pp) vs nPDF  $\times N_{\text{coll}}$  (Pb-Pb)

# Cross section Data/Theory, $R = 0.2$ & $0.4$

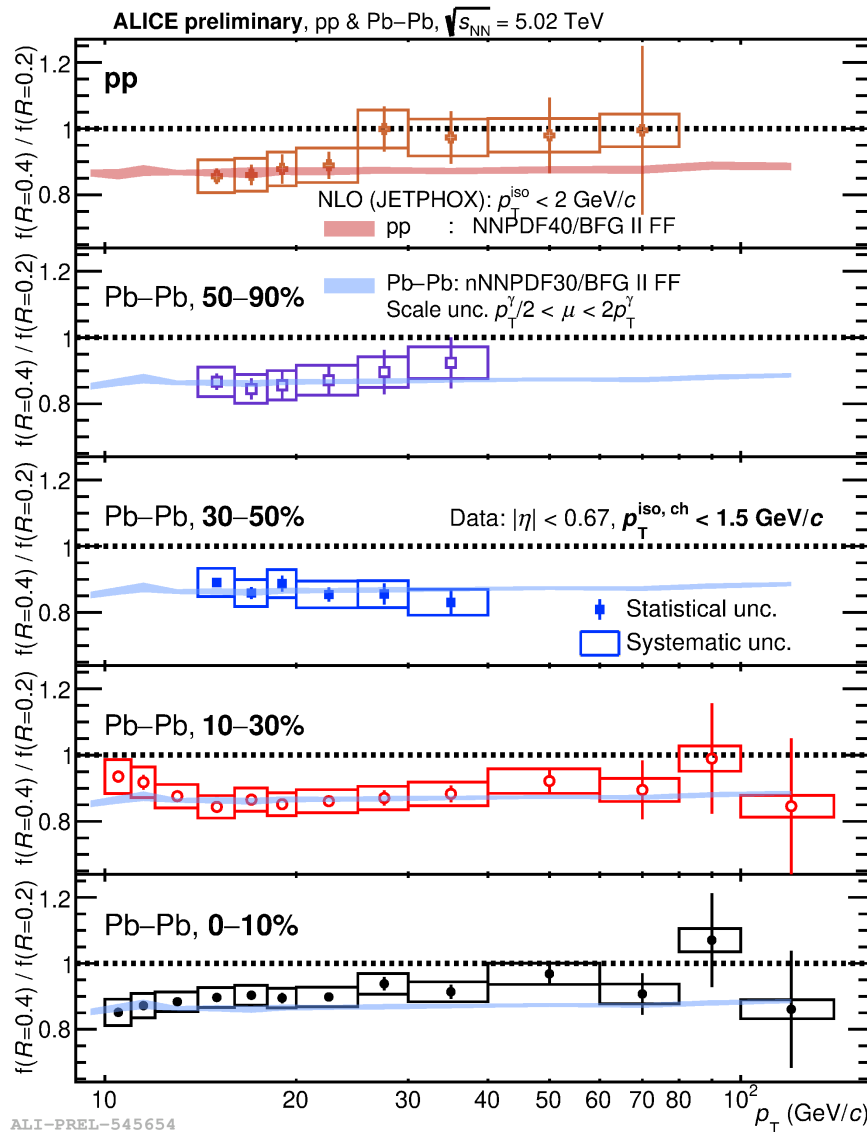


- NLO pQCD predictions (JETPHOX)
  - ➔ Note: Theory is centrality independent! only difference is PDF (pp) vs nPDF  $\times N_{coll}$  (Pb-Pb)
- Theory & data agreement for both  $R$  and coll. system within uncertainties



# Cross sections R ratios

$$\left. \frac{d^2\sigma}{dp_T d\eta} \right|_{(R=0.4)} / \left. \frac{d^2\sigma}{dp_T d\eta} \right|_{(R=0.2)}$$

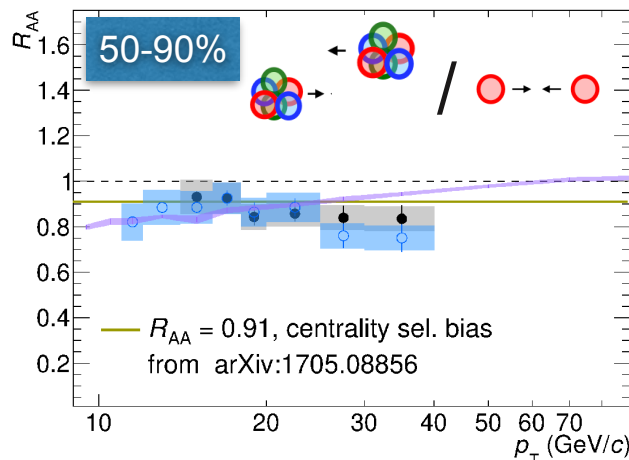
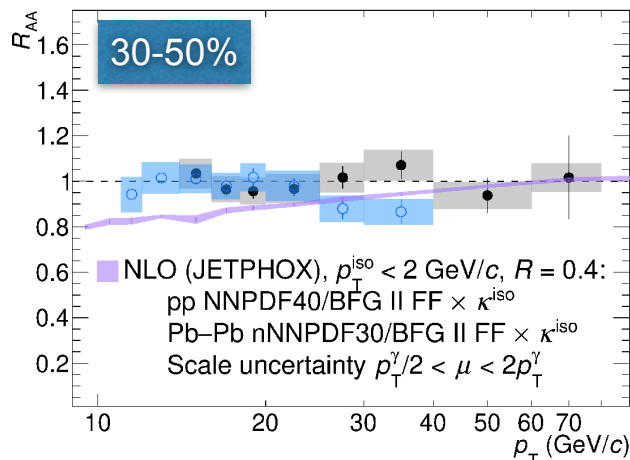
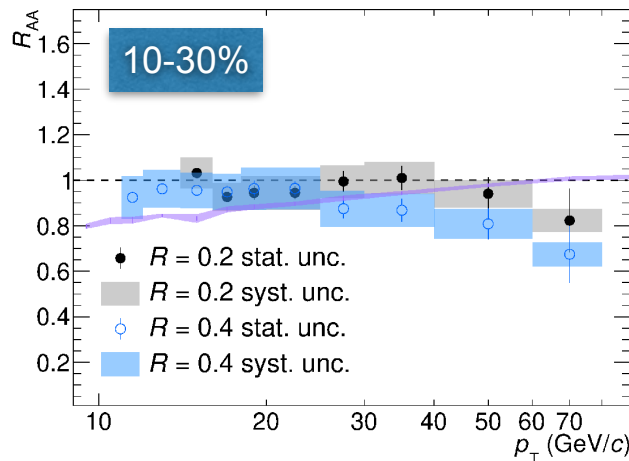
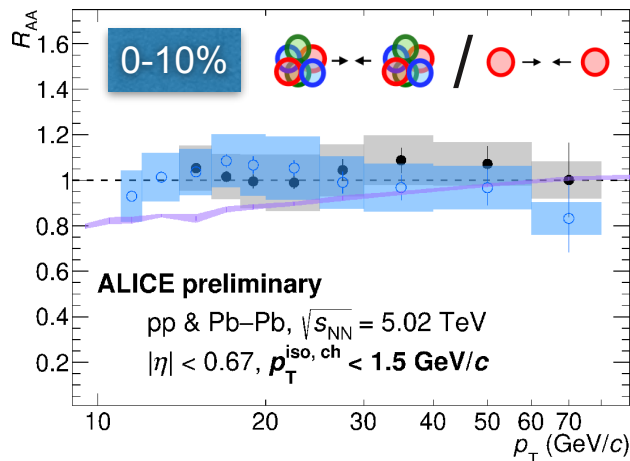


- Ratio sensitive to fraction of fragmentation  $\gamma$  surviving the isolation selection
  - ➔ Interesting for theory models
- Quite good agreement with theory on all collision systems
  - Theory (NLO) seems to control the isolation mechanism in  $2 \rightarrow 2$  processes and the direct fragmentation & prompt  $\gamma$  production even in Pb-Pb
  - Same measurement done by ATLAS in pp collisions at 13 TeV for  $p_T > 250$  GeV/c shows a good agreement with pQCD with even smaller uncertainties than theory: [JHEP 2023 \(2023\) 86](#) [arXiv:2302.00510](#) (back-up)



# Nuclear modification factor $R_{AA}$ , $R = 0.2$ & $0.4$

$$R_{AA} = \frac{1}{N_{\text{coll}}} \frac{d^2\sigma_{AA} / (dp_T d\eta)}{d^2\sigma_{pp} / (dp_T d\eta)}$$

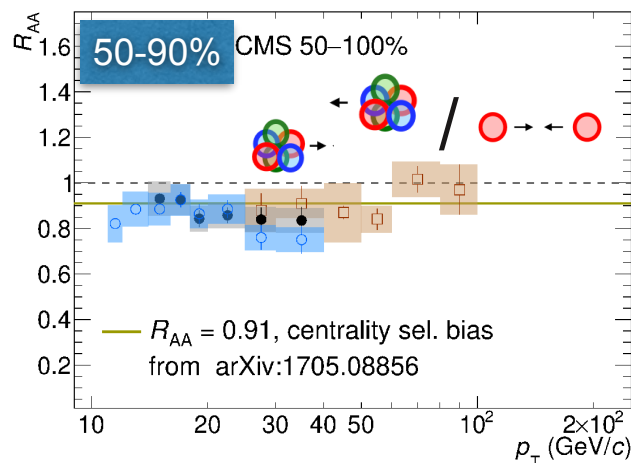
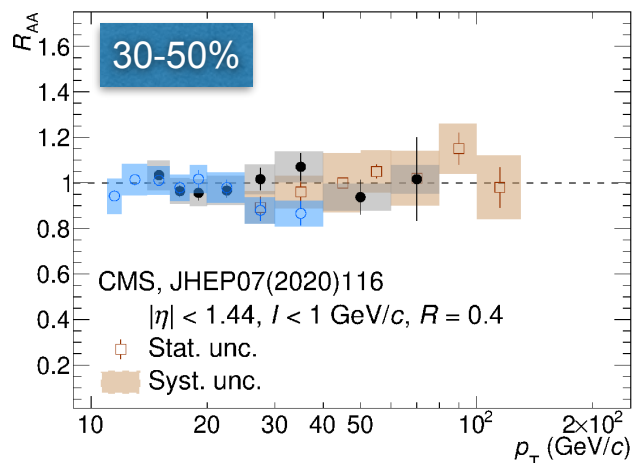
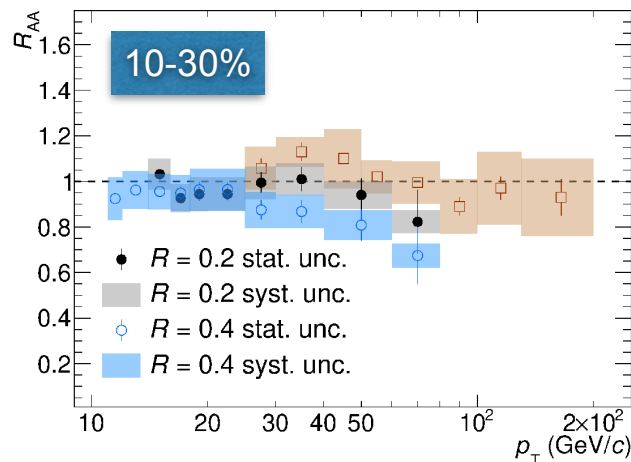
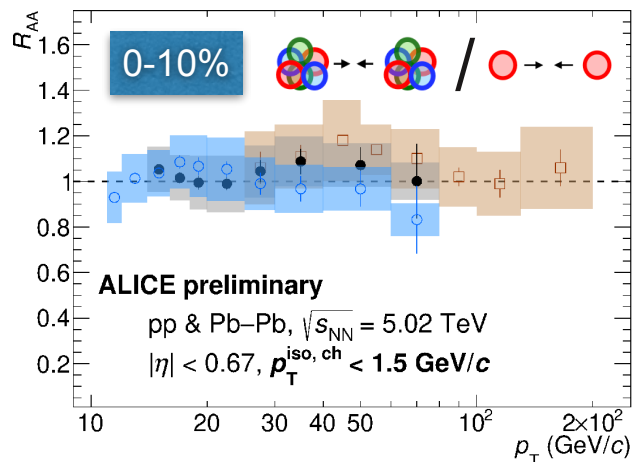


- **0-50%:**
  - ➔ Consistent with unity within the unc. for both  $R$
  - ❖ No modification of the prompt photon yield due to the QGP as expected
  - ➔ Agreement with NLO pQCD ratio above 20 GeV/c, a decrease is expected below due to PDF vs nPD
- **50-90%:**
  - ➔ Closer to 0.9 than 1 for both  $R$  likely due to centrality selection bias of Glauber model
  - ➔ Model by C. Loizides & A. Morsch expects a value of 0.91 ([arXiv:1705.08856](https://arxiv.org/abs/1705.08856))
  - ❖ In good agreement

ALI-PREL-545658

# Nuclear modification factor $R_{AA}$ , $R = 0.2$ & $0.4$

$$R_{AA} = \frac{1}{N_{\text{coll}}} \frac{d^2\sigma_{AA} / (dp_T d\eta)}{d^2\sigma_{pp} / (dp_T d\eta)}$$

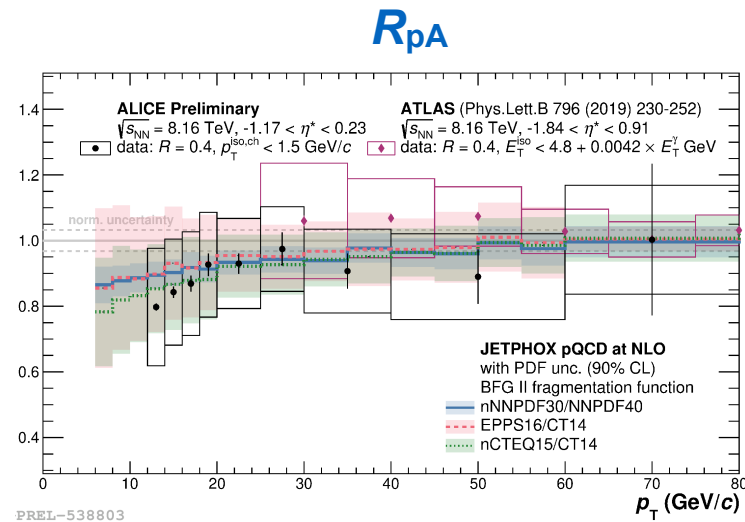
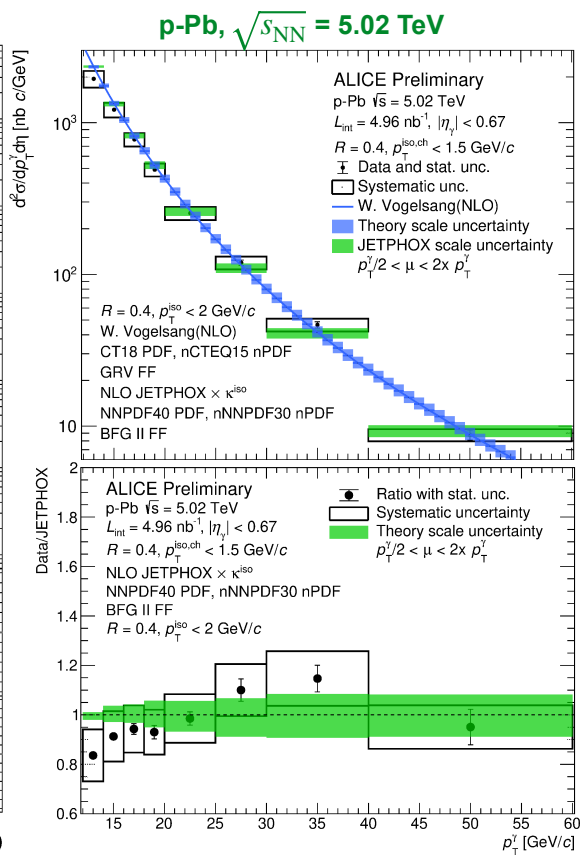
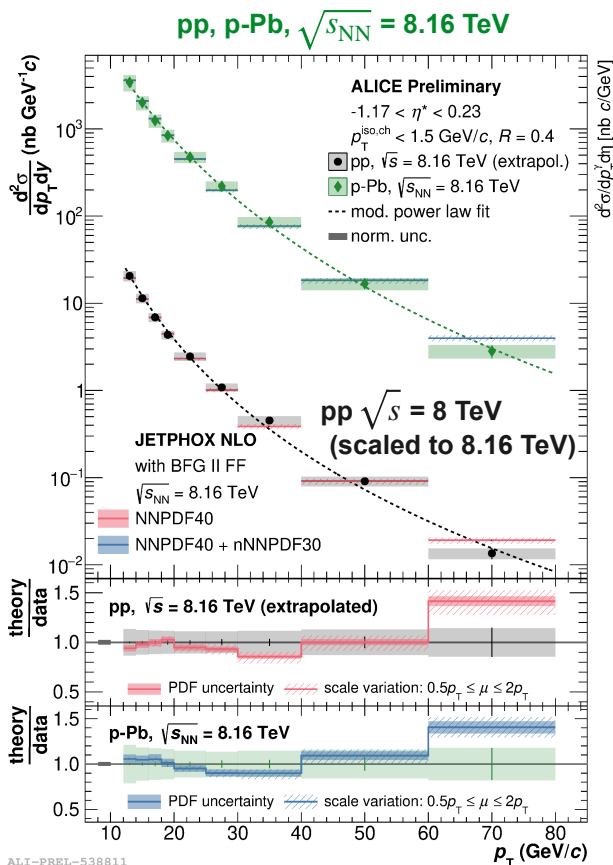


- **0-50%:**
  - ➔ Consistent with unity within the unc. for both  $R$
  - ❖ No modification of the prompt photon yield due to the QGP as expected
  - ➔ Agreement with NLO pQCD ratio above 20 GeV/c, a decrease is expected below due to PDF vs nPD
- **50-90%:**
  - ➔ Closer to 0.9 than 1 for both  $R$  likely due to centrality selection bias of Glauber model
  - ➔ Model by C. Loizides & A. Morsch expects a value of 0.91 ([arXiv:1705.08856](https://arxiv.org/abs/1705.08856))
  - ❖ In good agreement

- Agreement within the uncertainties with CMS in the overlapping region  $25 < p_T < 60$  GeV/c

ALI-PREL-545662

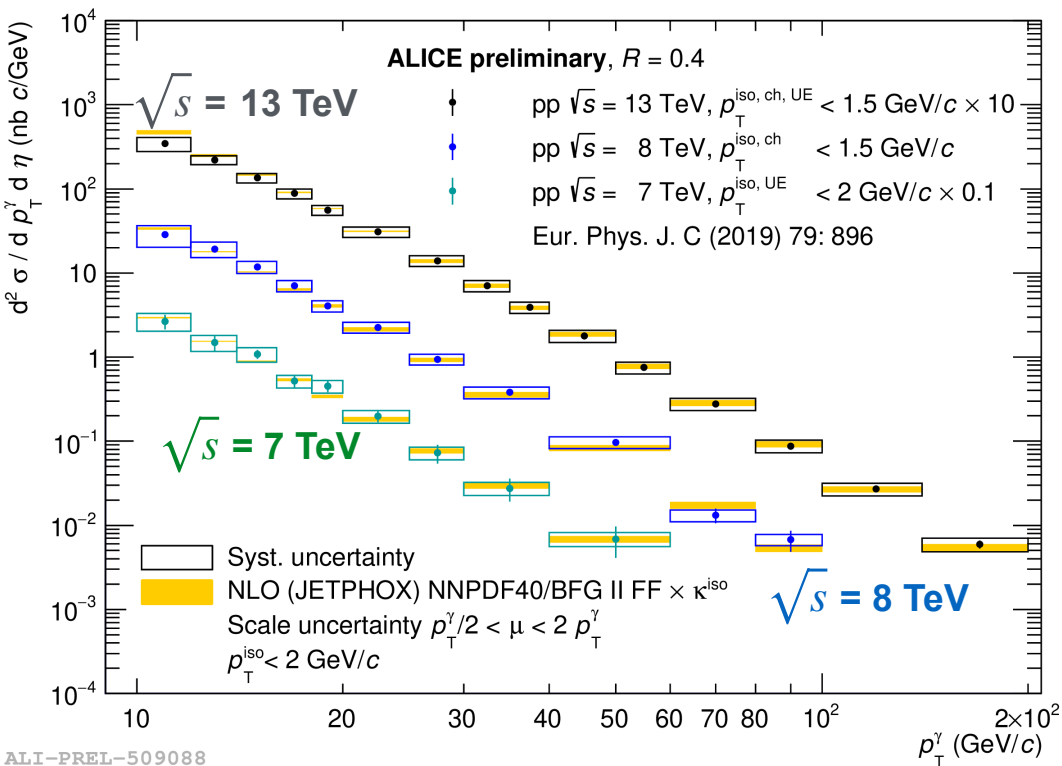
# Cross section in p-Pb col. with $R = 0.4$



Shown at HP 2023

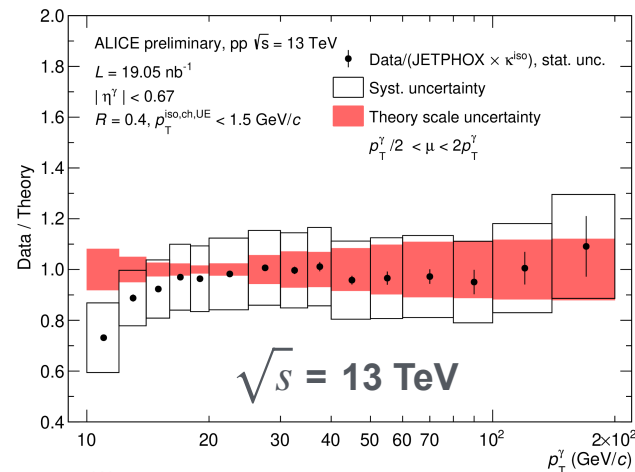
- NLO pQCD predictions (JETPHOX) and data agree
- $R_{p-Pb}$  in agreement with unity
  - Hints of lower than unity for  $p_T < 20$  GeV/c, expected in theory

# Cross section in pp col. and other $\sqrt{s}$ with $R = 0.4$

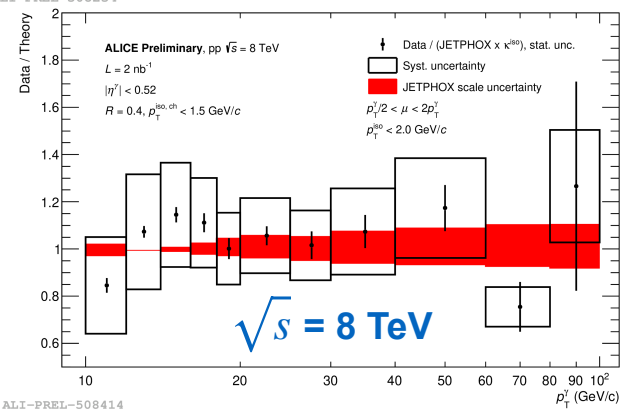


ALI-PREL-509088

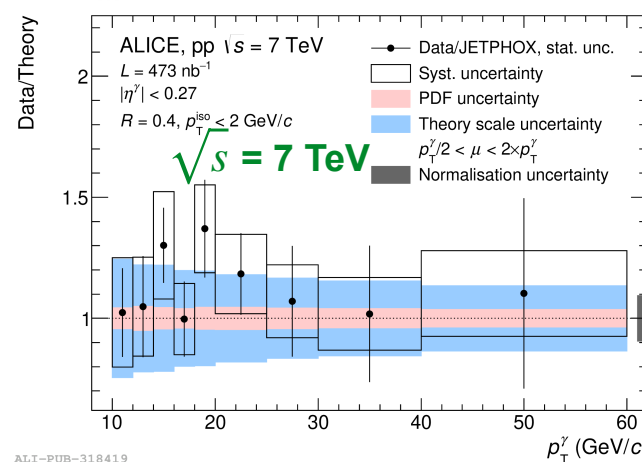
- NLO pQCD predictions (JETPHOX) and data agree measurement by Ran Xu @ LPSC & CCNU
  - $\sqrt{s} = 13 \text{ TeV}$  measurement by Ran Xu @ LPSC & CCNU, on arXiv in ~ a week!
    - Lower  $p_{\text{T}}$  &  $x_{\text{T}}$  than in preliminary
    - Lowest  $x_{\text{T}}$  LHC measurement at mid-rapidity
  - Strong involvement of LPSC on all ALICE isolated-photon measurements



ALI-PREL-508254

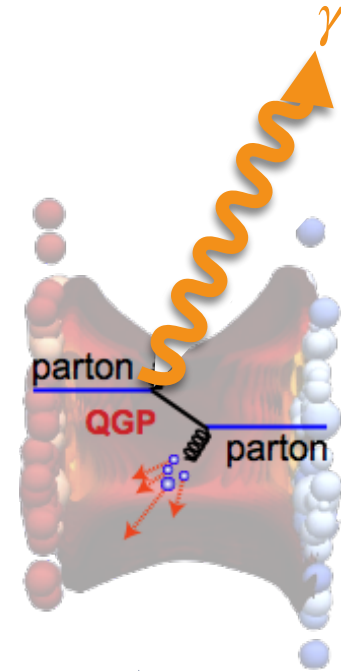


ALI-PREL-508414



ALI-PUB-318419

- Prompt  $\gamma$  associated to a parton emitted in opposite side
- Prompt  $\gamma$  measurement allow to **tag the parton initial energy**  
 $p_T^\gamma \simeq p_T^{\text{parton}}$ , before losing  $\Delta E$  in QGP
  - ➔ Aim: Measure FF modifications, where is the  $\Delta E$  radiated?



- Observables:

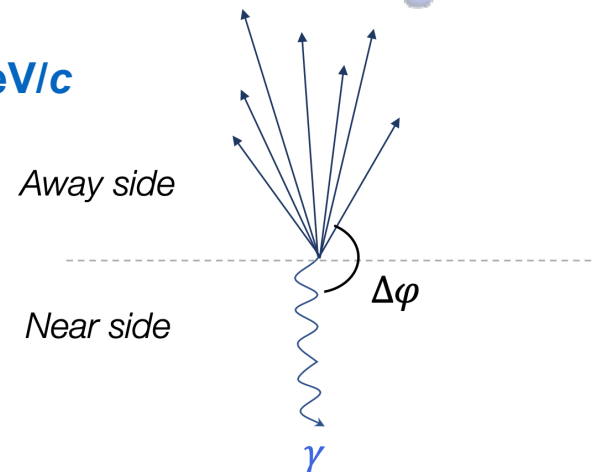
➔ Azimuthal correlation:  $\Delta\varphi = \varphi^{\text{trigger}} - \varphi^{\text{track}}$  with trigger isolated narrow or wide clusters,  **$R = 0.2$  &  $p_T^{\text{iso ch}} < 1.5 \text{ GeV}/c$**

➔ 
$$z_T = \frac{p_T^{\text{track}}}{p_T^{\text{trigger}}} \text{ and } D(z_T) = \frac{1}{N^{\text{trigger}}} \frac{d N^{\text{track}}}{d z_T}$$

for tracks in  $|\Delta\varphi| > 3/5\pi \text{ rad}$  (mirrored)

➔ **When trigger = prompt  $\gamma$ ,  $D(z_T)$  is a proxy for FF**

➔ Measurement:  $18 < p_T^{\text{trigger}} < 40 \text{ GeV}/c$  &  $p_T^{\text{track}} > 0.5 \text{ GeV}/c$



# Isolated $\gamma$ -hadron correlations in Pb-Pb: Azimuthal distribution

- UE in  $\Delta\phi$ : uncorrelated tracks shifting up the distribution
- UE subtraction with mixed event: artificial dataset created combining the trigger cluster with tracks on different MB collisions

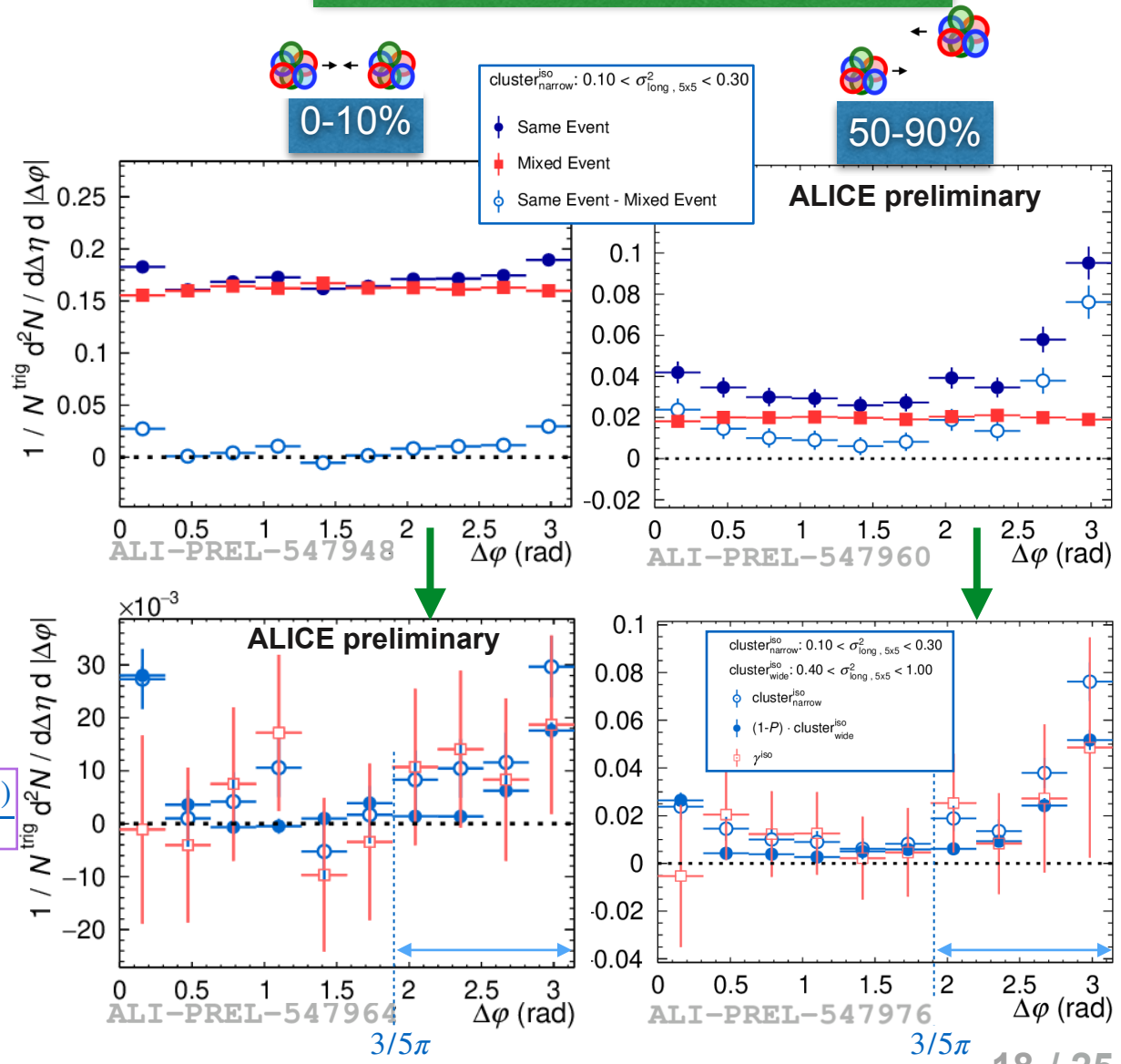


- Purity  $< 1$ , considering  $f(\Delta\phi^{\text{cls}_{\text{narrow}}^{\text{iso}}}) \text{ bkg} = f(\Delta\phi^{\text{cls}_{\text{wide}}^{\text{iso}}})$ :

$$f(\Delta\phi^{\gamma^{\text{iso}}}) = \frac{f(\Delta\phi^{\text{cls}_{\text{narrow}}^{\text{iso}}}) - (1 - P) \cdot f(\Delta\phi^{\text{cls}_{\text{wide}}^{\text{iso}}})}{P}$$

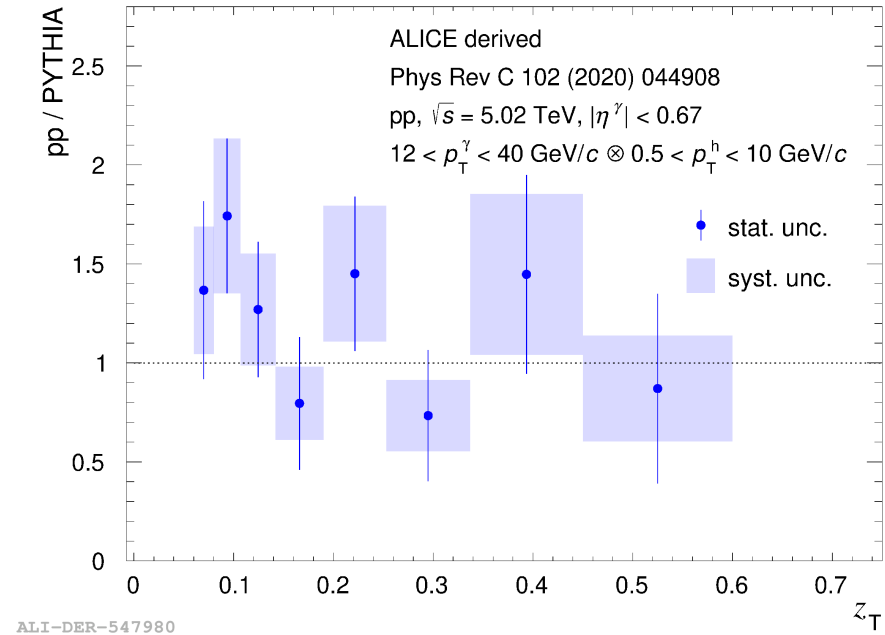
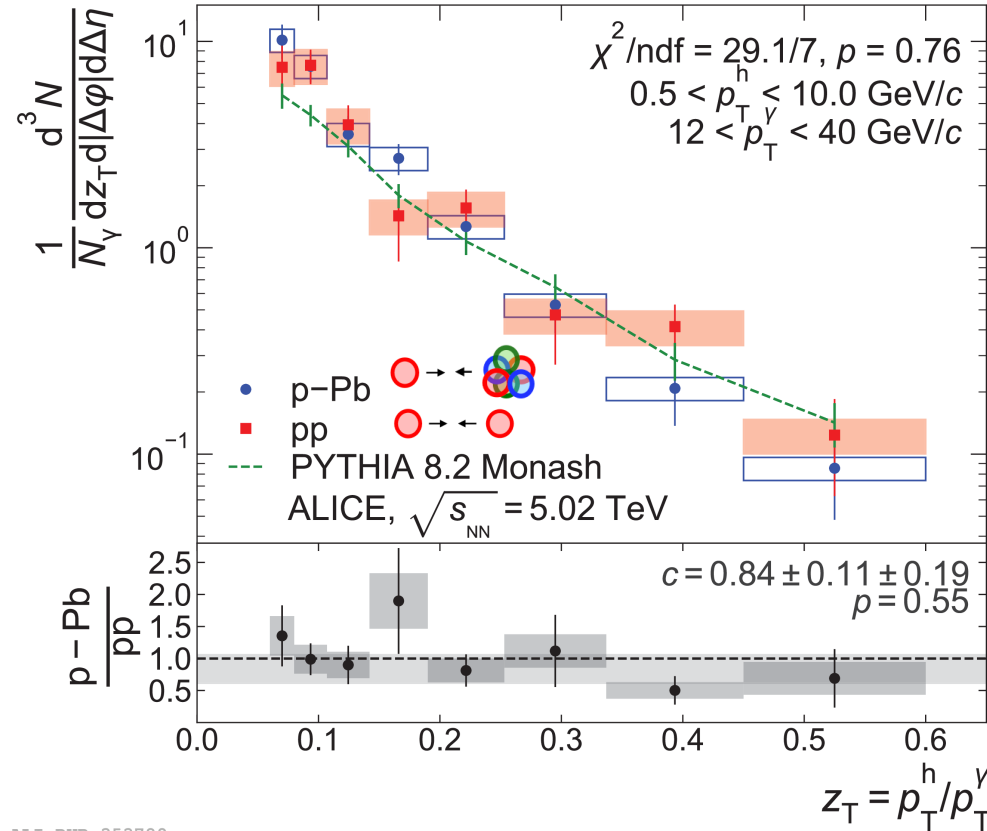
→  $D(z_T)$ : Integrate  $f(\Delta\phi^{\gamma^{\text{iso}}})$  in  $3/5\pi < |\Delta\phi| < \pi$  rad

20 <  $p_T$  < 25 GeV/c & 0.2 <  $z_T$  < 0.3

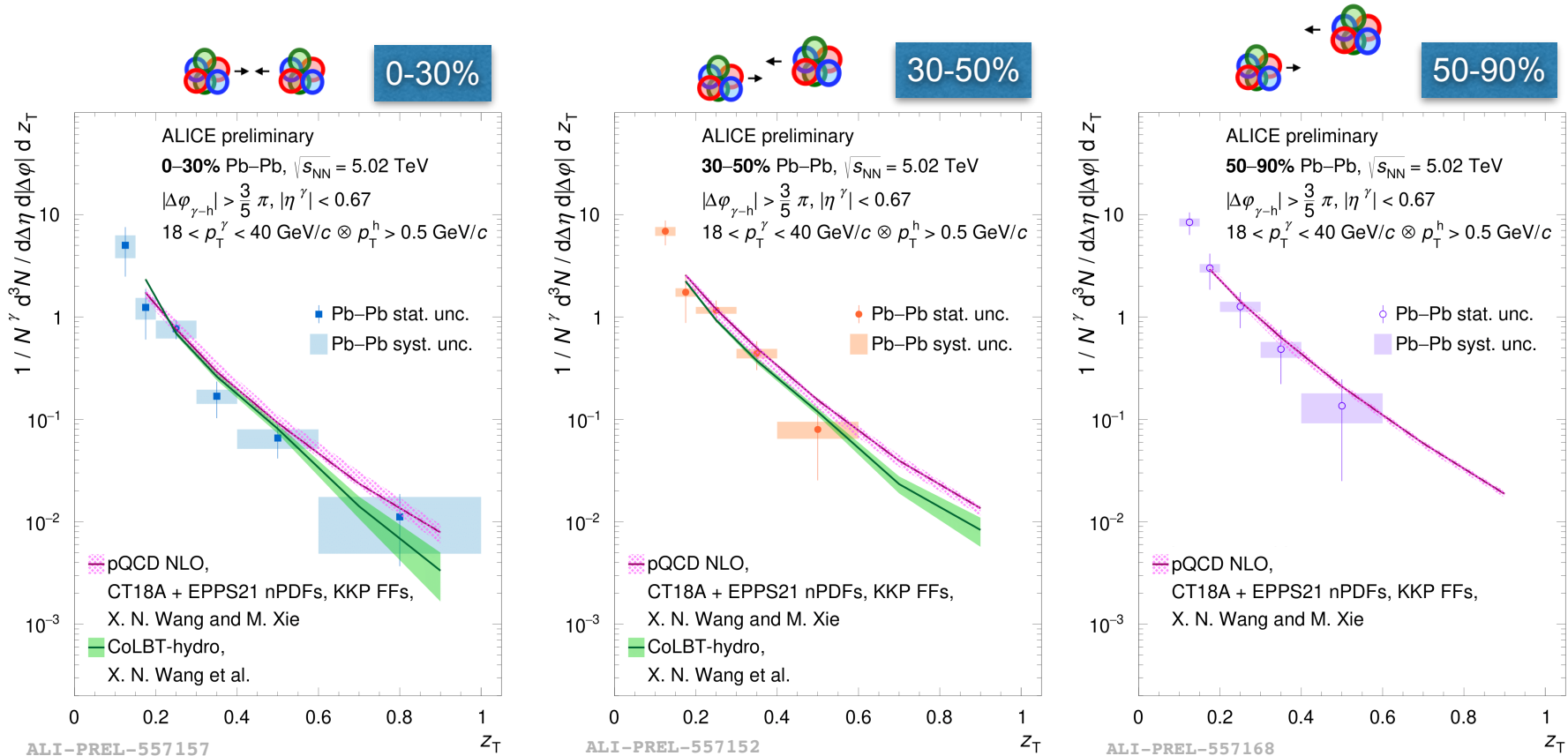


# Isolated $\gamma$ -hadron correlations in p-Pb & pp: $D(z_T)$

Phys Rev C 102 (2020) 044908



- Previous published results in p-Pb and pp collisions
  - ➔ Agreement between systems and with PYTHIA
- Note: Pb-Pb collisions measurement done in different  $p_T$  ranges and is compared directly to pQCD predictions



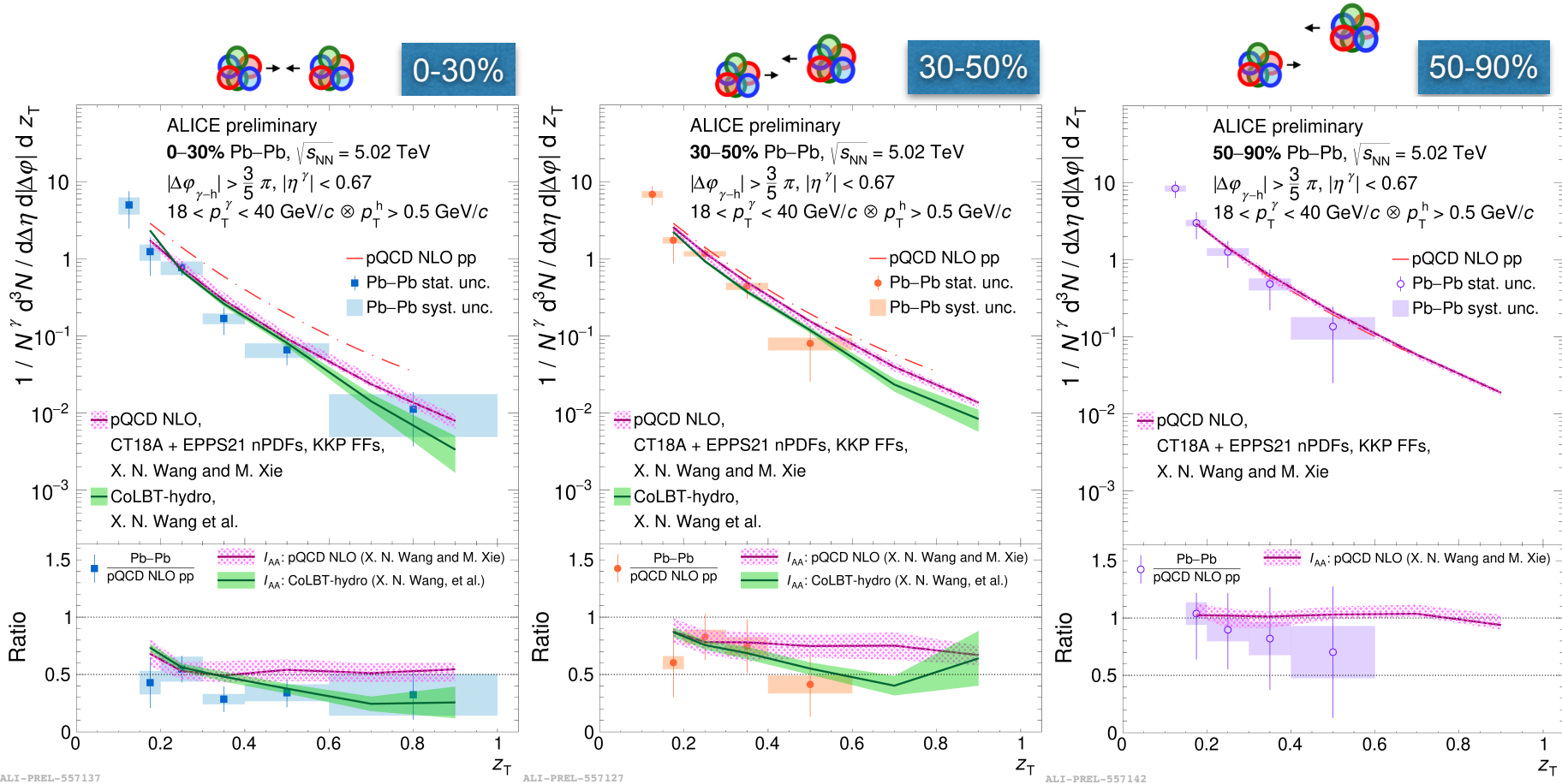
- Pb–Pb data compared with theory: **NLO pQCD** and **CoLBT (0-50% only)**

➔ There seems to be an agreement with both models

➔ Discrimination not possible yet

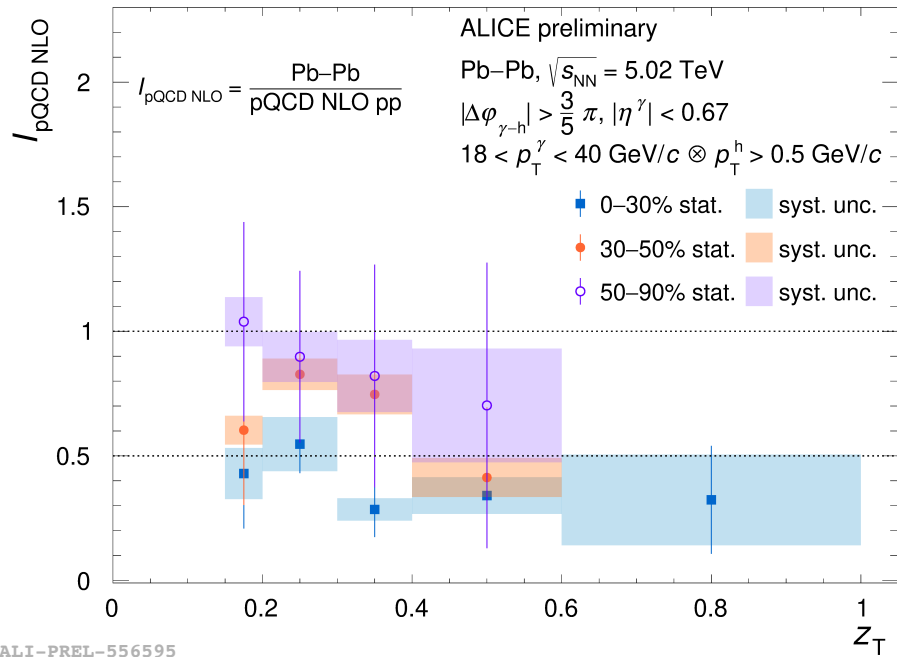
- [Phys. Rev. C 103, 034911](#), Xie, Wang and Zhang,
- [Phys. Rev. Lett. 103, 032302](#), Xie, Wang and Zhang
- [Phys. Lett. B 777 \(2018\) 86-90](#), Chen et al.





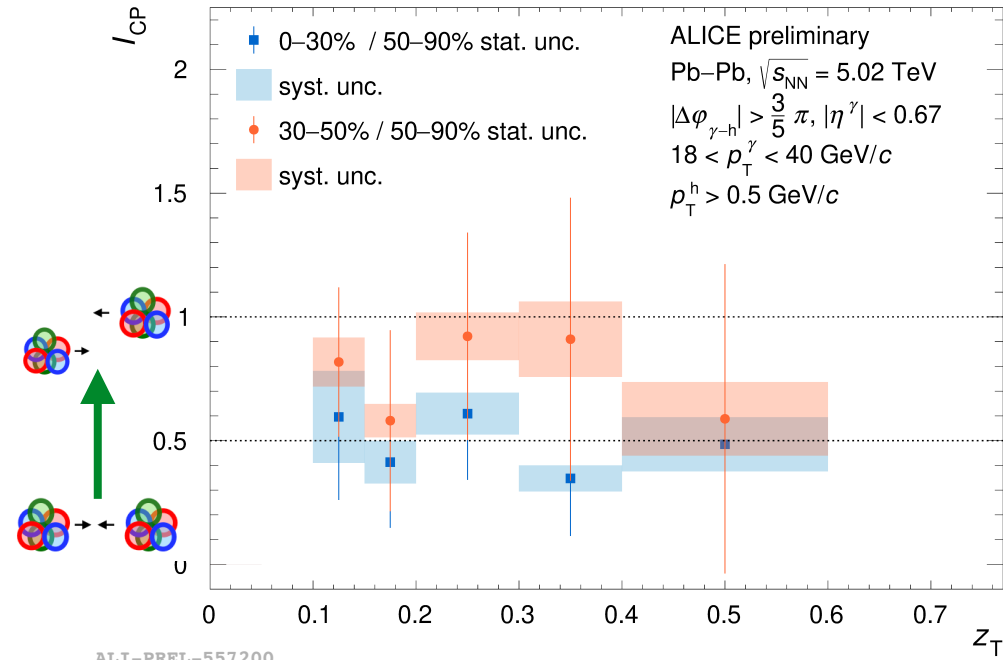
- Ratio with respect to NLO pQCD pp collision simulation  $\rightarrow$  sort of  $I_{AA} = \frac{D(z_T)_{\text{Pb-Pb}}}{D(z_T)_{\text{pp}}}$
- Clear modifications in data with respect to NLO pQCD pp simulation
- Comparison with  $I_{AA}$  from NLO pQCD and CoLBT models  $\rightarrow$  agreement

$$I_{\text{pQCD}} = \text{Pb–Pb Data} / \text{pp pQCD}$$



ALI-PREL-556595

$$I_{\text{CP}} = \text{Pb–Pb (semi) central} / \text{peripheral}$$

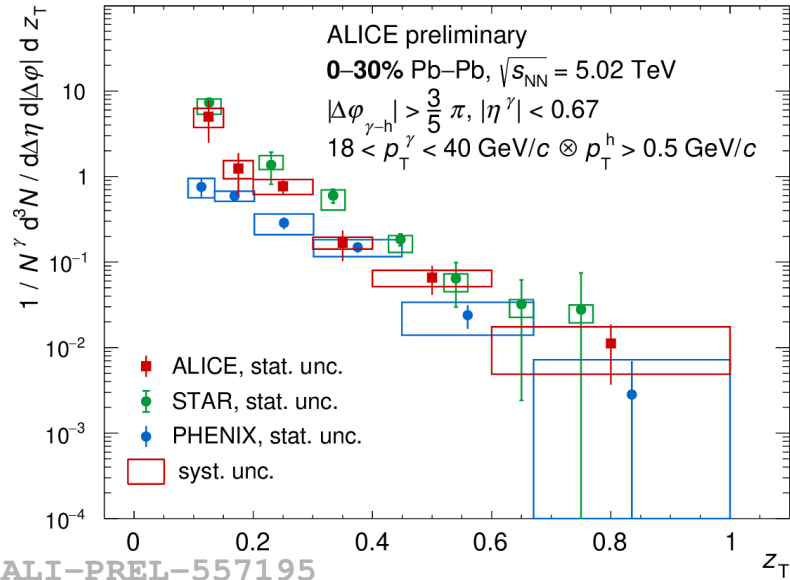
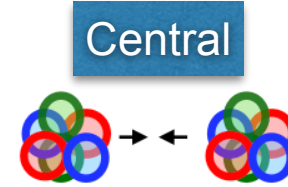


ALI-PREL-557200

- Ordering between centralities, central more suppressed than peripheral
- Hints of less suppression at lower  $z_T$  in  $I_{\text{pQCD}}$

# Isolated $\gamma$ -hadron correlations in Pb–Pb: RHIC & LHC

C. Arata thesis



STAR, Phys.Lett.B 760 (2016) 689-696

0–12% Au–Au,  $\sqrt{s_{NN}} = 200$  GeV

$|\Delta\phi_{\gamma-h} - \pi| \leq 1.4$

$12 < p_T^\gamma < 20$  GeV/c  $\otimes p_T^h > 1.2$  GeV/c

PHENIX, PRL 111, 032301 (2013)

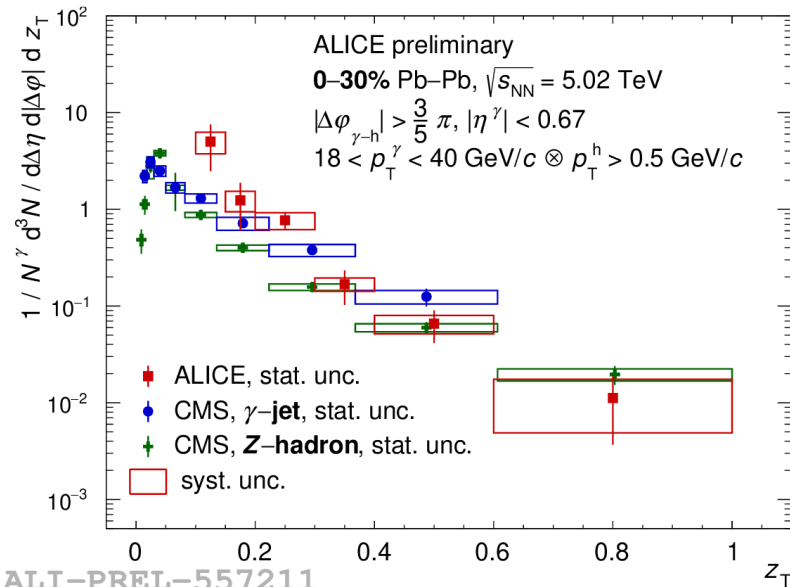
0–40% Au–Au,  $\sqrt{s_{NN}} = 200$  GeV

$|\Delta\phi_{\gamma-h} - \pi| < \pi/2$ ,  $|y| < 0.35$

$5 < p_T^\gamma < 9$  GeV/c  $\otimes 0.5 < p_T^h < 7$  GeV/c

- Similar behaviour as observed at RHIC and LHC experiments

➔ Note: not completely apples-to-apples comparisons!



CMS, Phys.Rev.Lett. 121 (2018) 24, 242301, 2018

$\gamma$ -jet, 0–10%

anti- $k_T$  jet R = 0.3,  $p_T^{\text{jet}} > 30$  GeV/c,  $|\eta^{\text{jet}}| < 1.6$

$|\Delta\phi_{\gamma\text{-jet}}| > \frac{7}{8}\pi$ ,  $|\eta^\gamma| < 1.44$ ,  $p_T^\gamma > 60$  GeV/c  $\otimes p_T^h > 1$  GeV/c

CMS, Phys.Rev.Lett. 128 (2022) 12, 122301, 2022

Z-hadron, 0–30%

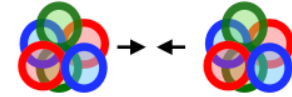
$|\Delta\phi_{Z-h}| > \frac{7}{8}\pi$ ,  $p_T^Z > 30$  GeV/c  $\otimes p_T^h > 1$  GeV/c

ALI-PREL-557211

# Isolated $\gamma$ -hadron correlations in Pb–Pb: RHIC & LHC

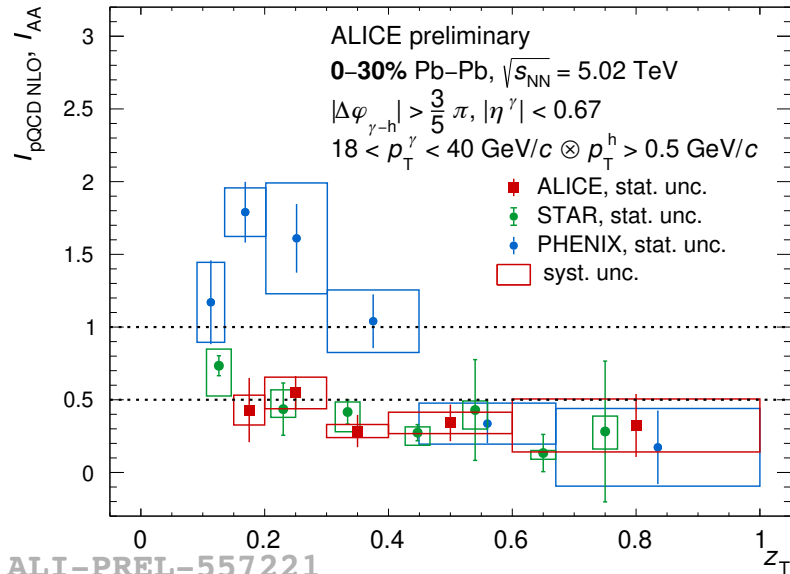
C. Arata thesis

Central

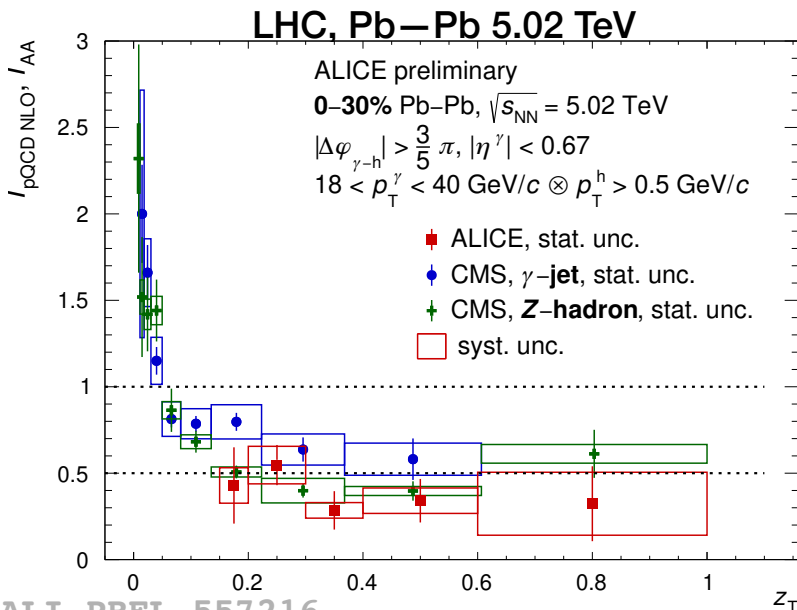


$$I_{AA}(z_T) = \frac{D(z_T, \text{Pb} - \text{Pb})}{D(z_T, \text{pp})}$$

- Similar behaviour as observed at RHIC and LHC experiments
- ➔ Note: not completely apples-to-apples comparisons!



ALI-PREL-557221



ALI-PREL-557216

STAR, Phys.Lett.B 760 (2016) 689-696

0-12% Au–Au,  $\sqrt{s_{NN}} = 200$  GeV

$|\Delta\varphi_{\gamma-h} - \pi| \leq 1.4$

$12 < p_T^\gamma < 20$  GeV/c  $\otimes$   $p_T^h > 1.2$  GeV/c

PHENIX, PRL 111, 032301 (2013)

0-40% Au–Au,  $\sqrt{s_{NN}} = 200$  GeV

$|\Delta\varphi_{\gamma-h} - \pi| < \pi/2$ ,  $|y| < 0.35$

$5 < p_T^\gamma < 9$  GeV/c  $\otimes$   $0.5 < p_T^h < 7$  GeV/c

CMS, Phys.Rev.Lett. 121 (2018) 242301, 2018

$\gamma$ -jet, 0-10%

anti- $k_T$  jet  $R = 0.3$ ,  $p_T^{\text{jet}} > 30$  GeV/c,  $|\eta^{\text{jet}}| < 1.6$

$|\Delta\varphi_{\gamma\text{-jet}}| > \frac{7}{8}\pi$ ,  $|\eta^\gamma| < 1.44$ ,  $p_T^\gamma > 60$  GeV/c  $\otimes$   $p_T^h > 1$  GeV/c

CMS, Phys.Rev.Lett. 128 (2022) 122301, 2022

Z-hadron, 0-30%

$|\Delta\varphi_{Z-h}| > \frac{7}{8}\pi$ ,  $p_T^Z > 30$  GeV/c  $\otimes$   $p_T^h > 1$  GeV/c

# Summary

## Isolated $\gamma$ , pp & Pb–Pb $\sqrt{s_{\text{NN}}} = 5.02 \text{ TeV}$

Various analyses on isolated photon in pp and p-Pb have been released or published during the last years:

- *the results in Pb–Pb were the last missing step*

### ➔ Cross section, with $R = 0.4$ (std) & $0.2$ (new)

- Spectra &  $R$  ratio agreement with pQCD
- 0-50% col.:  $R_{AA} \simeq 1$ , no  $\gamma$  suppression
- 50-90% col.:  $R_{AA} \simeq 0.9$ , expected bias of Glauber model in centrality selection
- $R_{AA}$ : agreement with CMS, tension with pQCD nPDF / PDF (0-100%) at low  $p_T$

### ➔ $\gamma$ –hadron correlations, Pb–Pb $\sqrt{s_{\text{NN}}} = 5.02 \text{ TeV}$ → C. Arata thesis

- Very statistically limited, challenging!
- FF modification stronger for central compared to peripheral collisions
- Results described by models, but discrimination not possible yet

Stay tuned for the final publications in the coming weeks (pp at  $\sqrt{s_{\text{NN}}} = 13 \text{ TeV}$ ) and months (Pb–Pb and p–Pb)!

# BACK-UP

# $\gamma$ measurement in ALICE

- $\gamma$  measurement

- $\rightarrow$  Calorimeters

- EMCal: Pb/scintillator towers ( $6 \times 6$  cm)

- 4.4 m from interaction point (IP)
- $|\eta| < 0.67$  for  $\Delta\varphi = 107^\circ$ ,  
 $0.22 < |\eta| < 0.67$  for  $\Delta\varphi = 60^\circ$  (DCal);
- Identification via EM shower dispersion selection
- $E_\gamma > 700$  MeV

- PHOS:  $\text{PWO}_4$  crystals ( $2.2 \times 2.2$  cm)

- 4.6 m from IP
- $|\eta| < 0.13$  for  $\Delta\varphi = 70^\circ$
- Identification via EM shower dispersion selection
- $E_\gamma > 200$  MeV

- $\rightarrow$  Tracking, TPC & ITS

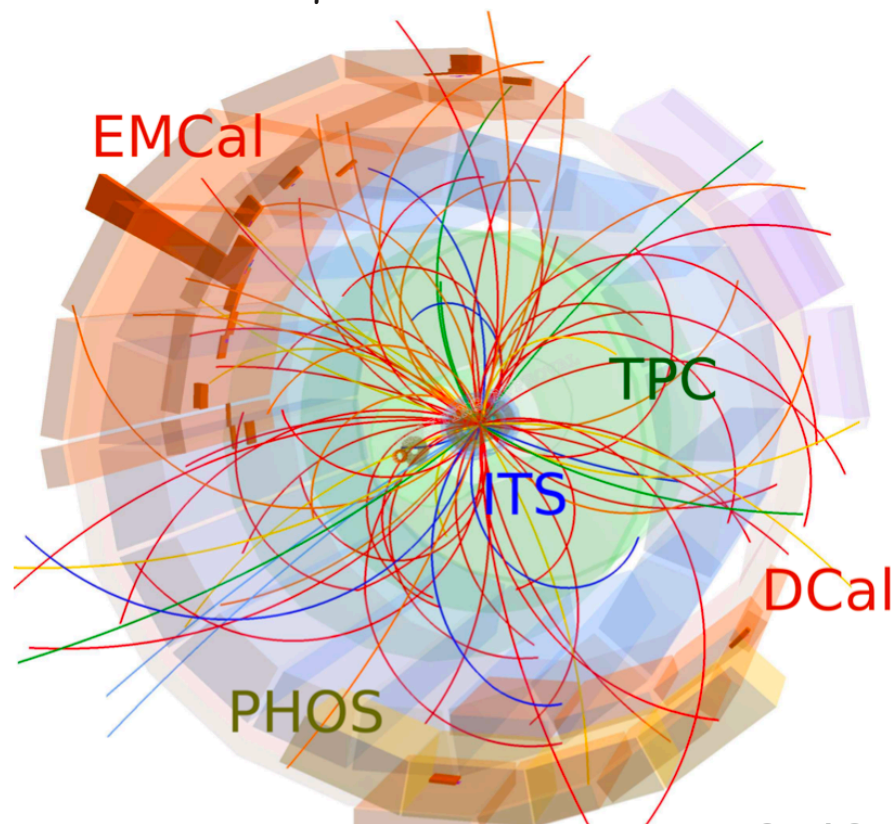
- $\gamma$  conversion method (PCM)

- $R < 180$  cm
- 8% conversion probability
- $|\eta| < 0.9$  for  $\Delta\varphi = 360^\circ$
- $E_\gamma > 100$  MeV

- $\gamma$  identification combining tracking+calorimeter

- $\rightarrow$  Inclusive  $\gamma$ : Charged particle veto

- $\rightarrow$  Prompt  $\gamma$ : Isolation (next slides)



# Direct prompt $\gamma$ measurement with EMCal:

## Isolated $\gamma$

New ALICE results shown today for the first time, LHC Run 2 at  $\sqrt{s_{NN}} = 5.02$  TeV:

- ▶ Isolated  $\gamma$  cross section in pp & Pb–Pb collisions
- ▶ Isolated  $\gamma$ -hadron correlations in Pb–Pb collisions

□ Calorimeter: EMCal

□ Tracking:

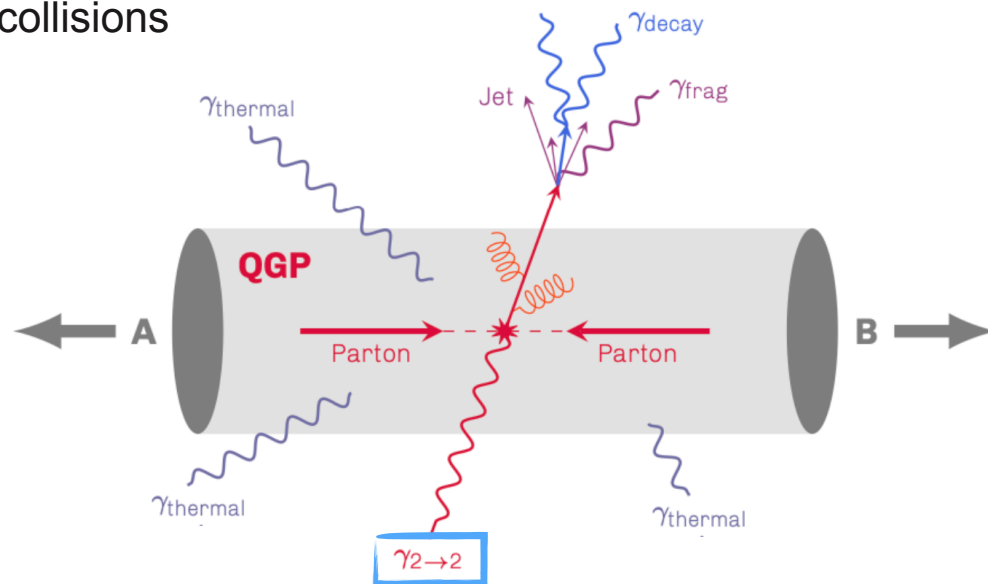
- ✱ Pb–Pb, TPC+ITS tracks
- ✱ pp, ITS-only tracks

□ Simulation: PYTHIA pp events randomly embedded in Pb–Pb Minimum bias (MB) data

□ Triggers: MB & EMCal L1- $\gamma$  trigger at  $E_{\text{threshold}} = 12$  (Pb–Pb) and 4 (pp) GeV

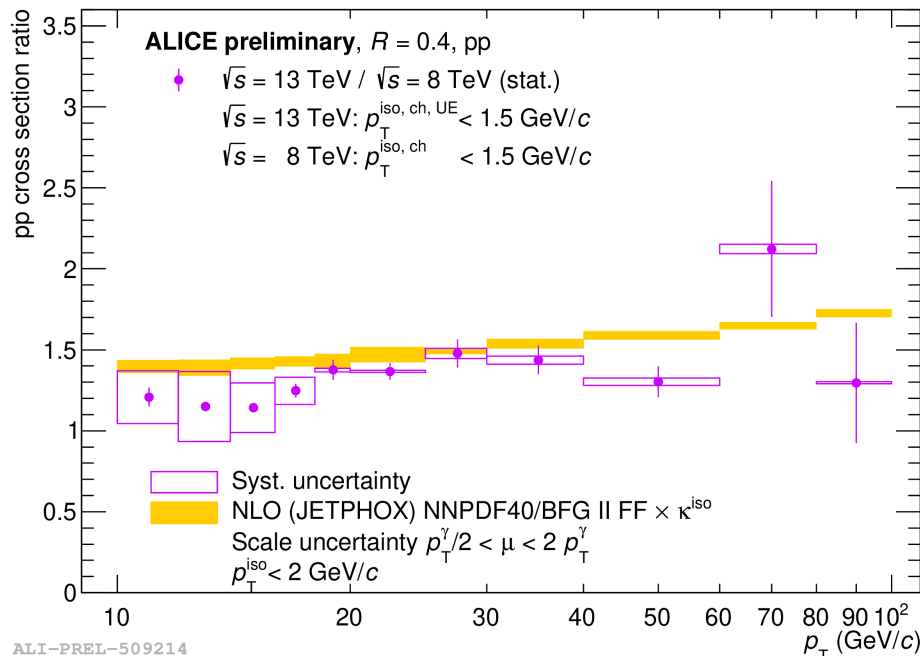
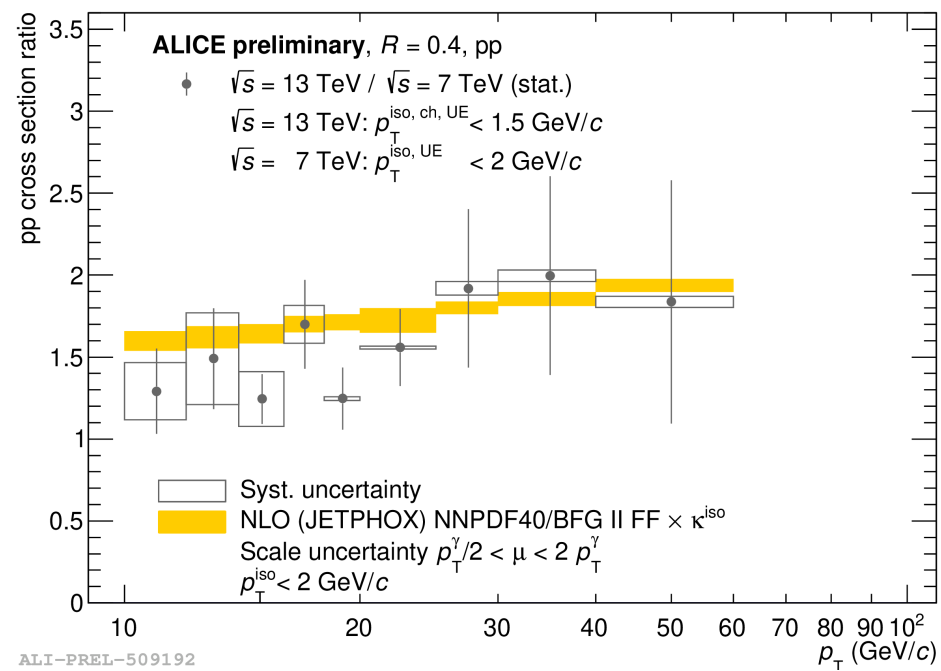
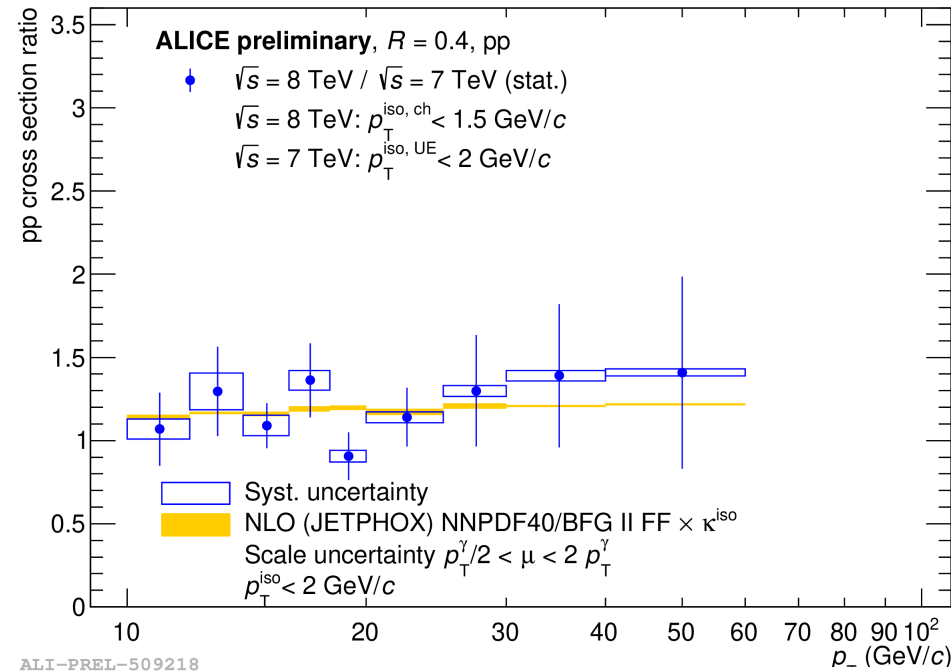
✱ Pb–Pb,  $L_{\text{int}} = 18 \text{ nb}^{-1}$ ; pp  $L_{\text{int}} = 245 \text{ nb}^{-1}$

✱ Pb–Pb centrality bins: **0-10%, 10-30%, 30-50%, 50-90%**



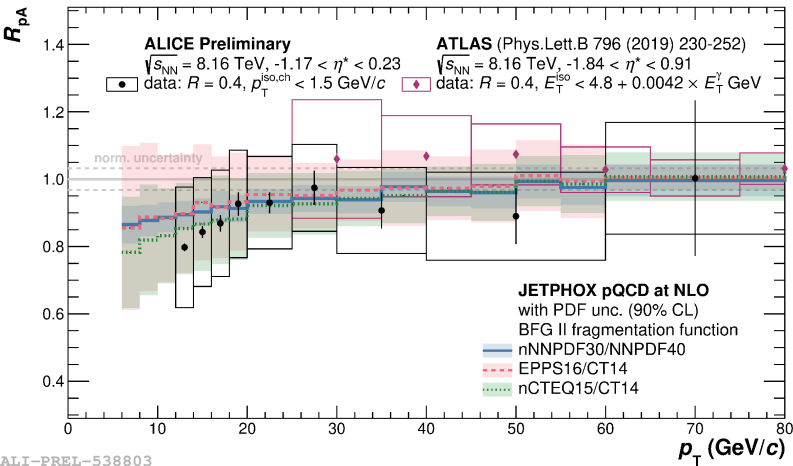


# Isolated $\gamma$ in pp collisions

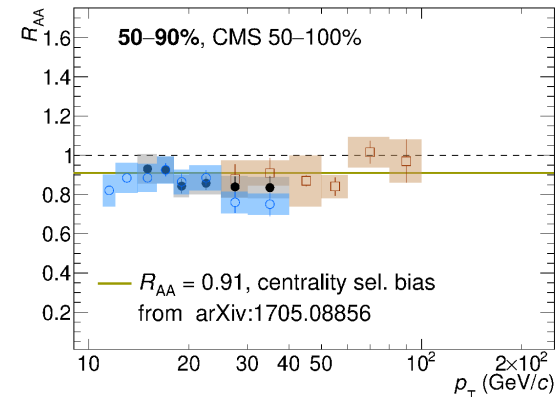
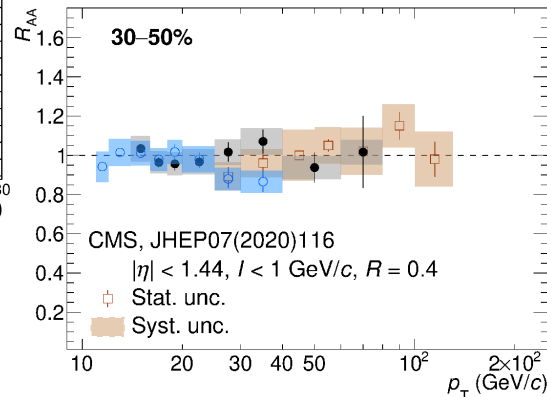
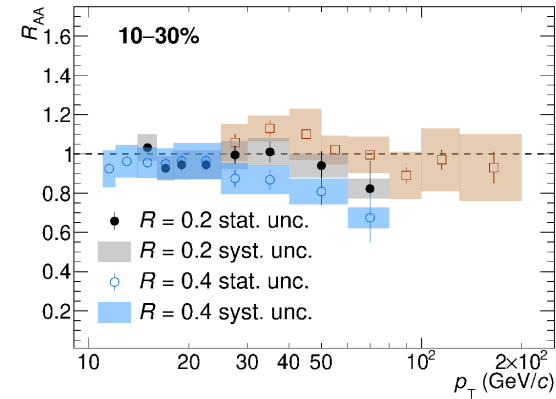
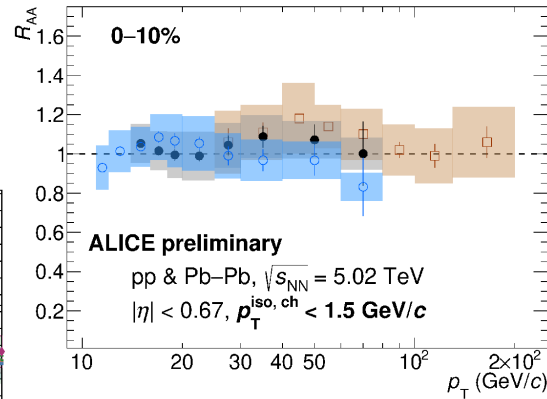


# Isolated $\gamma$ $R_{AA}$ & $R_{pA}$

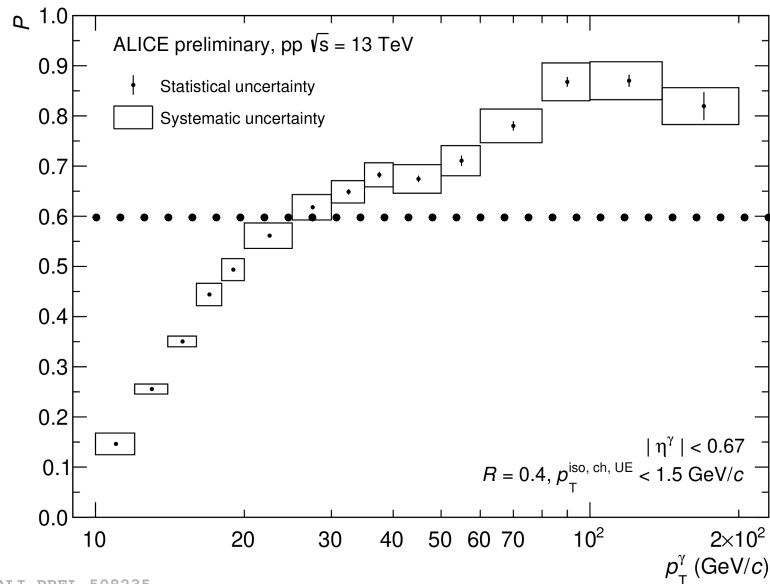
p-Pb / pp



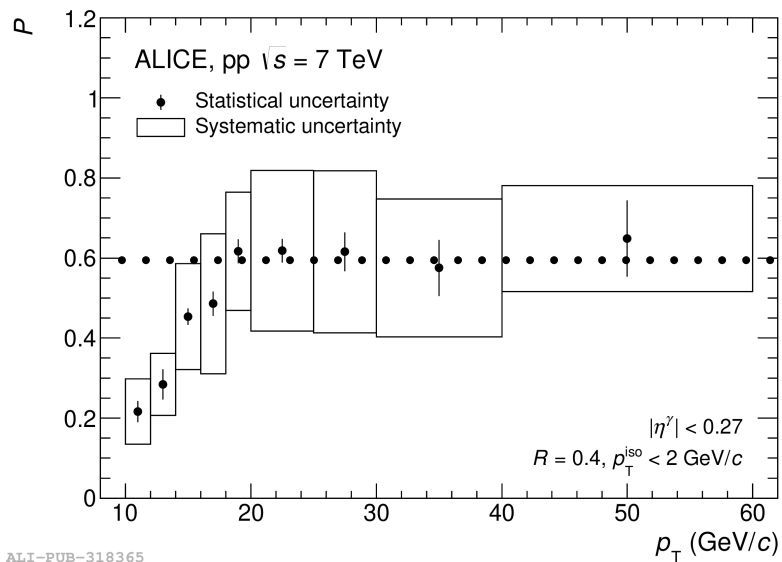
Pb-Pb / pp



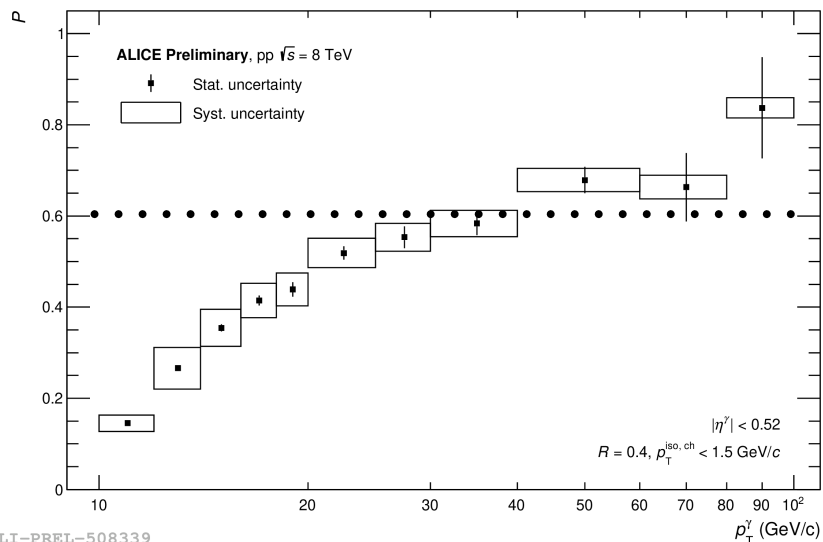
# Isolated $\gamma$ purity in pp & p-Pb collisions



ALI-PREL-508235

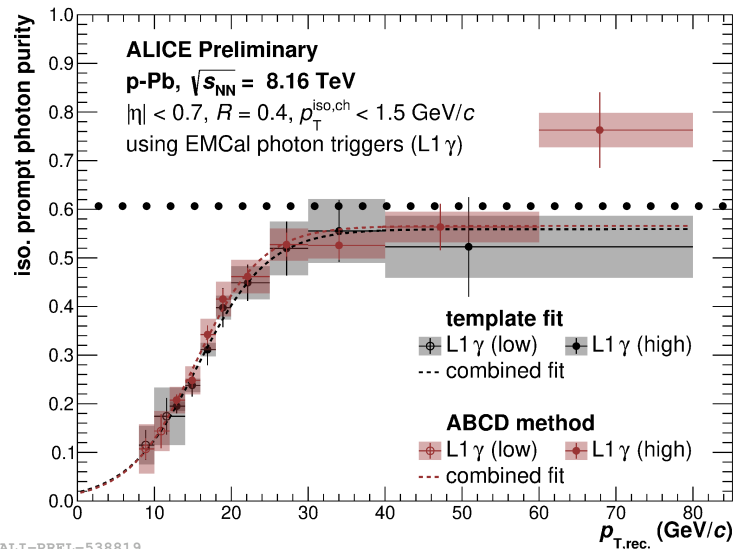


ALI-PUB-318365



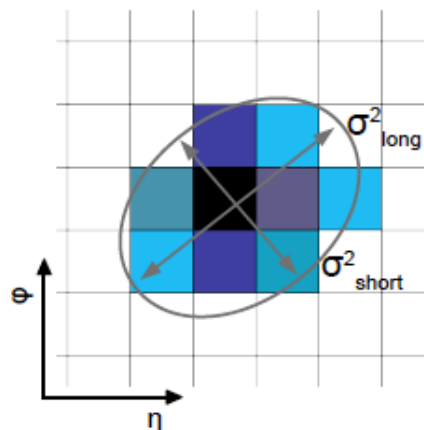
ALI-PREL-508339

FCPPN/L | 13/06/24 | G. Conesa Balbastre



ALI-PREL-538819

# EMCal cluster shower lateral dispersion parameter



- Shower shape parameter  $\sigma^2_{\text{long}}$  is related to the longer axis of the cluster ellipse
- Parameter depends on cluster cells location and its energy

$$\sigma_{\alpha\beta}^2 = \sum_i \frac{w_i \alpha_i \beta_i}{w_{\text{tot}}} - \sum_i \frac{w_i \alpha_i}{w_{\text{tot}}} \sum_i \frac{w_i \beta_i}{w_{\text{tot}}}$$

$$w_i = \text{Maximum}(0, w_0 + \ln(E_{\text{cell}, i}/E))$$

$$w_{\text{tot}} = \sum_i w_i$$

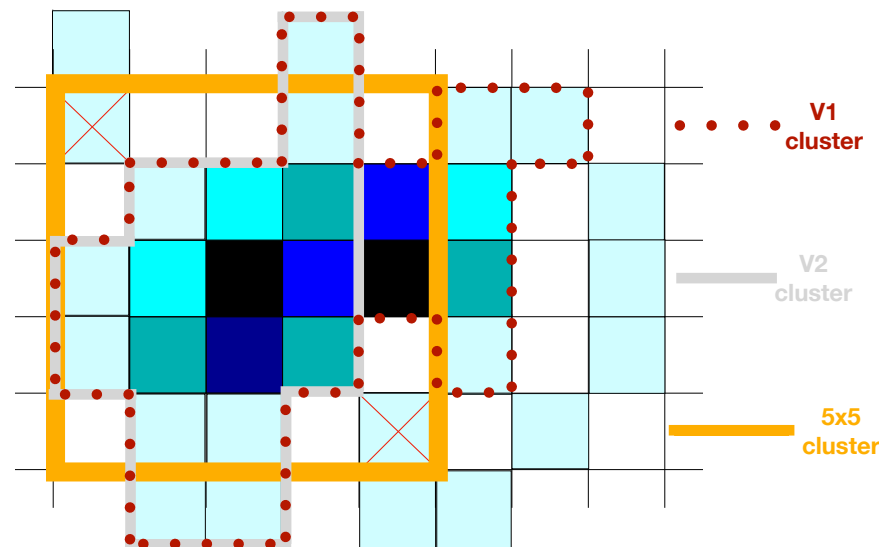
$$\sigma_{\text{long}}^2 = 0.5(\sigma_{\phi\phi}^2 + \sigma_{\eta\eta}^2) + \sqrt{0.25(\sigma_{\phi\phi}^2 - \sigma_{\eta\eta}^2)^2 + \sigma_{\eta\phi}^2},$$

$$\sigma_{\text{short}}^2 = 0.5(\sigma_{\phi\phi}^2 + \sigma_{\eta\eta}^2) - \sqrt{0.25(\sigma_{\phi\phi}^2 - \sigma_{\eta\eta}^2)^2 + \sigma_{\eta\phi}^2},$$

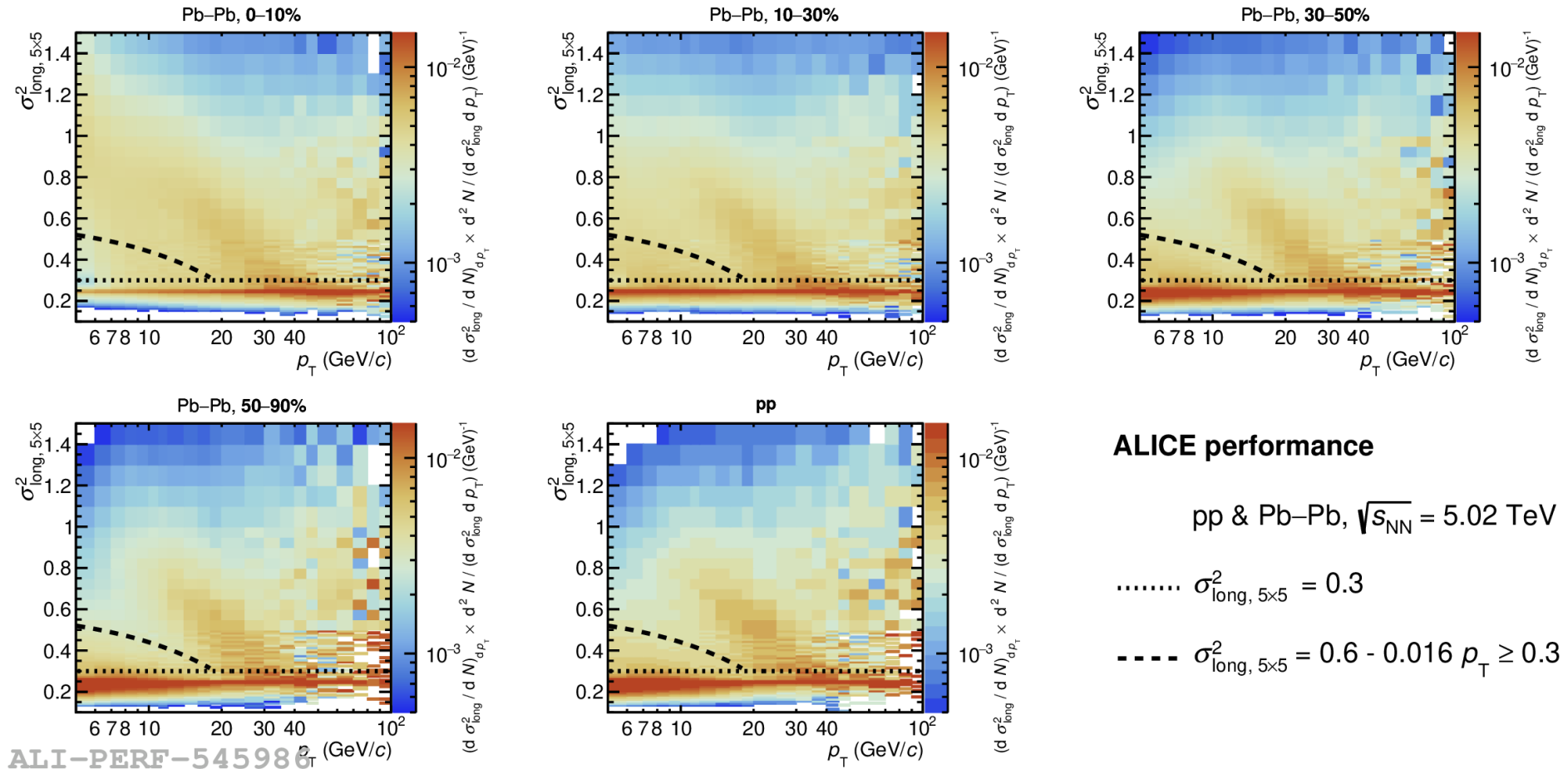
- For Pb–Pb, let's just consider the cells around the highest energy cell in a 5x5 fixed window in the  $\sigma^2_{\text{long}}$  calculation, independently if cells were assigned to the V3 cluster

▶ Those cells must be all neighbours

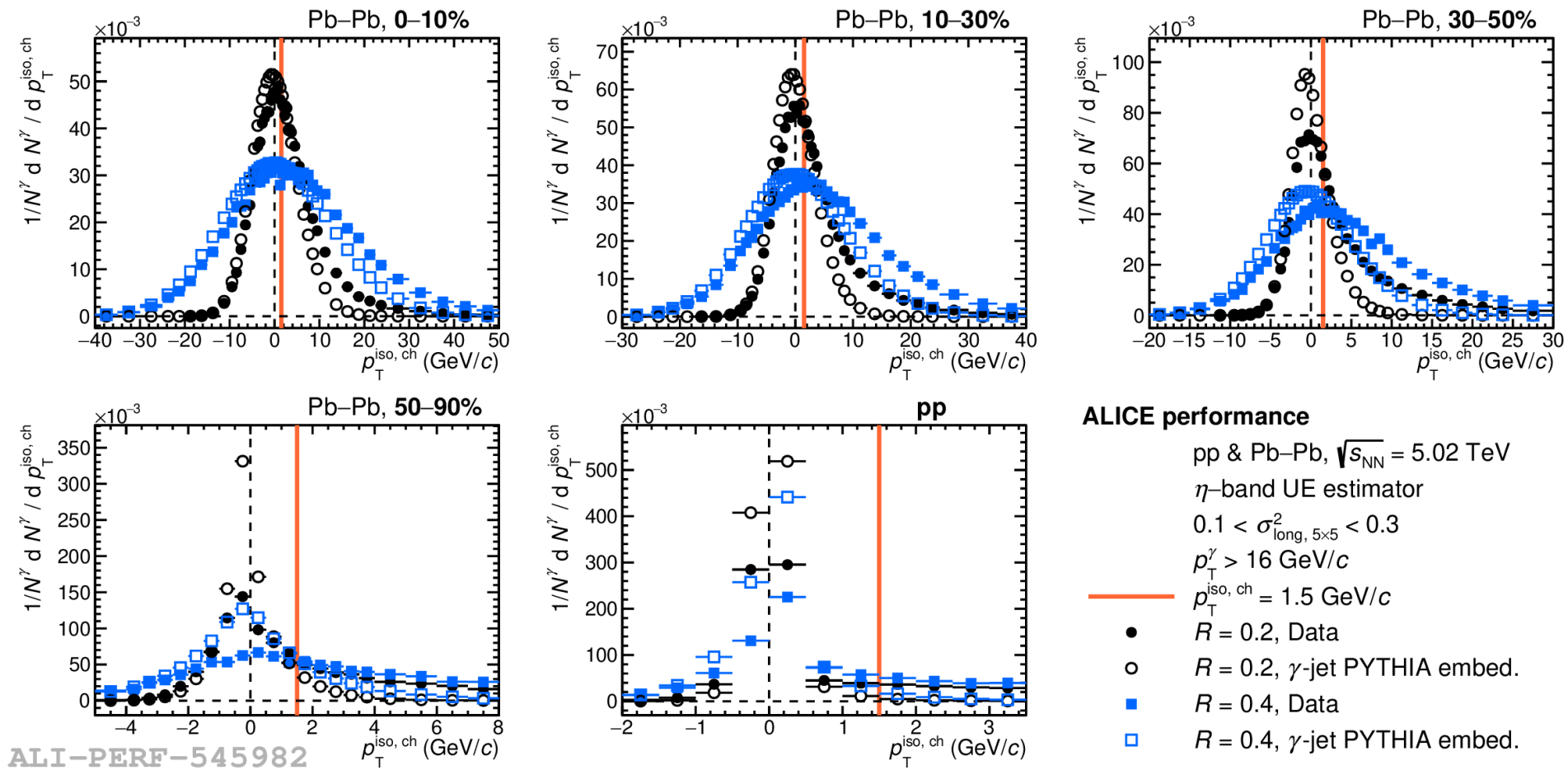
- **The cluster energy and position remains the same as the V3 cluster**
- **Use same definition in pp and Pb–Pb collisions**



# EMCal cluster shower shape

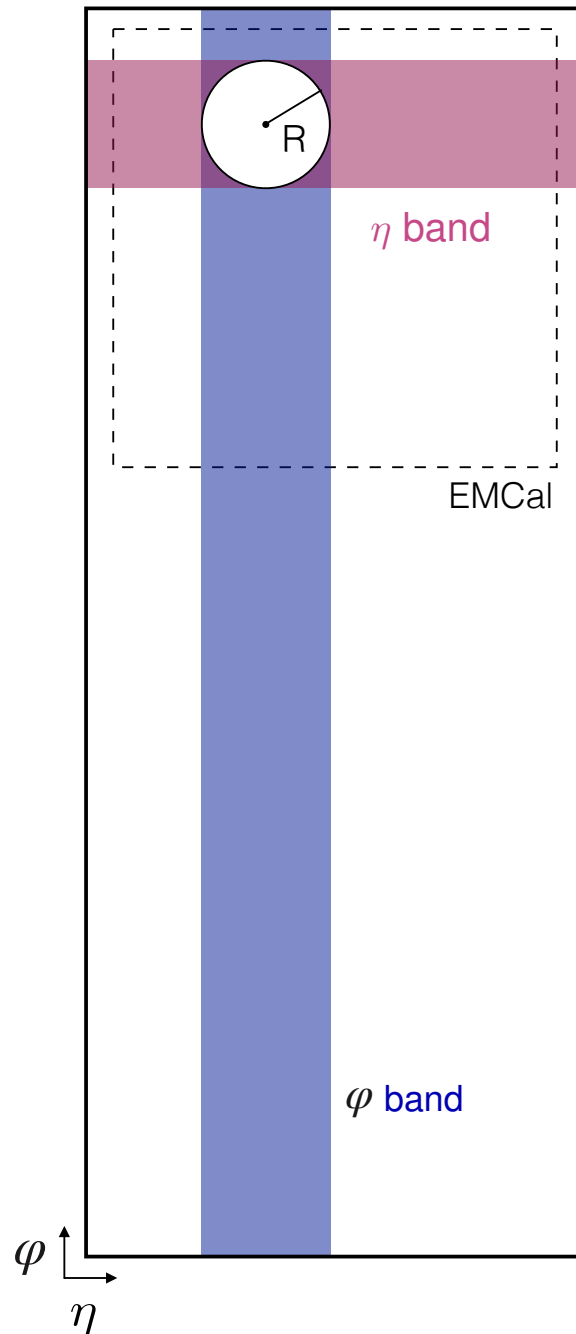


# Isolation energy in cone for $R = 0.2$ & $0.4$



ALI-PERF-545982

# TPC acceptance



# ISOLATED CROSS SECTION CALCULATION

$$\frac{d^2 \sigma}{d p_T d \eta} = \frac{\sigma_{MB}}{N_{col} \times \sum^n \text{periods \& triggers} (N_{events} \times RF_{\epsilon_{trig}})} \times \sum^n \text{triggers \& periods} \left( \frac{d^2 N}{d p_T d \eta} \right) \times \frac{Purity}{Acc. \times \epsilon_{\gamma}^{iso} \times \epsilon_{trig}}$$

Ingredients:

- Trigger efficiency:  $\epsilon_{trig}$
- Rejection factor:  $RF_{trig}$
- EMCal acceptance correction Acc: 0.527
- Minimum bias cross section:  $\sigma_{MB}$
- $N_{coll}$
- Purity
- Efficiency:

	$\sigma_{MB}$ (mb)	$N_{coll}$
pp	50.87 (2.1%)	1
Pb-Pb	67.6 (0.88%)	
0-10%		1572 ± 17.4 (1.1%)
10-30%		783.05 ± 7.0 (0.9%)
30-50%		264.75 ± 3.3(1.2%)
50-90%		38.42 ± 0.6 (1.6%)

Efficiency per selection cut:

$$\epsilon^{sel} = \frac{dN_{\gamma_{prompt}}^{cluster\ sel.} / dp_T^{rec}}{dN_{\gamma_{prompt}}^{gener.} / dp_T^{gen}}$$

- Reconstruction
- PID (shower shape)
- Isolation

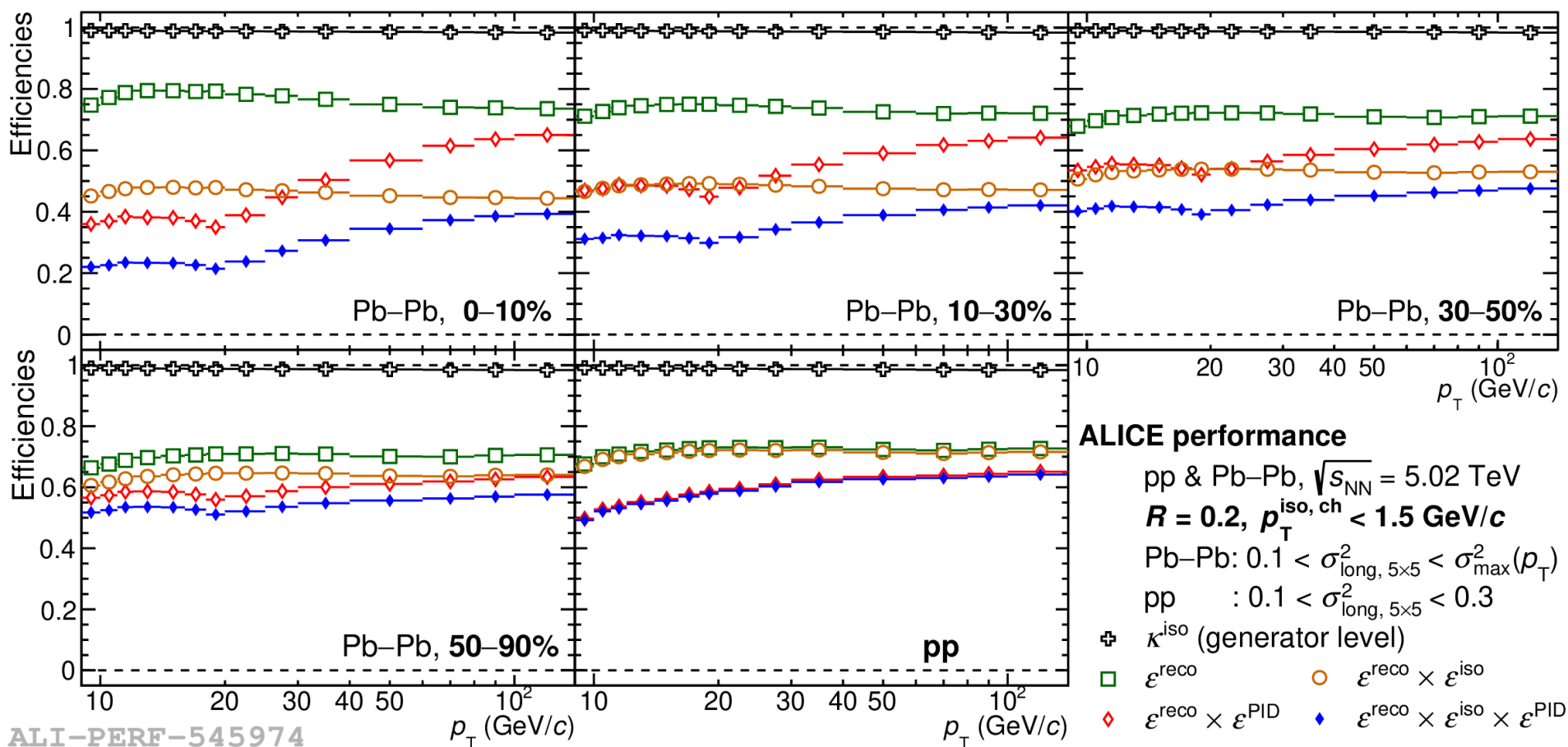
Final efficiency:

$$\epsilon_{\gamma}^{iso} = \frac{dN_{\gamma_{prompt}}^{cluster\ iso.\ narrow} / dp_T^{rec}}{dN_{\gamma_{prompt}}^{gener.\ iso.} / dp_T^{gen}}$$



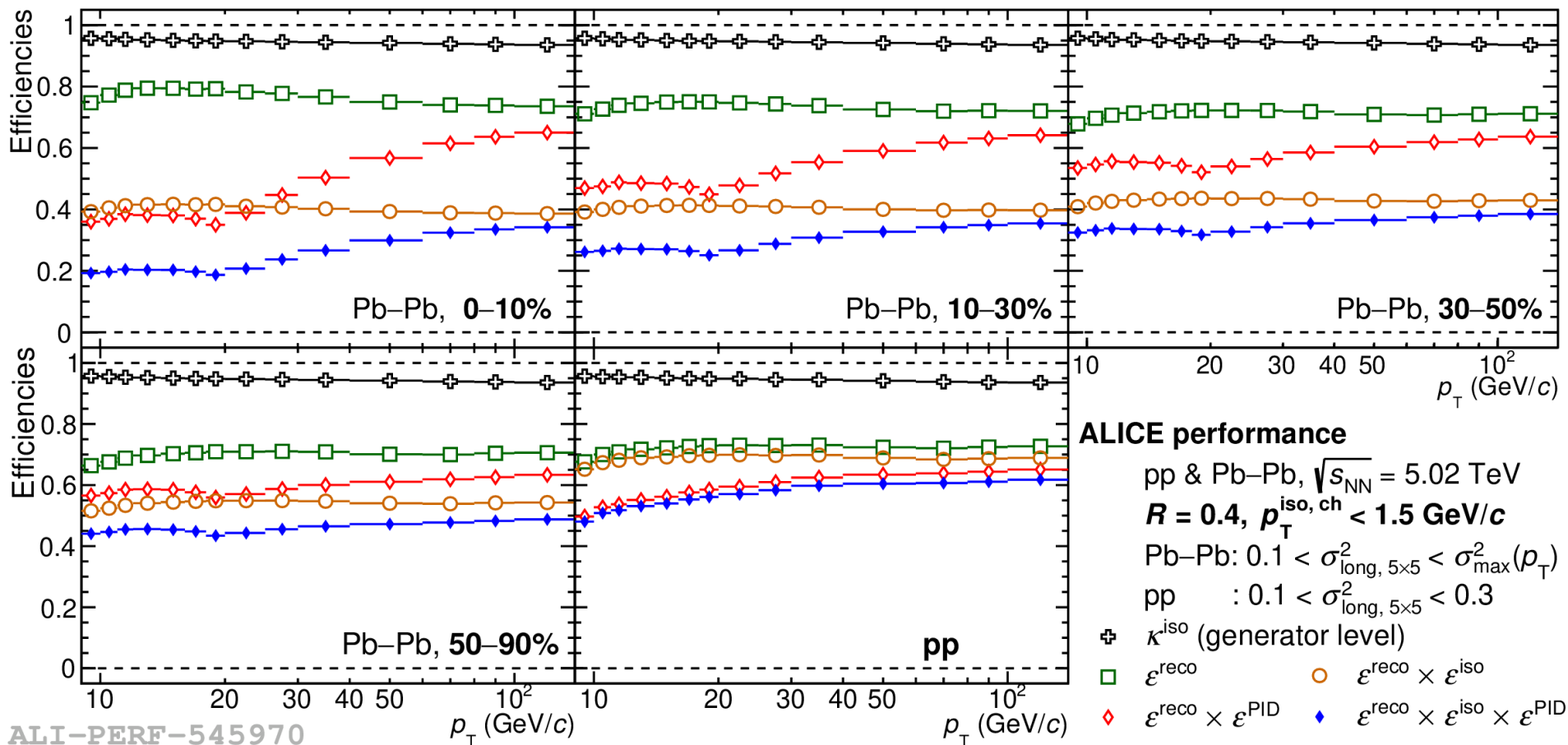
# Isolated $\gamma$ efficiency components, $R = 0.2$

$$\epsilon^{\text{sel}} = \frac{dN_{\gamma_{\text{prompt}}}^{\text{cluster sel.}}/dp_{\text{T}}^{\text{rec}}}{dN_{\gamma_{\text{prompt}}}^{\text{gener.}}/dp_{\text{T}}^{\text{gen}}}$$



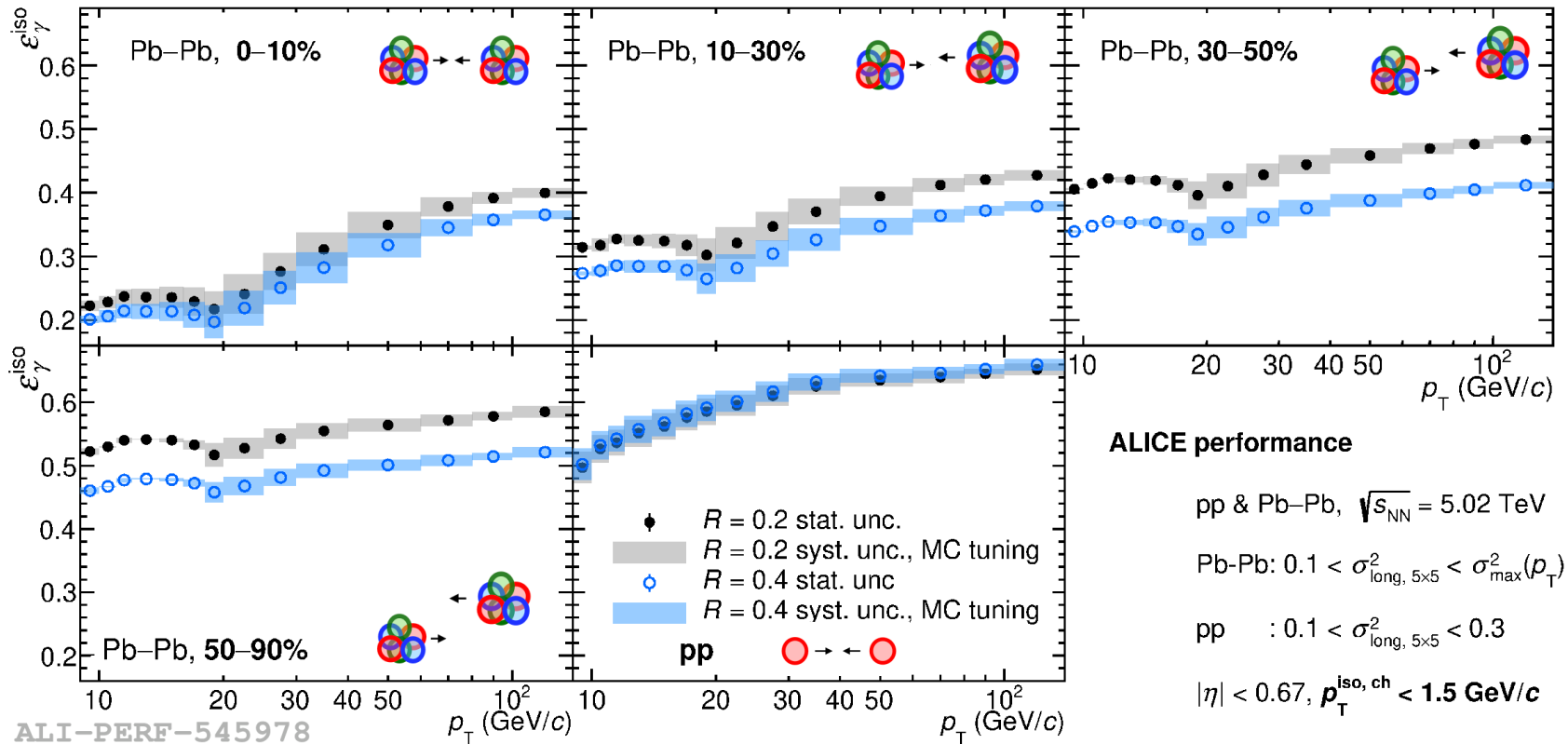
# Isolated $\gamma$ efficiency components, $R = 0.4$

$$\epsilon^{\text{sel}} = \frac{dN_{\gamma_{\text{prompt}}}^{\text{cluster sel.}}/dp_{\text{T}}^{\text{rec}}}{dN_{\gamma_{\text{prompt}}}^{\text{gener.}}/dp_{\text{T}}^{\text{gen}}}$$



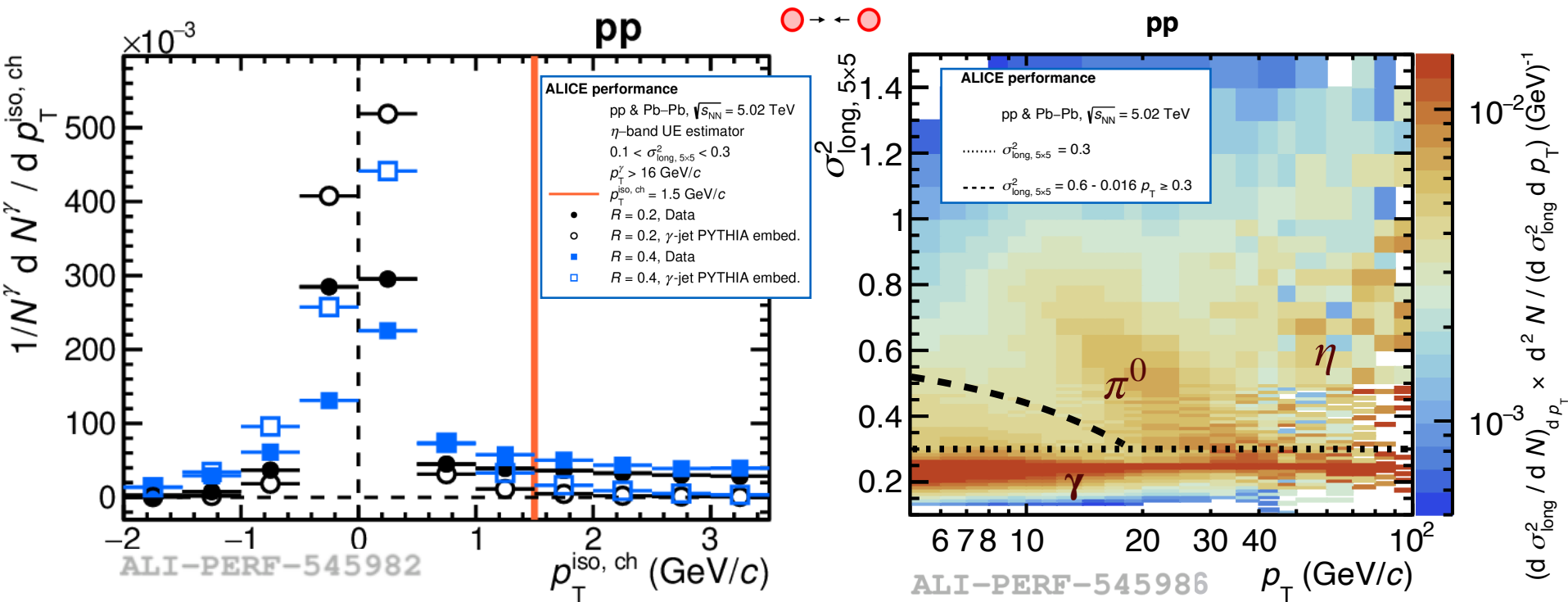
# Efficiency, $R = 0.2$ & $0.4$

$$\epsilon_{\gamma}^{\text{iso}} = \frac{dN_{\gamma_{\text{prompt}}}^{\text{cluster iso. narrow}}/dp_{\text{T}}^{\text{rec}}}{dN_{\gamma_{\text{prompt}}}^{\text{gener. iso.}}/dp_{\text{T}}^{\text{gen}}}$$



- $\epsilon_{\gamma}^{\text{iso}} (0-10\%) < \epsilon_{\gamma}^{\text{iso}} (50-90\%)$ : UE increases cluster size in more central collisions
- In Pb-Pb,  $\epsilon_{\gamma}^{\text{iso}} (R = 0.2) > \epsilon_{\gamma}^{\text{iso}} (R = 0.4)$  a factor  $\sim 0.9$  due to lower UE fluctuations
- In pp,  $\epsilon_{\gamma}^{\text{iso}} (R = 0.2) \approx \epsilon_{\gamma}^{\text{iso}} (R = 0.4)$ , due to the less performing ITS-only tracks

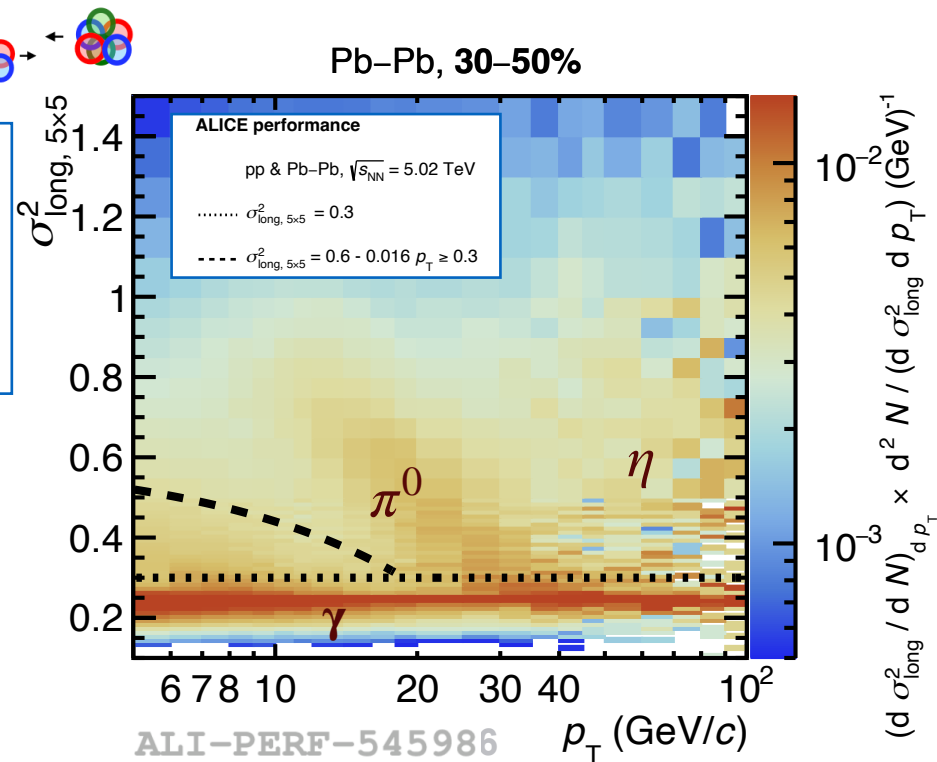
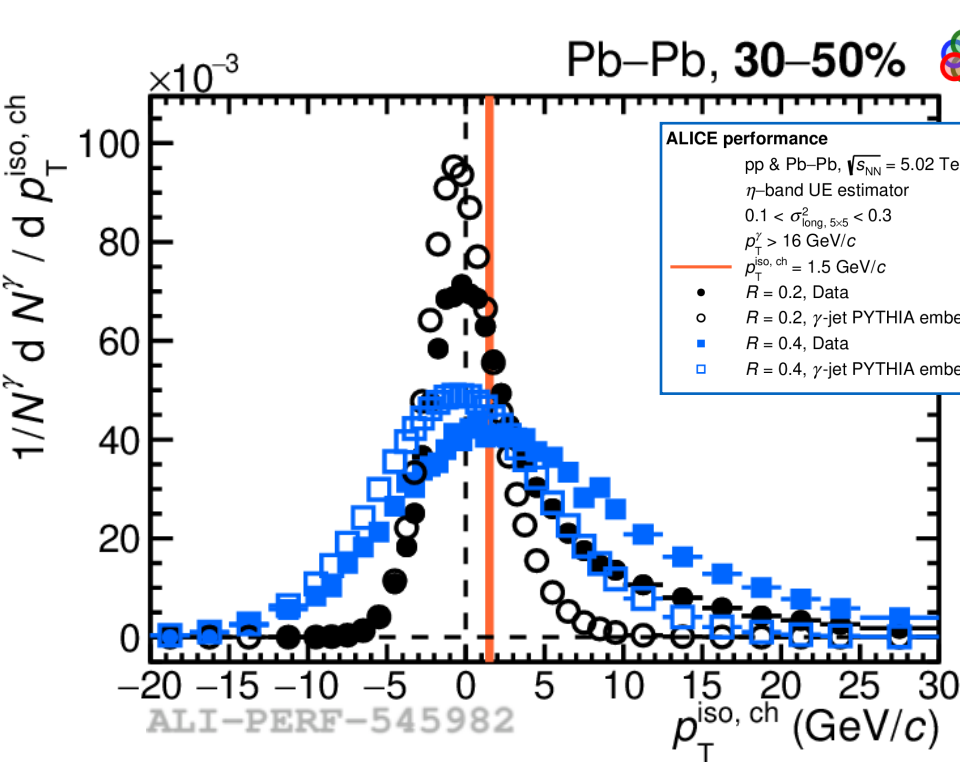
# Prompt $\gamma$ identification: EMCal EM shape & isolation



- Similar narrow peaked distribution for both  $R$ , more peaked for  $R = 0.2$
- In data, more jet contribution to the right tail for  $R = 0.4$

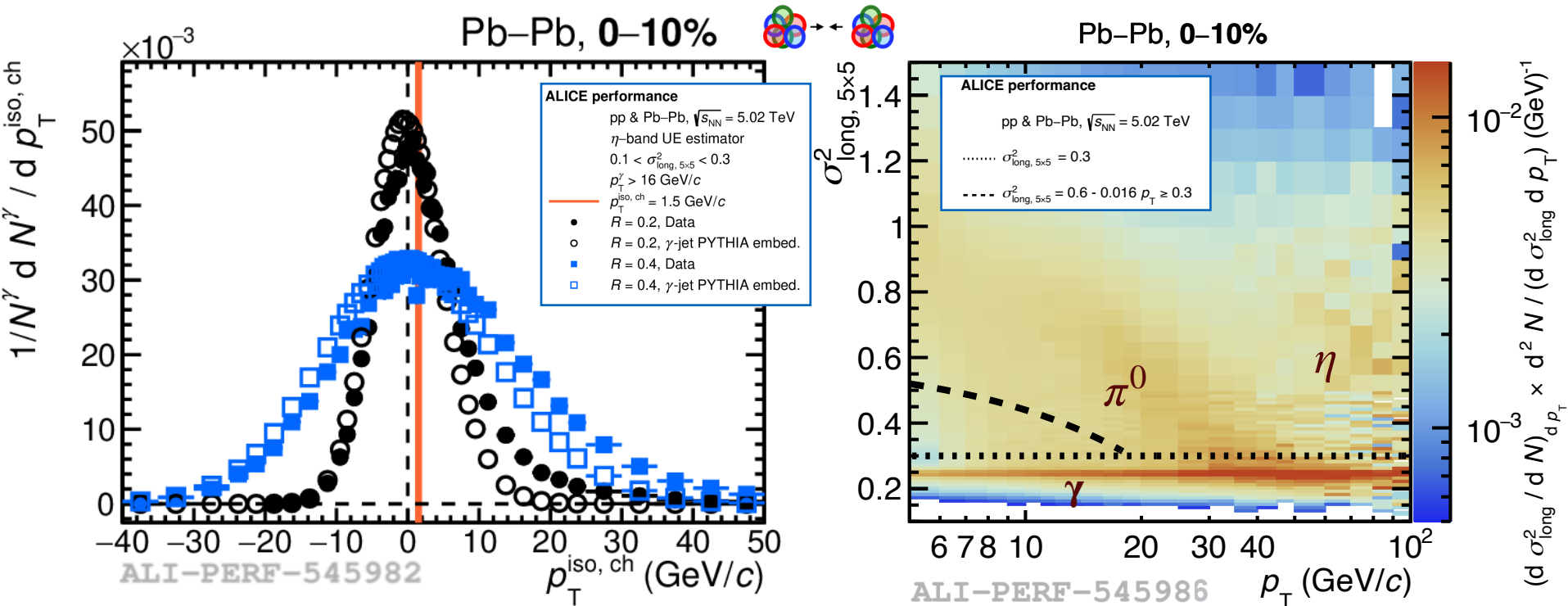
- Select as  $\gamma$  clusters with  $0.1 < \sigma_{\text{long}, 5 \times 5}^2 < 0.3$
- $\gamma$  &  $\pi^0$  bands well separated for  $p_T < 20$  GeV/c, then overlap

# Prompt $\gamma$ identification: EMCal EM shape & isolation



- Significantly wider for  $R = 0.4$
- Embedded pp PYTHIA simulation into MB data, symmetric distribution
- In data, more asymmetric distribution due to jet contribution
- Select as  $\gamma$  clusters with  $0.1 < \sigma_{\text{long}, 5 \times 5}^2 < 0.6 - 0.016 \cdot p_T \geq 0.3$
- $\gamma$  &  $\pi^0$  bands visible from pp to Pb-Pb semi-central collisions

# Prompt $\gamma$ identification: EMCal EM shape & isolation



- Significantly much wider for  $R = 0.4$
- Embedded pp PYTHIA simulation into MB data, symmetric distribution
- In data, more asymmetric distribution due to jet contribution

- Select as  $\gamma$  clusters with  $0.1 < \sigma_{\text{long}, 5 \times 5}^2 < 0.6 - 0.016 \cdot p_T \geq 0.3$
- $\gamma$  &  $\pi^0$  bands visible from pp to Pb-Pb central collisions
- ➔ but many  $\gamma$  increase their  $\sigma_{\text{long}, 5 \times 5}^2$  due to the UE contribution to the cluster

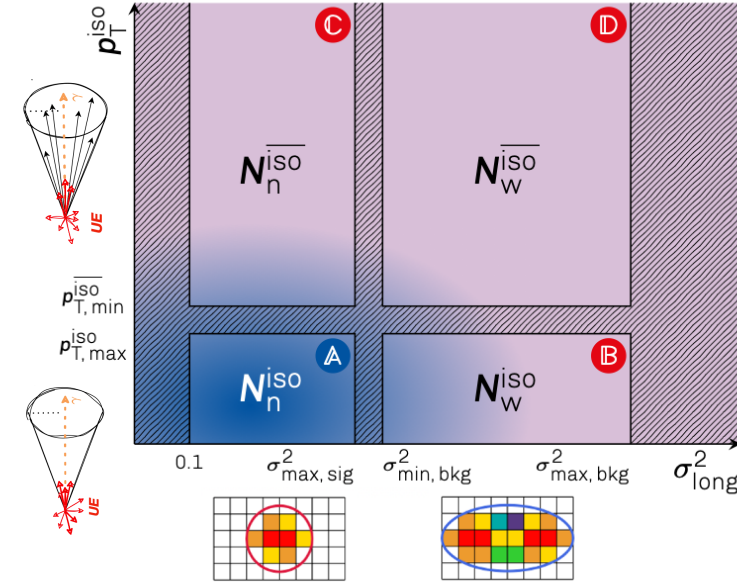
# Purity

- Phase space of calorimeter clusters divided in 4 regions:

$\Delta$ , signal dominated & B-C-D, background dominated

- $\rightarrow$  A:  $0.1 < \sigma_{\text{long}, 5 \times 5}^2 < \sigma_{\text{max}}^2(p_T)$ ,  $p_T^{\text{iso, ch}} < 1.5 \text{ GeV}/c$
- $\rightarrow$  B:  $0.1 + \sigma_{\text{max}}^2(p_T) < \sigma_{\text{long}, 5 \times 5}^2 < 2.0$ ,  $p_T^{\text{iso, ch}} < 1.5 \text{ GeV}/c$
- $\rightarrow$  C:  $0.1 < \sigma_{\text{long}, 5 \times 5}^2 < \sigma_{\text{max}}^2(p_T)$ ,  $4 < p_T^{\text{iso, ch}} < 25 \text{ GeV}/c$
- $\rightarrow$  D:  $0.1 + \sigma_{\text{max}}^2(p_T) < \sigma_{\text{long}, 5 \times 5}^2 < 2.0$ ,  $4 < p_T^{\text{iso, ch}} < 25 \text{ GeV}/c$

with  $\sigma_{\text{max}}^2 = 0.6 - 0.016 \cdot p_T \geq 0.3$  (Pb-Pb) or  $\sigma_{\text{max}}^2 = 0.3$  (pp)



- Purity in  $\Delta$  region extracted as:

$$P = 1 - \left( \frac{N_n^{\text{iso}} / N_n^{\text{iso}}}{N_w^{\text{iso}} / N_w^{\text{iso}}} \right)_{\text{data}} \times \left( \frac{B_n^{\text{iso}} / N_n^{\text{iso}}}{N_w^{\text{iso}} / N_w^{\text{iso}}} \right)_{\text{MC}}$$

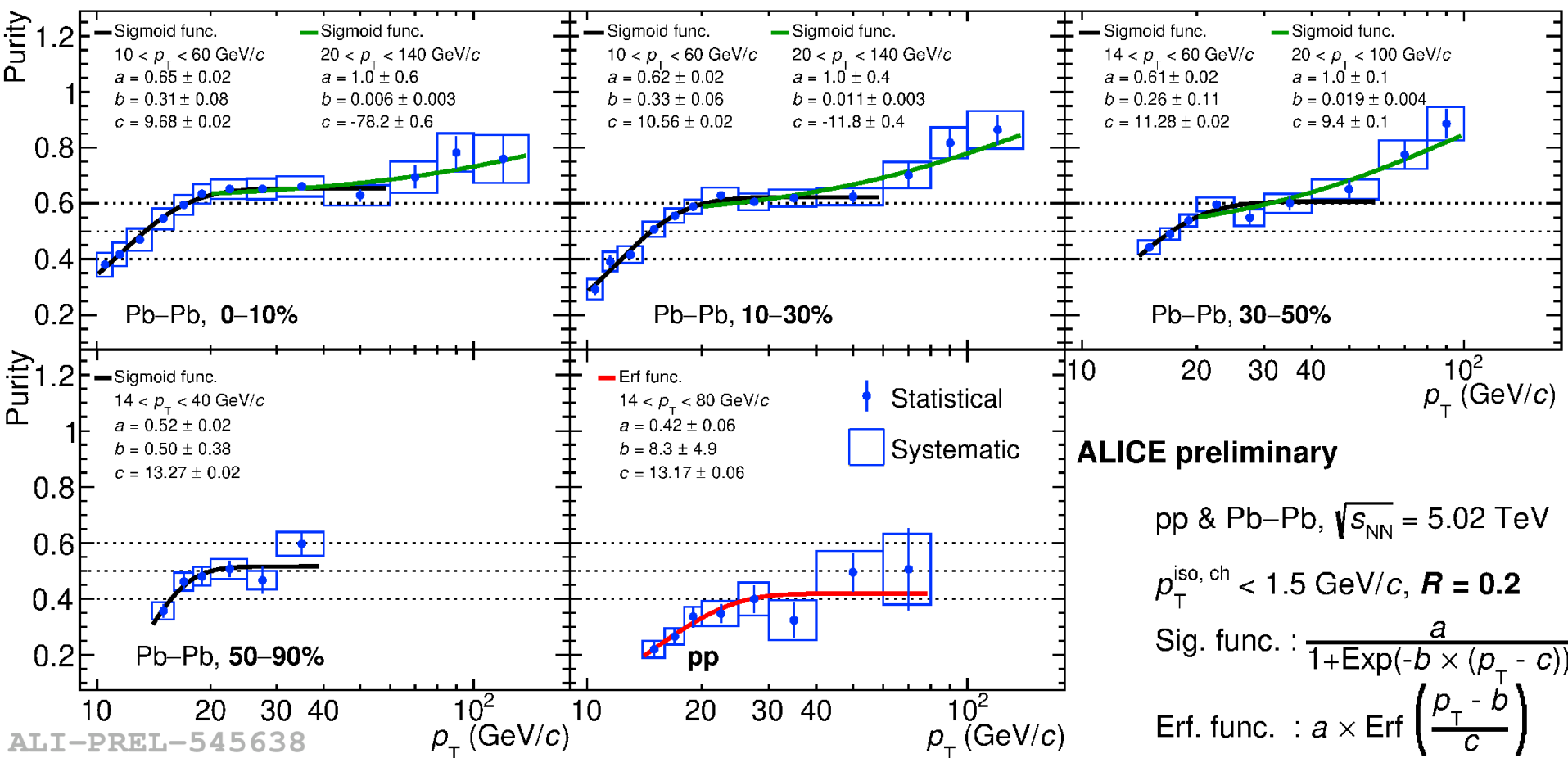
data-driven

PYTHIA:

$$N_{n,w}^{\text{iso, iso}} = \text{jet-jet } (B_{n,w}^{\text{iso, iso}}) + \gamma\text{-jet } (S_{n,w}^{\text{iso, iso}})$$

- $\rightarrow$  Semi data-driven approach, simulation to correct correlations between  $p_T^{\text{iso, ch}}$  and  $\sigma_{\text{long}, 5 \times 5}^2$

# Isolated $\gamma$ purity, $R = 0.2$



**ALICE preliminary**

pp & Pb-Pb,  $\sqrt{s_{NN}} = 5.02$  TeV

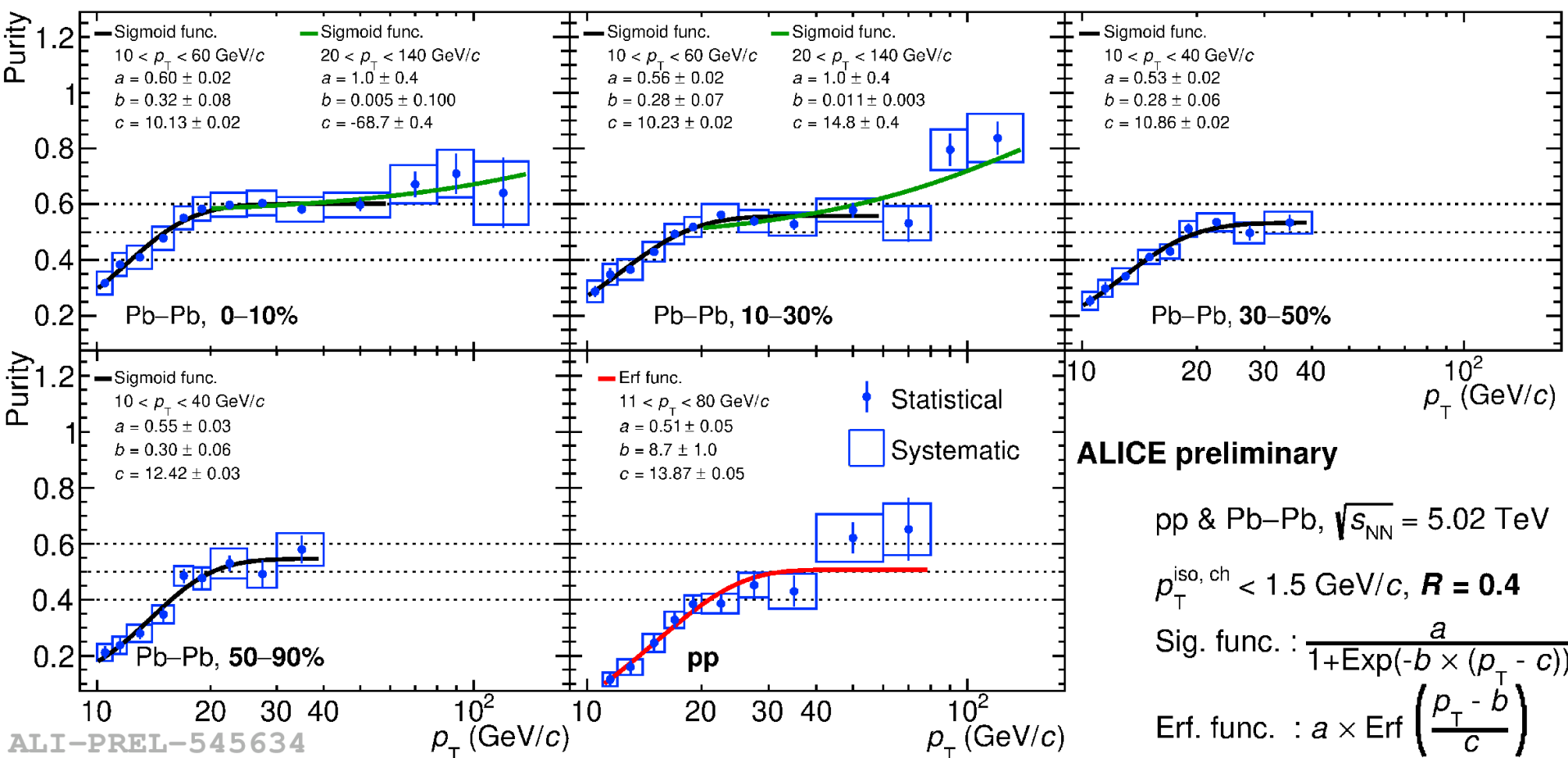
$p_T^{iso, ch} < 1.5$  GeV/c,  $R = 0.2$

Sig. func. : 
$$\frac{a}{1 + \text{Exp}(-b \times (p_T - c))}$$

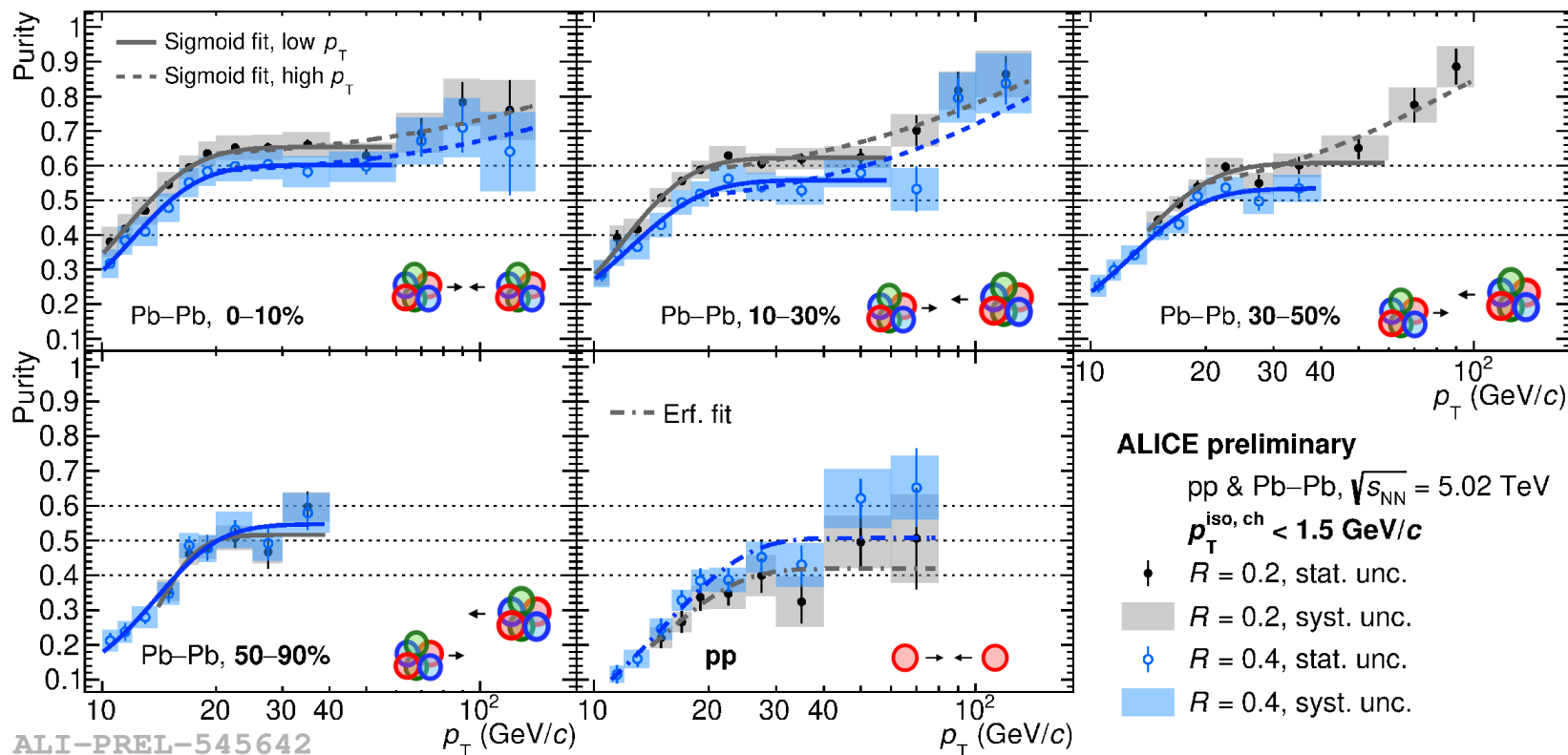
Erf. func. : 
$$a \times \text{Erf} \left( \frac{p_T - b}{c} \right)$$



# Isolated $\gamma$ purity, $R = 0.4$

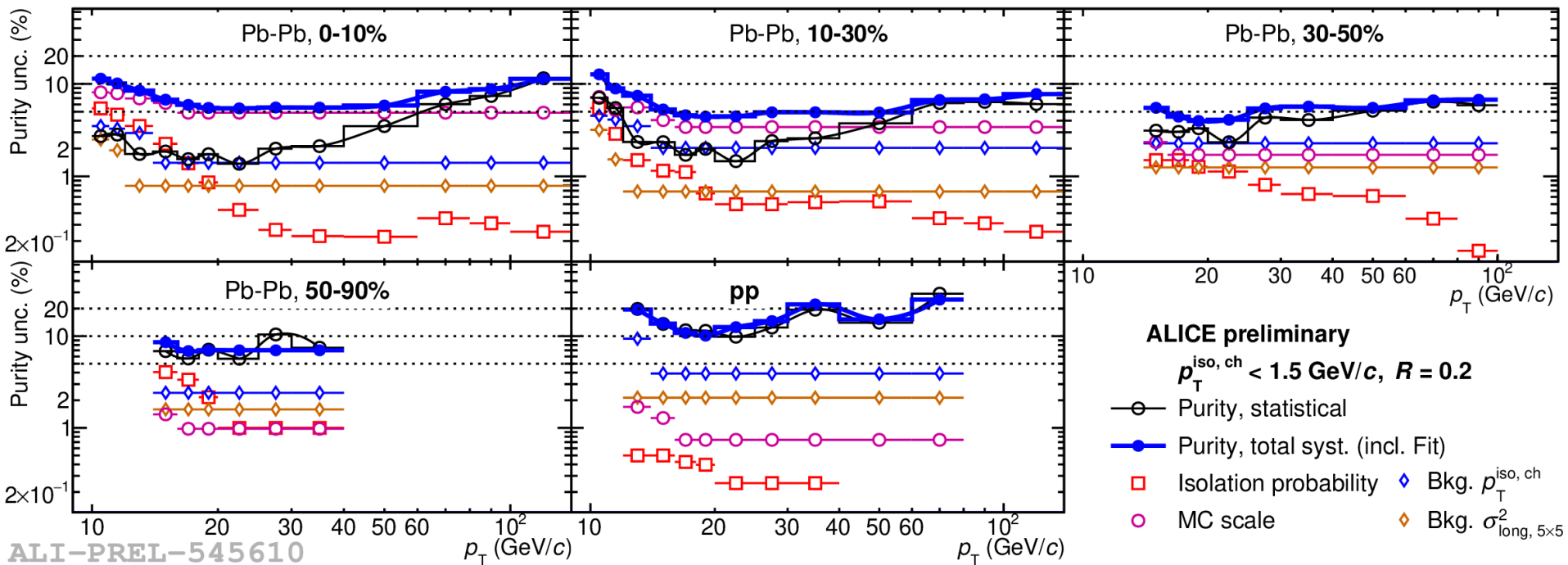


# Purity for $R = 0.2$ & $0.4$

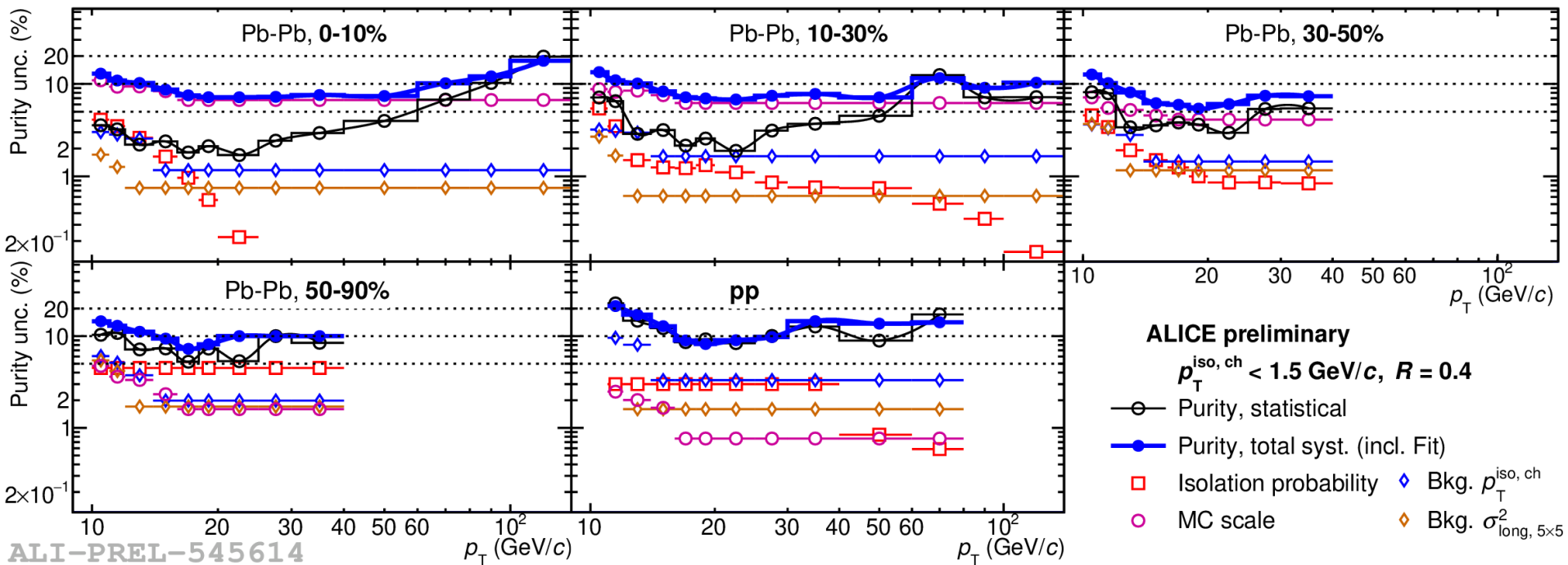


- Distributions fitted to Sigmoid or Erf functions to reduce influence of fluctuations, fits used to correct the spectra
- $P(R = 0.4) > P(R = 0.2)$  in pp collisions, more jet particles in cone, but decreasing centrality  $P(R = 0.2) > P(R = 0.4)$ , due to UE fluctuations, although not significantly different
- $P(\text{Pb-Pb}) > P(\text{pp})$  due to better tracking and higher  $N(\gamma) / N(\pi^0)$  ratio ( $R_{AA}(\pi^0) \ll 1$ )

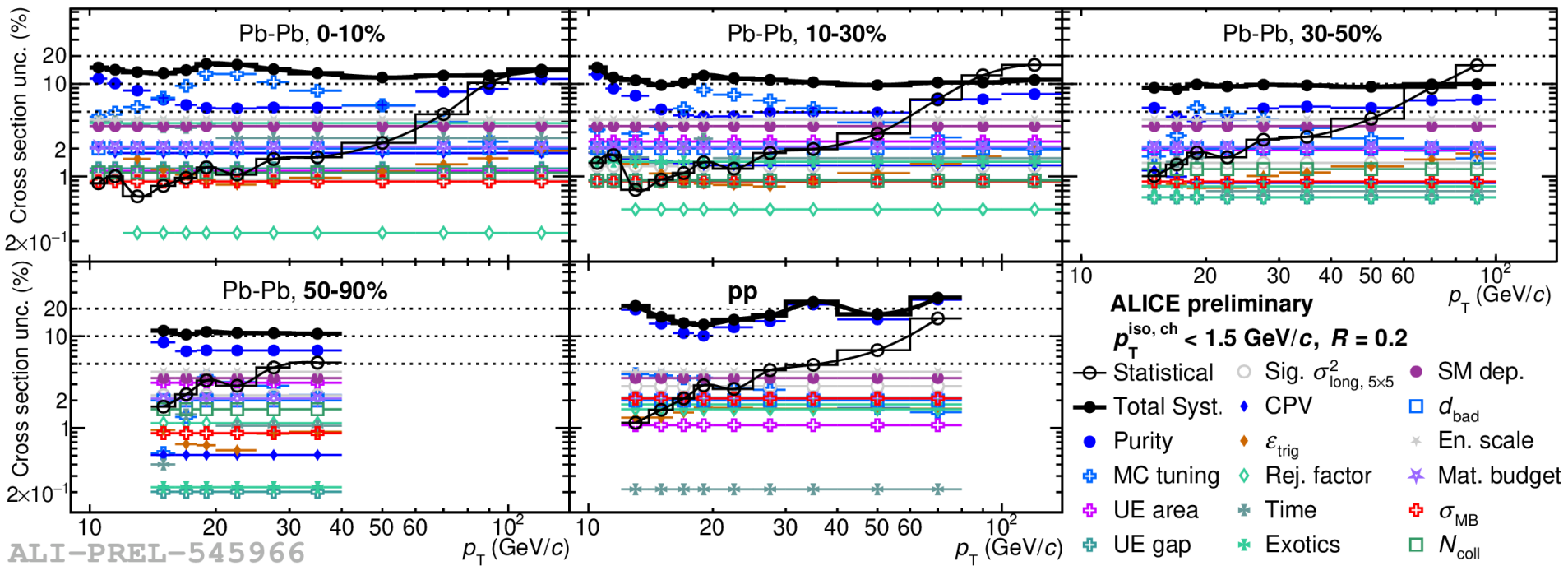
# Isolated $\gamma$ purity uncertainty, $R = 0.2$



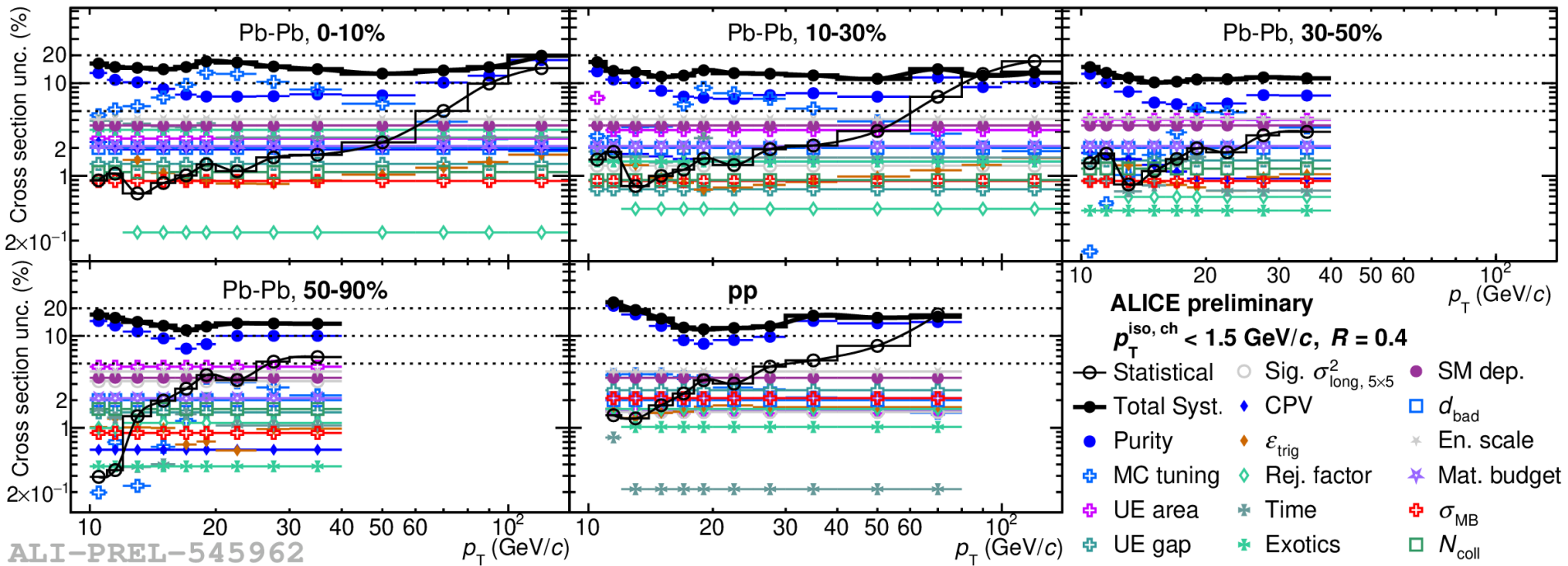
# Isolated $\gamma$ purity uncertainty, $R = 0.4$



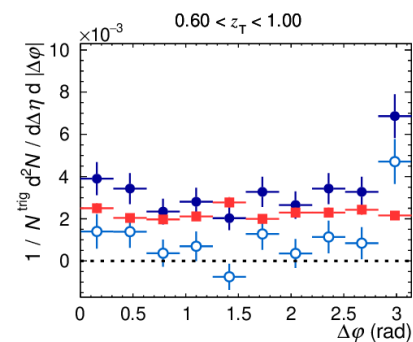
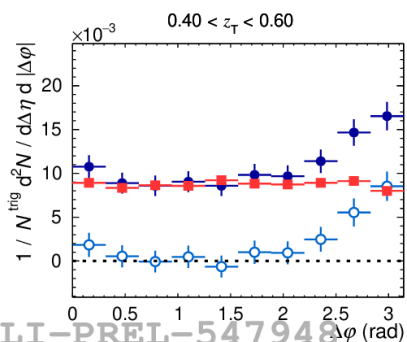
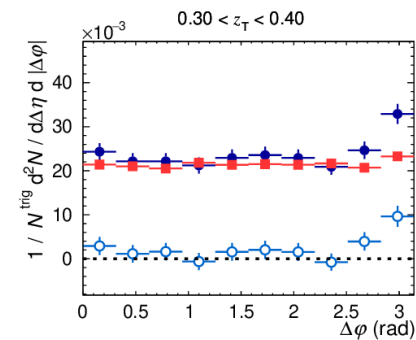
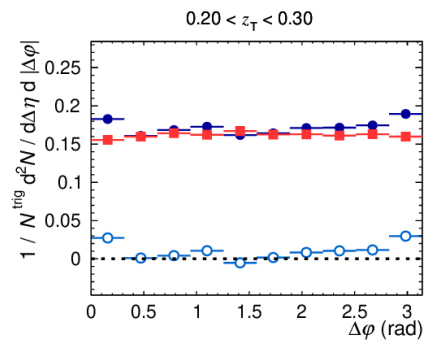
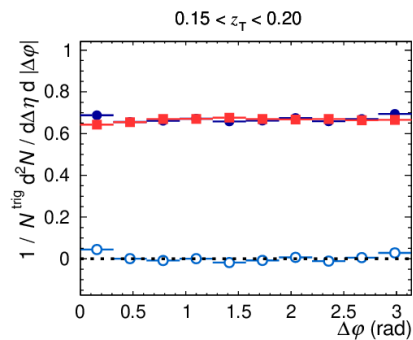
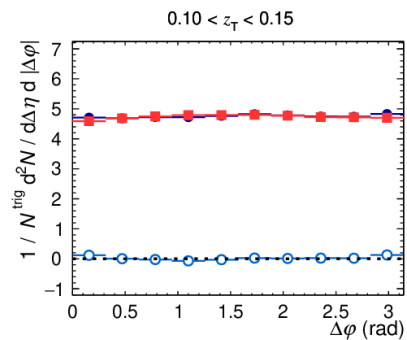
# Isolated $\gamma$ cross section uncertainty, $R = 0.2$



# Isolated $\gamma$ cross section uncertainty, $R = 0.4$



# Isolated $\gamma$ -hadron correlations in Pb-Pb: $D(z_T)$



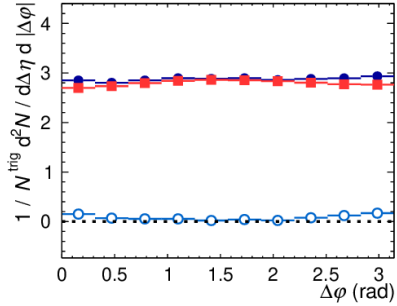
ALICE preliminary  
 0–10% Pb–Pb,  $\sqrt{s_{NN}} = 5.02$  TeV,  $|\eta^{trig}| < 0.67$   
 $20 < p_T^{trig} < 25$  GeV/c  $\otimes$   $p_T^h > 0.5$  GeV/c  
 cluster<sub>narrow</sub><sup>iso</sup>:  $0.10 < \sigma_{long, 5 \times 5}^2 < 0.30$

- ◆ Same Event
- Mixed Event
- ◇ Same Event - Mixed Event

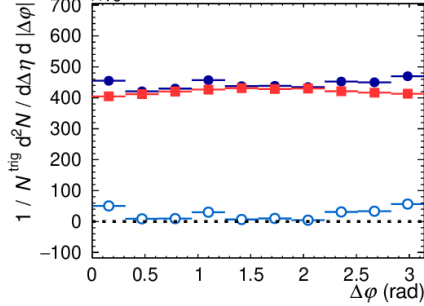
ALI-PREL-547948

# Isolated $\gamma$ -hadron correlations in Pb-Pb: $D(z_T)$

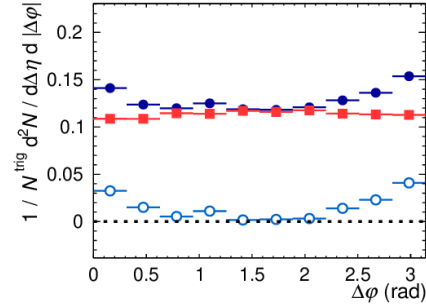
$0.10 < z_T < 0.15$



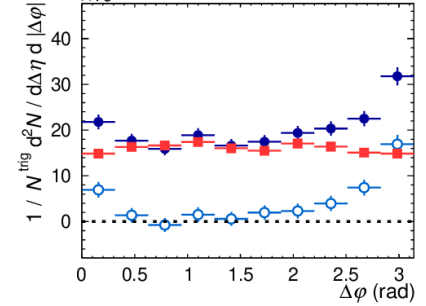
$0.15 < z_T < 0.20$



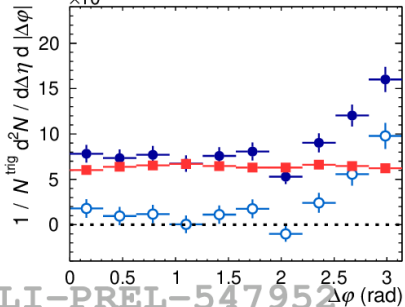
$0.20 < z_T < 0.30$



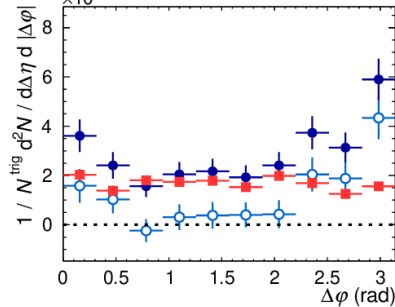
$0.30 < z_T < 0.40$



$0.40 < z_T < 0.60$



$0.60 < z_T < 1.00$



ALICE preliminary

10–30% Pb–Pb,  $\sqrt{s_{NN}} = 5.02$  TeV,  $|\eta^{trig}| < 0.67$

$20 < p_T^{trig} < 25$  GeV/c  $\otimes$   $p_T^h > 0.5$  GeV/c

cluster<sub>narrow</sub><sup>iso</sup>:  $0.10 < \sigma_{long, 5x5}^2 < 0.30$

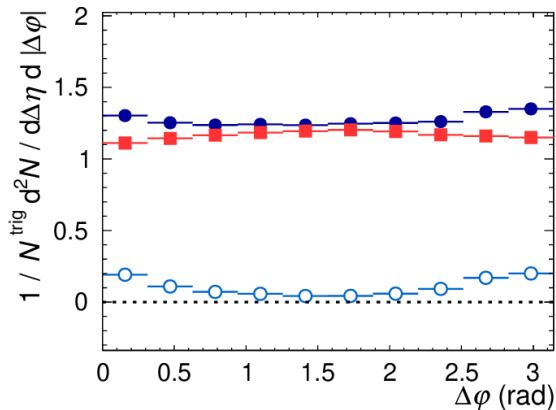
- ◆ Same Event
- Mixed Event
- Same Event - Mixed Event

ALI-PREL-547952

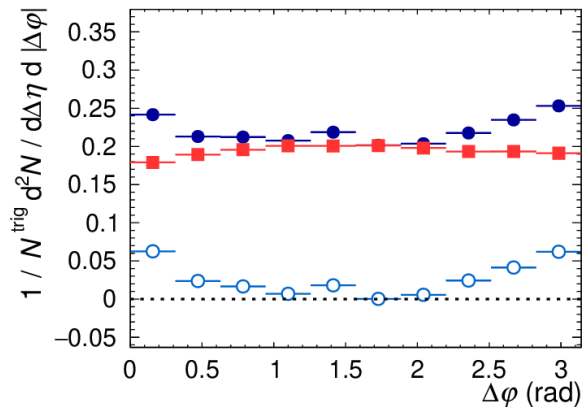


# Isolated $\gamma$ -hadron correlations in Pb-Pb: $D(z_T)$

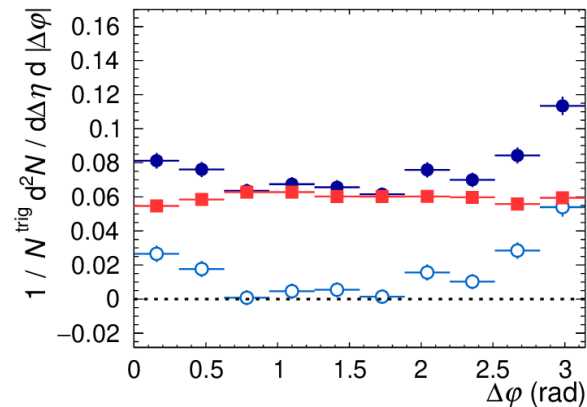
$0.10 < z_T < 0.15$



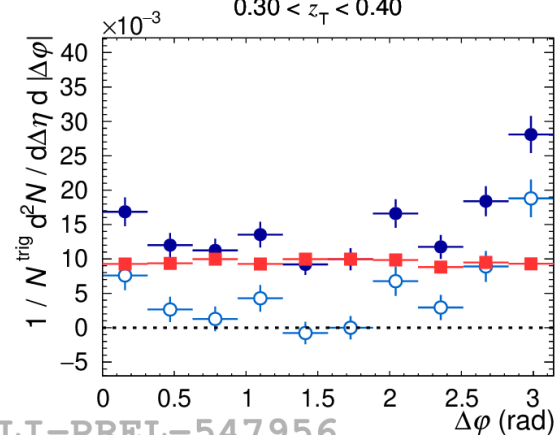
$0.15 < z_T < 0.20$



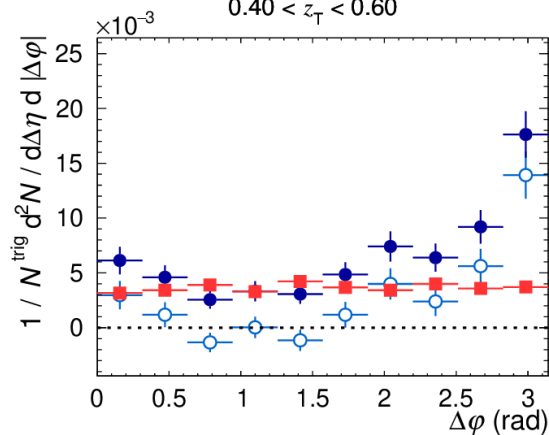
$0.20 < z_T < 0.30$



$0.30 < z_T < 0.40$



$0.40 < z_T < 0.60$



ALICE preliminary

**30–50% Pb–Pb**,  $\sqrt{s_{NN}} = 5.02$  TeV,  $|\eta^{\text{trig}}| < 0.67$

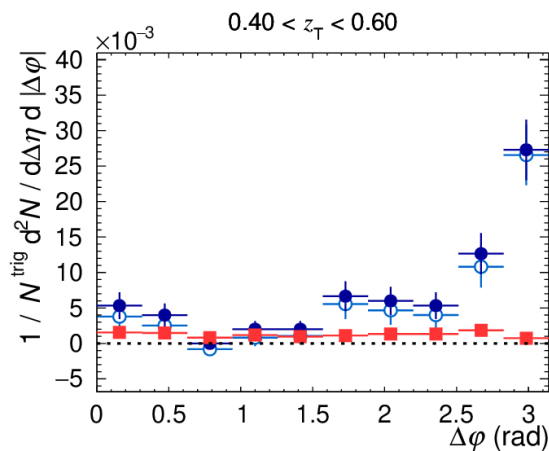
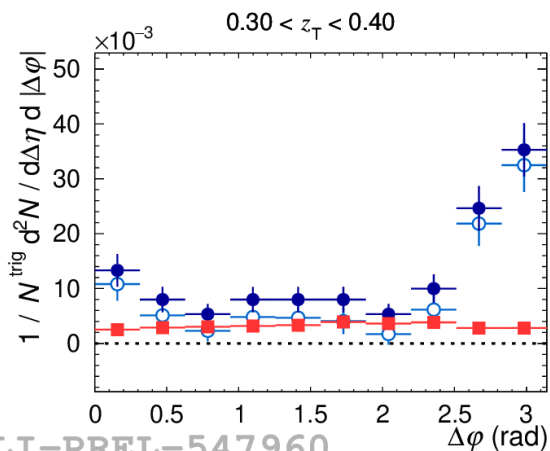
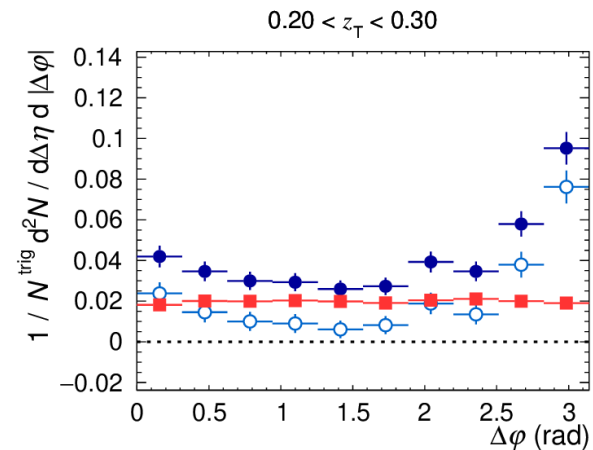
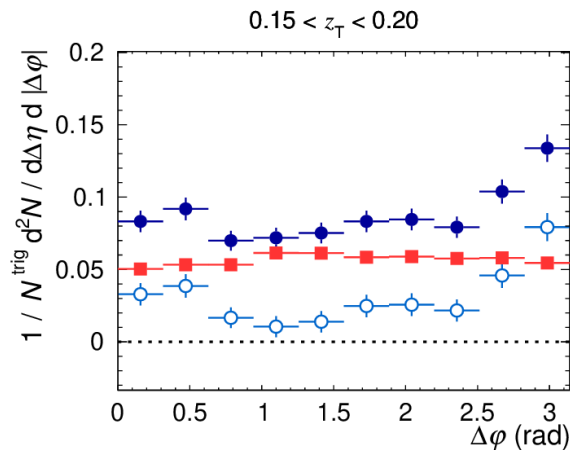
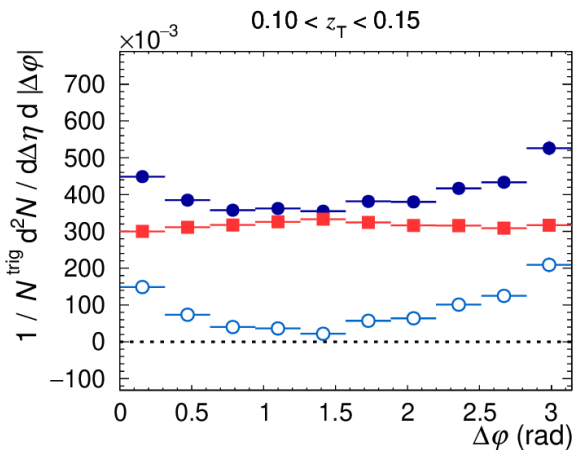
$20 < p_T^{\text{trig}} < 25$  GeV/c  $\otimes$   $p_T^h > 0.5$  GeV/c

cluster<sub>narrow</sub><sup>iso</sup>:  $0.10 < \sigma_{\text{long}, 5 \times 5}^2 < 0.30$

- Same Event
- Mixed Event
- Same Event - Mixed Event

ALI-PREL-547956

# Isolated $\gamma$ -hadron correlations in Pb–Pb: $D(z_T)$



ALICE preliminary

50–90% Pb–Pb,  $\sqrt{s_{NN}} = 5.02$  TeV,  $|\eta^{trig}| < 0.67$

$20 < p_T^{trig} < 25$  GeV/c  $\otimes$   $p_T^h > 0.5$  GeV/c

cluster<sub>narrow</sub><sup>iso</sup>:  $0.10 < \sigma_{long, 5x5}^2 < 0.30$

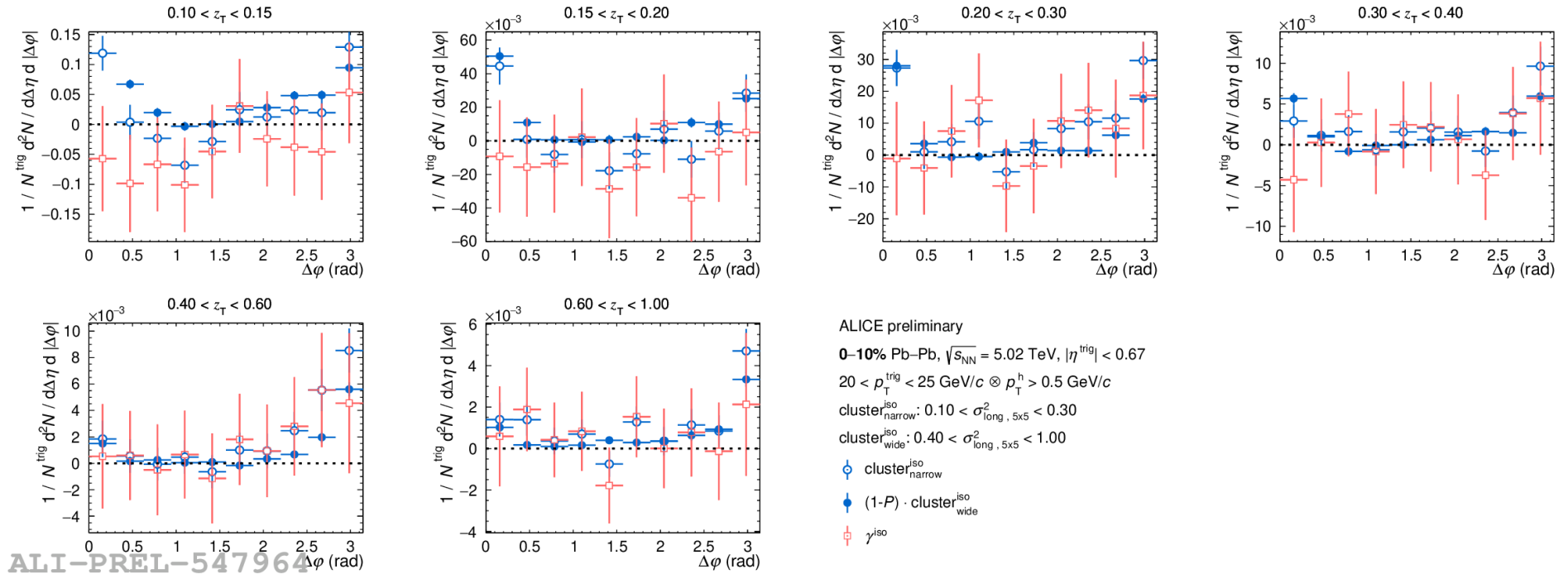
● Same Event

■ Mixed Event

○ Same Event - Mixed Event

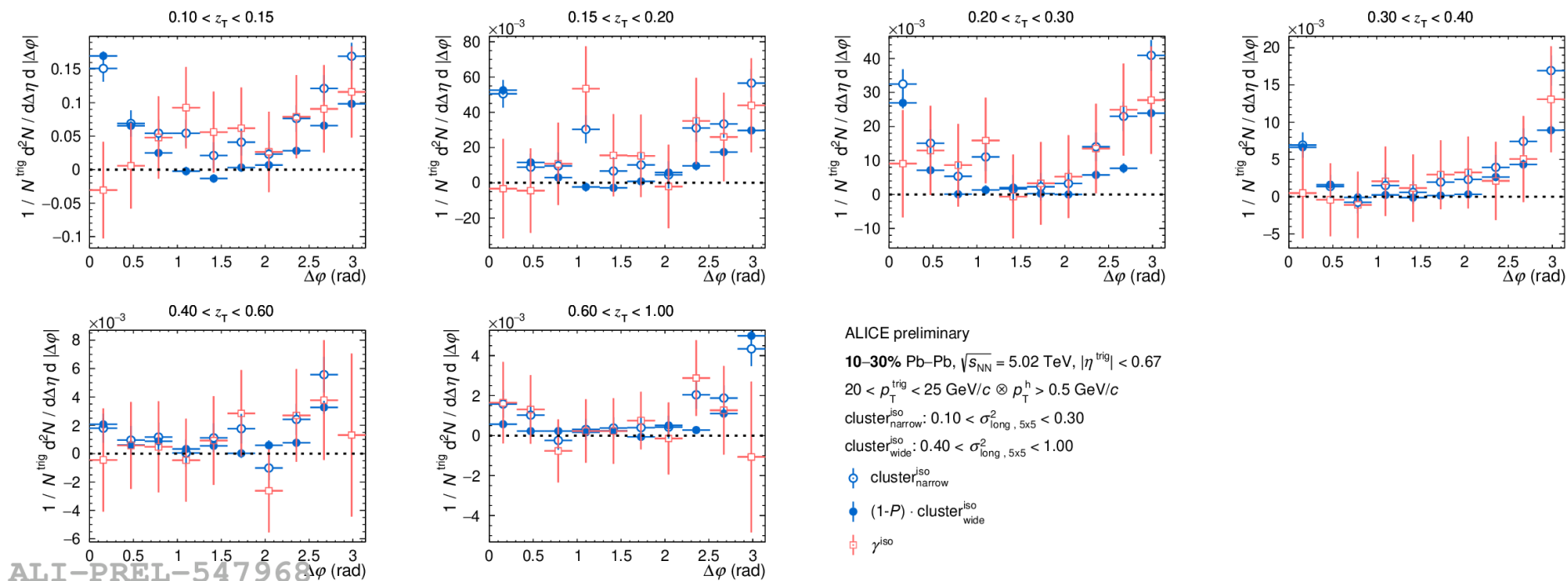
ALI-PREL-547960

# Isolated $\gamma$ -hadron correlations in Pb-Pb: $D(z_T)$



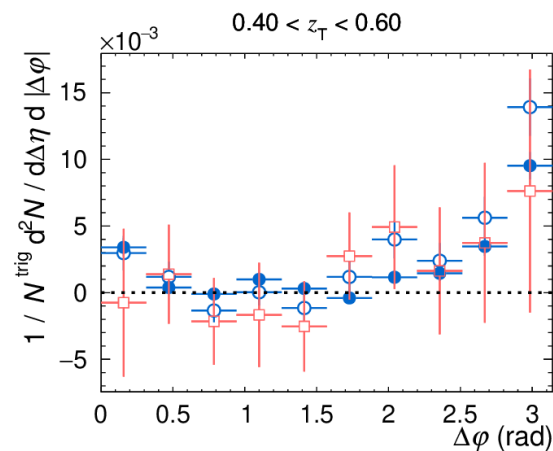
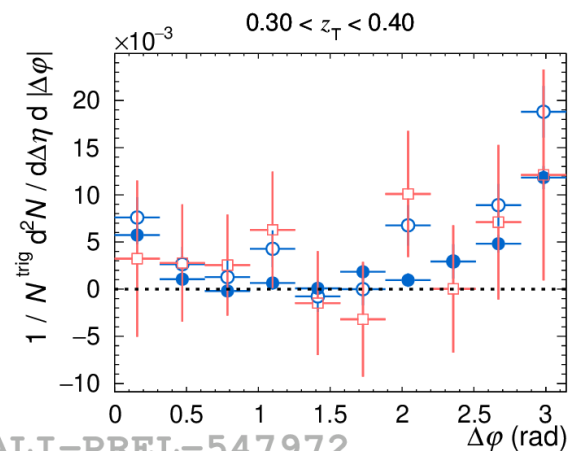
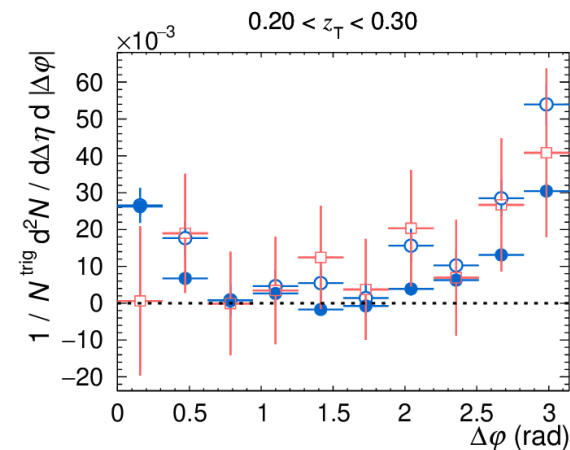
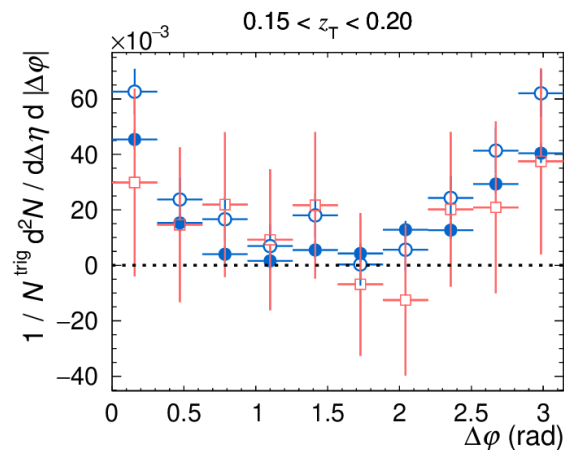
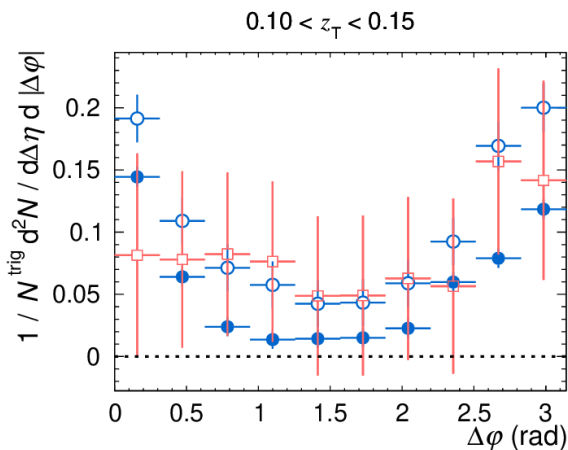
ALI-PREL-547964

# Isolated $\gamma$ -hadron correlations in Pb-Pb: $D(z_T)$



ALI-PREL-547968

# Isolated $\gamma$ -hadron correlations in Pb–Pb: $D(z_T)$



ALICE preliminary

30–50% Pb–Pb,  $\sqrt{s_{NN}} = 5.02$  TeV,  $|\eta^{trig}| < 0.67$

$20 < p_T^{trig} < 25$  GeV/c  $\otimes$   $p_T^h > 0.5$  GeV/c

cluster<sub>narrow</sub><sup>iso</sup>:  $0.10 < \sigma_{long, 5x5}^2 < 0.30$

cluster<sub>wide</sub><sup>iso</sup>:  $0.40 < \sigma_{long, 5x5}^2 < 1.00$

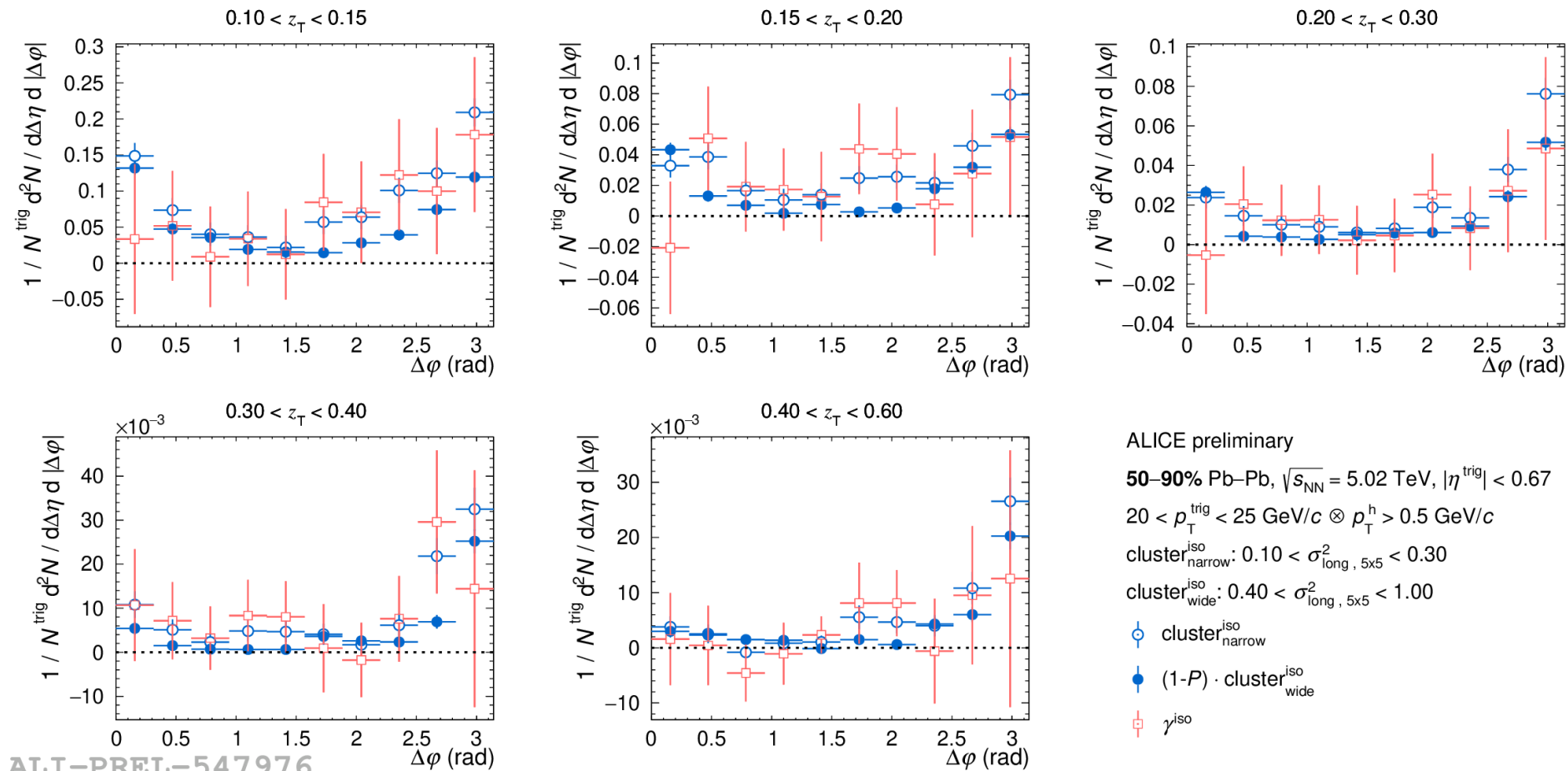
○ cluster<sub>narrow</sub><sup>iso</sup>

● (1- $P$ ) · cluster<sub>wide</sub><sup>iso</sup>

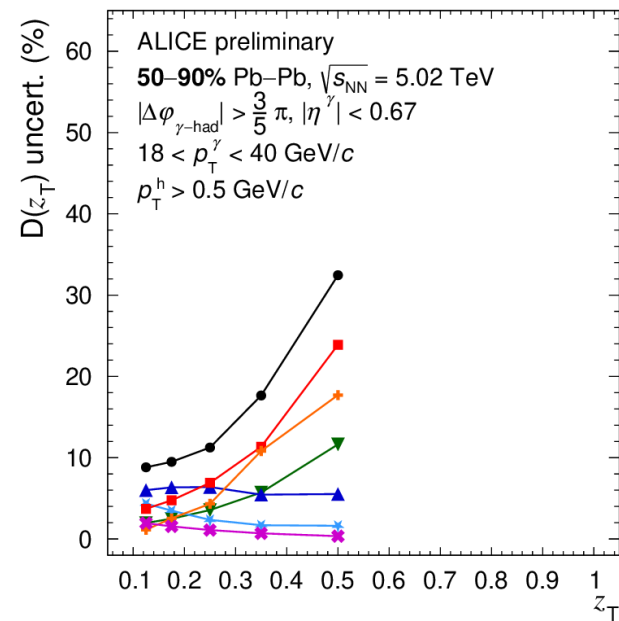
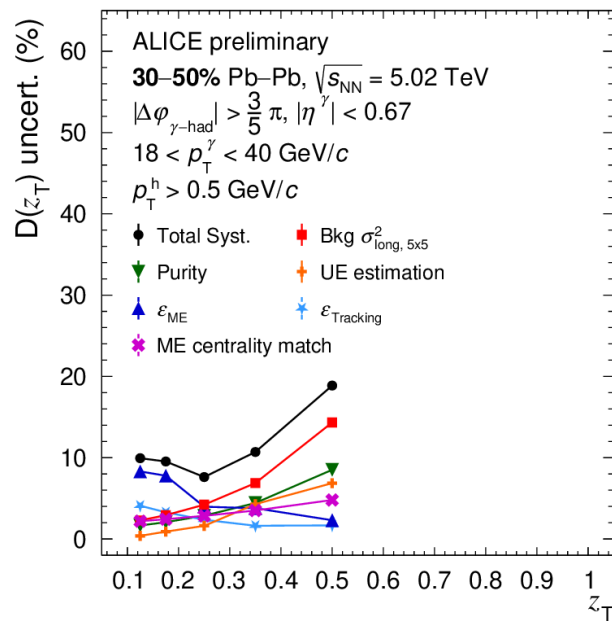
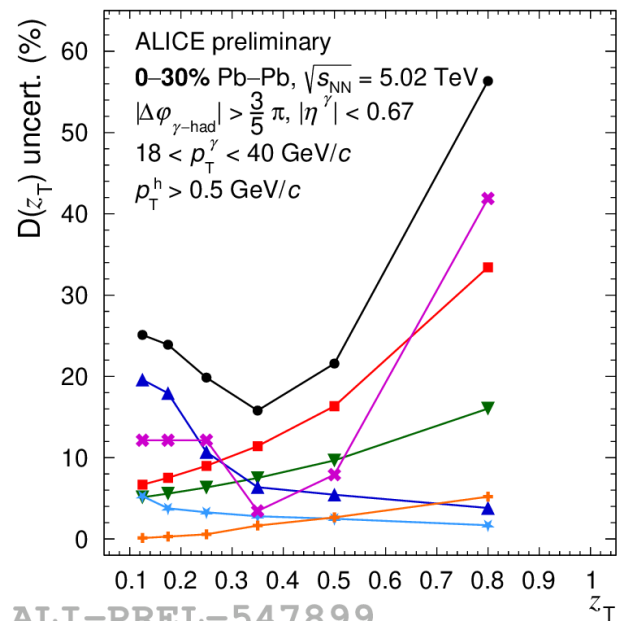
□  $\gamma^{iso}$

ALI-PREL-547972

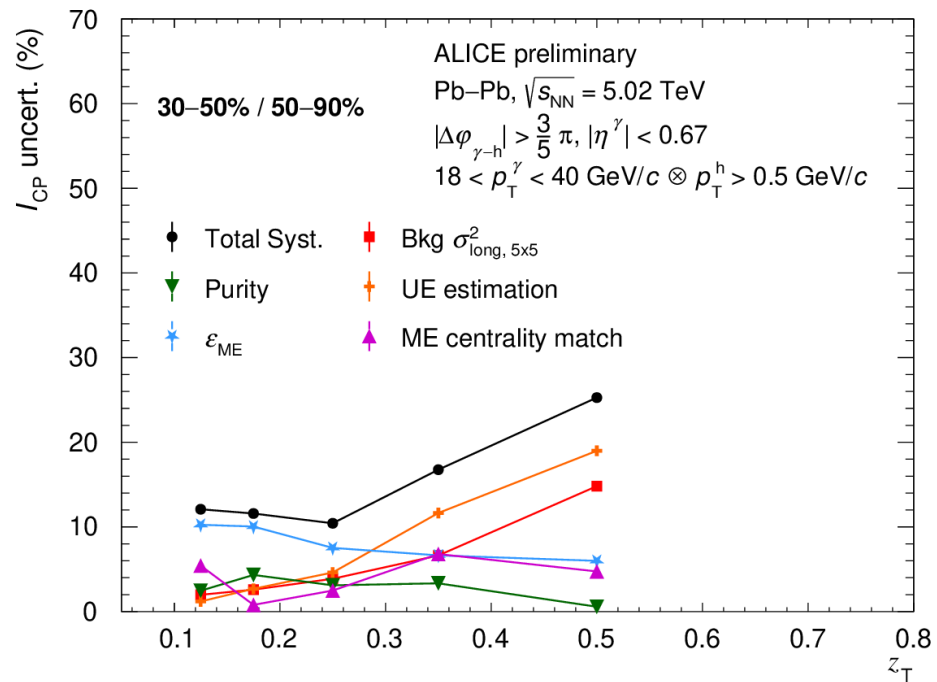
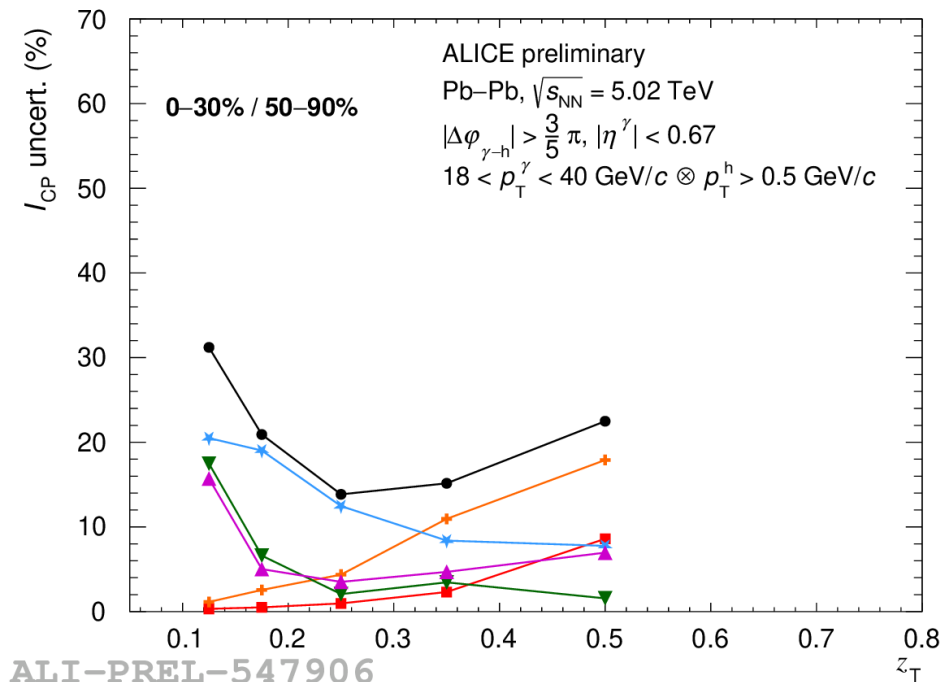
# Isolated $\gamma$ -hadron correlations in Pb–Pb: $D(z_T)$



# Isolated $\gamma$ -hadron correlation uncertainty: $D(z_T)$



# Isolated $\gamma$ -hadron correlation uncertainty: $I_{CP}$





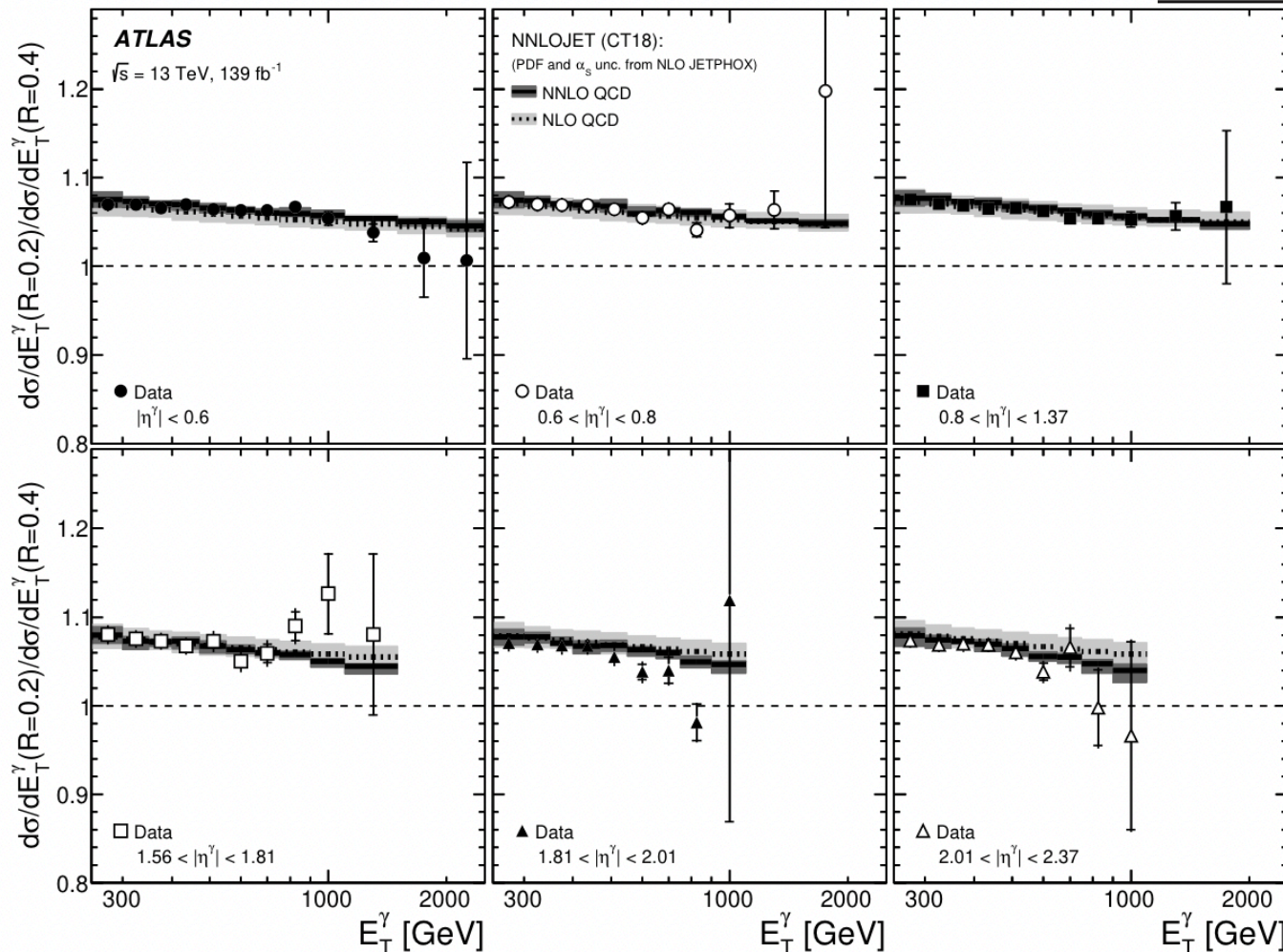


Figure 21: Measured ratios of the differential cross sections for inclusive isolated-photon production for  $R = 0.2$  and  $R = 0.4$  as functions of  $E_T^\gamma$  in different  $\eta^\gamma$  regions. The NLO (dotted lines) and NNLO (solid lines) pQCD predictions from NNLOJET based on the CT18 PDF set are also shown. The inner (outer) error bars represent the statistical uncertainties (statistical and systematic uncertainties added in quadrature) and the shaded bands represent the theoretical uncertainties. For some of the points, the inner and outer error bars are smaller than the marker size and, thus, not visible.